Evaluation of Carbon Nanopearls as D-SPME Sorbent for Global Metabolomics of Human Plasma

Rosalynde Ann Sonnenberg

A Thesis

in

the Department

of

Chemistry and Biochemistry

Presented in Partial Fulfillment of the Requirements

For the Degree of Master of Science (Chemistry) at

Concordia University

Montreal, Quebec, Canada

March 2019

This is to certify that the thesis prepared

By: Rosalynde Ann Sonnenberg

Entitled: Evaluation of Carbon Nanopearls as D-SPME Sorbent For Global Metabolomics of Human Plasma

and submitted in partial fulfilment of the requirements for the degree of

Master of Science in Chemistry

complies with the regulations of the University and meets the accepted standards with respect to originality and quality

Signed by the final Examining Committee:

_____ Chair

Dr. Rafik Naccache

_____ Examiner

Dr. John Oh

_____ Examiner

Dr. Cameron Skinner

_____ Supervisor

Dr. Dajana Vuckovic

Approved by:

_____

Dr. Peter Pawelek, Graduate Program Director

_____

Dr. André Roy, Dean of Faculty

Date: March 21, 2019

Abstract

Metabolomics is the comprehensive analytical study of the metabolome, which is composed of all of the low molecular weight (≤1500 Da) species in a biological system. Chromatographic separation of samples is implemented before detection by mass spectrometry to increase metabolome coverage. To ensure coverage of as many metabolites as possible, from hydrophobic to hydrophilic, both reversed phase liquid chromatography (RPLC) and hydrophilic interaction liquid chromatography (HILIC) are used. A variety of stationary phases are available for HILIC and can be grouped into three categories: neutral, charged, and zwitterionic. Each stationary phase varies by relative hydrophobicity, hydrogen bonding ability, and electrostatic interaction capabilities. There is currently no consensus in the literature on which of the available HILIC stationary phases provides the best results for global metabolomics applications. The first objective of this study was to compare a sulfobetaine zwitterionic ZIC-HILIC stationary phase to a charged underivatized silica HILIC stationary phase, specifically the Ascentis Si Express. The effects of salt concentration in the mobile phase and the mobile phase gradient were both investigated. The quality of peak shapes, analyte retention time, peak separation, and metabolite coverage were used to compare the results from each stationary phase. The methods were evaluated using a mixture of 37 standards covering a range of logP values (-10 to 3.73), molecular weights (59 to 776 Da), and metabolite classes. Good quality results for 7 and 14 of the metabolite standards were achieved using the silica and ZIC-HILIC columns, respectively. 14 and 2 of the standards could not be detected at all on the two phases respectively. Phospholipids, separated by HILIC based on the polarity of their head group, regardless of fatty acyl chain length or degree of saturation, can cause ion suppression. Lipid standards were analyzed to determine their retention times for both HILIC methods, aiding the interpretation of plasma analysis results. The developed methods were further compared using a complex biological sample: methanol-precipitated plasma. Metabolome coverage was greater with the silica column (3520 and 2734 compounds in positive and negative ESI respectively) compared to the ZIC-HILIC column (1612 and 1643 respectively), however peak quality and retention time reproducibility was greater with the ZIC-HILIC column. Thus, it is possible that automated data processing may overestimate the number of metabolite peaks in silica HILIC due to wider peaks and more variability in retention times. Finally, the addition of 10 mM ammonium phosphate to samples was evaluated and determined to improve the peak shape quality for standards in solvent, however no similar improvement was observed for plasma samples. The second objective of this study was to develop a dispersive solid-phase microextraction (D-SPME) protocol for global metabolomics of human plasma. Solid phase microextraction is a non-exhaustive, equilibrium-based extraction technique governed by the partitioning of analytes between the sample matrix and

sorbent material. Advantages of the technique include decreased ionization suppression, decreased solvent consumption, the capability to measure free metabolite concentrations, and the large variety of sorbent materials available. Each sorbent material comes with different extraction efficiencies and selectivities. To evaluate the use of carbon nanopearls (CNPs) for D-SPME, the effect of extraction time, sorbent volume, desorption solvent, desorption solvent volume, extraction temperature and desorption temperature was evaluated in detail. Extraction time experiments indicated that short extraction times, 2 minutes in the case of standards in buffer, can be used since equilibrium appears to have been reached. The evaluation of different desorption solvents is important because the choice of desorption solvent can influence not only which compounds are detected but also the concentration of these compounds in the desorbed sample. Acetonitrile was determined to provide the greatest desorption efficiency. The extraction of metabolite standards indicated that those with greater hydrophobicity, for example diosmin and diosmetin, and those with iodine atoms in their structure, for example thyroxine and triiodothyronine, have larger distribution coefficients however further investigation of the selectivity of CNPs is required. In conclusion, both chromatographic separation and sample preparation play a role in improving metabolome coverage. HILIC remains a promising tool for the separation of the polar metabolome prior to MS although further understanding of retention mechanisms is required, and SPME is a promising tool for improving the detection of novel, possibly low abundance metabolites not detected using less selective methods such as solvent precipitation.

Acknowledgements

Firstly, I would like to thank my supervisor, Dr. Dajana Vuckovic, for believing in my potential and providing me with the opportunity to grow as a scientist and researcher. Your dedication and enthusiasm are an inspiration. It has been my absolute pleasure to learn from you.

Secondly, I would like to acknowledge the input of my thesis supervisory committee members: Dr. Cameron Skinner and Dr. John Oh. Your questions and suggestions helped to broaden my perspective, allowing me to view my research in a new light.

Thirdly, I would like to thank my lab mates: Dmitri Sitnikov, Irina Slobodchikova, Cian Monnin, Mariana Russo, Alexander Napylov, Ankita Gupta, Shama Naz, Oluwatosin Kuteyi, and Abeer Malkawi. Your friendship means the world to me.

And last, but definitely not least, thank you to my parents, Meg and Fred, and my sister, Olivia, for their unconditional love, constant support, and for always believing in me. I love you more than words can express.

Contribution of Authors

Chapter 2

This chapter entitled “A Comparison of an Underivatized Silica and Zwitterionic Sulfobetaine HILIC Stationary Phases for Global Metabolomics of Human Plasma” authored by Rosalynde Sonnenberg and Dajana Vuckovic is the first draft of a manuscript in preparation that will be submitted for publication in summer 2019.

R. S. and D. V. designed all experiments and interpreted results. All experiments were executed by R. S.and she wrote the first draft of the manuscript.

All authors will review and revise the manuscript prior to final submission for publication.

Chapter 3

This chapter entitled “Evaluation of Carbon Nanopearls as Dispersive Solid-phase Microextraction Sorbent for Global Metabolomics of Human Plasma” authored by Rosalynde Sonnenberg, Oluwatosin Kuteyi, and Dajana Vuckovic is the first draft of a manuscript in preparation that will be submitted for publication in Fall 2019.

R. S. and D. V. designed all experiments and interpreted results. All experiments were executed by R.S. and she wrote the first draft of the manuscript. R.S. performed all targeted data processing of metabolite standards. R.S. and O.K. performed all data processing and manual curation of the data for global metabolomics.

All authors will review and revise the final manuscript prior to final submission for publication.

Table of Contents

List of Figures

List of Tables

List of Equations

List of Abbreviations

a	Area of each peak slice
ACN	Acetonitrile
ADP	Adenosine diphosphate
AJS	Agilent Jet Steam
AMP	Adenosine monophosphate
ATP	Adenosine triphosphate
CEM	Chain ejection model
CE-MS	Capillary electrophoresis-mass spectrometry
CNPs	Carbon nanopearls
C_o	Analyte concentration in the sample
CRM	Charged residue model
CSF	Cerebrospinal fluid
DC	Direct current
D-SPME	Dispersive solid-phase microextraction
EIC	Extracted ion chromatogram
ESI	Electrospray ionization
GABA	Gamma-aminobutyric acid
GC-MS	Gas chromatography-mass spectrometry
H	Height of the peak
HBA	Hydrogen bond acceptor
HBD	Hydrogen bond donor
H_f	Height of the front inflection point
HILIC	Hydrophilic interaction liquid chromatography
HMDB	Human Metabolome Database
HPLC	High-performance liquid chromatography
H_r	Height of the rear inflection point
HRTEM	High resolution transmission electron microscopy
IC	Ion chromatography
IEM	Ion evaporation model
IM	Ion mobility
IPA	Isopropanol
k’	Capacity factor
K_{fs}	Distribution coefficient between the fiber coating and sample matrix
LC-MS	Liquid chromatography-mass spectrometry
LLE	Liquid-liquid extraction
logP	Logarithm of partition coefficient
LPE	Lyso phosphatidylethanolamine
LPS	Lyso phosphatidylserine
MCP	Microchannel plates
MeOH	Methanol
MTBE	Methyl tert-butyl ether
MWCNTs	Multi walled carbon nanotubes
n	Mass of analyte extracted
nLC-nESI	Nano liquid chromatography-nano electrospray ionization
NMR	Nuclear magnetic resonance
NPLC	Normal phase liquid chromatography

PA	Phosphatidic acid
PBS	Phosphate buffered saline
PC	Phosphatidylcholine
PE	Phosphatidylethanolamine
PG	Phosphatidylglycerol
PI	Phosphatidylinositol
PP	Protein precipitation
PS	Phosphatidylserine
Q-TOF	Quadrupole-time-of-flight
RCF	Relative centrifugal force
RF	Radio frequency
RPLC	Reversed phase liquid chromatography
RPLC-MS	Reversed phase liquid chromatography-mass spectrometry
RSD	Relative standard deviation
SA	Surface area
SEM	Scanning electron microscope
SPE	Solid-phase extraction
SPME	Solid-phase microextraction
SWCNTs	Single walled carbon nanotubes
t	Time of each peak slice
t_R	Retention time
TOF	Time-of-flight
UHPLC	Ultra high-performance liquid chromatography
V_f	Volume of the fiber coating
V_s	Volume of sample
β-NAD	Nicotinamide adenine dinucleotide

Chapter 1: Introduction

1.1 Metabolomics

Metabolites are low molecular weight (<1500 Da) compounds produced as the intermediate or end products of metabolic, enzymatic reactions.[1] The variety and concentration of metabolites in a biological system at any given time are influenced by biological and environmental factors, making them an invaluable source of information on an organism's biological activity.[1] Altogether, all metabolites in a biological system are referred to as the metabolome. The metabolome of a biological system is the most predictive of its phenotype compared against the proteome, transcriptome, and genome and may provide a link between the genotype of an organism and its expressed phenotype.[2] As of 2018, the Human Metabolome Database (HMDB) contains information on 114,100 human metabolites.[3]

Metabolomics is the study of the metabolome and can be subdivided into two key approaches; untargeted, or global, and targeted. Targeted studies aim to prove or disprove a predetermined hypothesis by looking at a metabolite class or specific group of metabolites in a given pathway.[4] Such studies are ideally carried out with high accuracy and precision, obeying clinical laboratory standards as set out by regulating bodies such as the Food and Drug Administration in the U.S. or Health Canada, however this is not the case for all developed methods.[1,4] Untargeted metabolomics is hypothesis-generating and aims to look at the entire metabolome.[2] All of the detectable metabolites are studied in an attempt to determine which metabolites differ between groups of samples in a semi-quantitative way to generate a metabolic hypothesis.[4]

Global metabolomics faces a multitude of challenges including a large variety of chemical structures, a large range of biological concentrations spanning multiple orders of magnitude, and a large range of solubilities and polarities.[2,5,6] This physico-chemical diversity makes non-selective sample preparation and comprehensive chromatographic separation by one method impossible. In addition to these biological and chemical factors, the number of metabolites and which metabolites are detectable is also affected by the sample type, sample collection, sample preparation method, separation parameters, and detection instrumentation.[2,4,5] The most common instrumentation used in global metabolomics is liquid chromatography-mass spectrometry (LC-MS) although separation can also be achieved using gas chromatography or capillary electrophoresis.[2,5] Liquid chromatography-mass spectrometry is preferred over direct infusion into the MS in global studies since chromatographic separation improves the selectivity of the analysis, improves the coverage of the metabolome, and can be done using soft ionization (electrospray ionization, ESI) which produces intact gas phase molecular ions to aid in the

identification efforts.[2,5] Ion mobility (IM) provides gas-phase size-based separation complementary to the polarity separation of reversed phase liquid chromatography (RPLC)/hydrophilic interaction liquid chromatography (HILIC) and mass separation of MS, so it can be added to LC-MS analysis as LC-IM-MS to aid in separation of isomers and isobars.[2] In addition to MS, detection can also be achieved by nuclear magnetic resonance (NMR). Nuclear magnetic resonance is advantageous for its simple sample preparation, short analysis time, and high reproducibility.[1,7] It provides quantitative and structural data and can be used to analyze intact tissue samples for high abundance metabolites using magic angle spinning.[1,4] Unfortunately, NMR is not highly sensitive, does not provide adequate metabolome coverage, detecting less than 100 metabolites in a sample due to its poor limits of detection, and can suffer from chemical shift overlap which can make distinguishing between specific metabolites within a class, for example lipids, an extremely difficult if not impossible task.[8] This thesis will focus on how to enhance metabolite coverage in LC-MS global metabolomics, so these other analytical approaches will not be further discussed.

1.1.1 Workflow for Global Metabolomics

Untargeted metabolomics studies follow a general workflow shown in Figure 1.1. Initially, the design of the experiment must be established. This includes planning the type and number of samples, the study subjects, and the selection of analytical and statistical approaches to use during the study. The experimental design step is then followed by the collection and storage of samples, sample preparation, data acquisition, data processing and analysis, metabolite identification, and the biological interpretation of the final data set. Each step of the process comes with its own set of challenges, and consistency and appropriate selection of all steps across a study is crucial to the collection of high-quality data and reliable biological interpretation.[9] The critical steps of the workflow that are the most relevant to this thesis are discussed in more detail in subsequent sections.

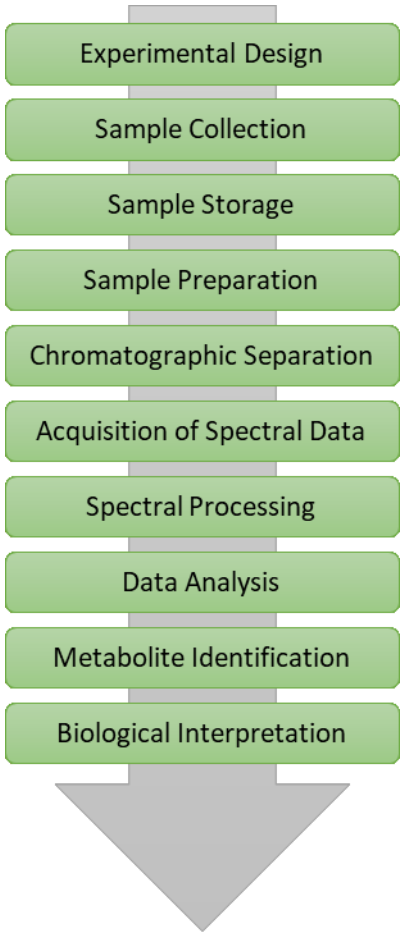

Figure 1.1 General workflow for global metabolomics study using LC-MS.

1.1.2 Sample Collection and Storage

Before samples can be collected, the type of sample appropriate to a specific study must be determined. The number and character of the metabolites detected will be partially dependent on the sample type chosen.[4] Preexisting knowledge about the system being studied from previous studies, databases, predictive models, and informatics resources can be used to determine what type of sample will provide the most relevant data.[6] The most common types of samples used in clinical studies are plasma and serum.[9] Both provide information on both the anabolic and catabolic processes occurring in the biological system.[6] Along with urine, which provides information on only the catabolic processes, these three sample types are advantageous as they provide information on the whole individual, are easily collected, and are readily available.[6] For studies where metabolites in the central nervous system are key, cerebrospinal fluid (CSF) is preferred, especially if the metabolites of interest are unable to cross the blood brain barrier.[6] Tissue samples can be used if spatial resolution is required, for example, to study the mechanism of action

of a drug in a specific location within the body.[6] Additional candidates for sample type of human origin include cells, tissues, amniotic fluid, breast milk, saliva, and exhaled breath.[2,6]

When designing metabolomics studies, it is crucial to limit the amount of variability between samples due to confounding variables, to decrease the chances of false interpretation of the data. The age, gender, physical activity, body mass index, environmental exposure and diet of an individual can all affect metabolome composition of the sample.[10] Additionally, sample types controlled by homeostasis like serum, tissue, or plasma present lower variability than biospecimens such as urine which can vary greatly depending on the physiology, and water/food intake of the individual as well as the volume of the sample.[6] The amount of time spent fasting pre-collection, the time of day, and the time of year when collection occurs can also affect the sample composition. For example, Townsend *et al.* looked at 166 metabolites in plasma and showed that both time of day and season affected the diet and amount of light exposure for an individual which in turn affected specific classes of metabolites, namely purines, pyrimidines, organic acids, bile acids, and water soluble vitamins.[10]

If opting to use a blood-derived biofluid, a choice must be made between serum and plasma. Serum is the fraction of the blood that remains when separation of the blood cells is undertaken after clotting occurs. Plasma is the fraction of blood that remains when separation of the blood cells is done in the presence of an anticoagulant in order to avoid clotting process. A survey of the literature showed that plasma is the most commonly employed blood-derived sample type for LC-MS metabolomics studies with serum coming in second.[11] Several studies have compared the two sample types.[9,12,13] All three studies observed higher metabolite concentrations in serum, possibly due to the removal of some proteins during coagulation and/or the release of cellular metabolites during coagulation.[9,12] If opting to work with plasma, a choice of anticoagulant must be made. Different anticoagulants as well as counter ions, and collection tubes can introduce interferences and cause matrix effects during analysis influencing the biological interpretation of the collected data.[4] In this thesis, human plasma with citrate anti-coagulant was used for all experiments.

1.1.3 Sample Preparation

The archetypal sample preparation method for global metabolomics must meet five criteria; be non-selective, reproducible, simple, quench the metabolome, and result in an LC-MS compatible sample with the same metabolite contents as the original sample. It is vital that these requirements are met in order to determine, as accurately as possible, the metabolome at the sampling time.[14] Any changes to the metabolome after collection decrease the quality of the data acquired and may influence the biological

interpretation of the acquired data.[14] Additionally, it is ideal if the preparation technique enriches the metabolites and removes interferences to improve the detection of low abundance metabolites.[6] Multiple sample preparation techniques have been applied to metabolomics. The advantages and disadvantages of these techniques are summarized in Table 1.1.

The most common sample preparation method in metabolomics, considered to be the gold standard, is protein precipitation (PP) by organic solvent.[15] This method provides high metabolite coverage and allows for the quantitation of the total metabolite concentration (free plus bound) by disrupting protein-metabolite binding. While this method is considered the best to date, it does not remove all of the protein from the samples. Between two and ten percent of the protein remains in the sample and can cause deterioration of high-performance liquid chromatography (HPLC) columns.[14] Additionally, some metabolites can be partially removed or lost in the protein pellet.[14]

Protein precipitation by organic solvent has been carried out using a variety of solvents or solvent mixtures. Want *et al.* tested four solvents and six solvent mixtures and determined that methanol (MeOH) provided the best coverage and most reproducible results for serum samples.[15] They also compared the solvent based methods to PP by heat or acid and concluded that they both improved the efficiency of protein removal, but at the cost of metabolome coverage. Michopoulos *et al.* compared MeOH and acetonitrile (ACN) as the organic solvent for PP of plasma samples and concluded that MeOH was preferable based on better repeatability.[16] Polson *et al.* compared the use of organic solvents, acids, salts, and metals for PP of plasma samples and concluded that ACN was the most effective for removing proteins.[17] Bruce *et al.* compared five concentrations of MeOH and ACN from 50-100%, concluding that 100% MeOH provided the best results, including improved recovery of the lipophilic metabolome.[18] A second study compared ACN, acetone, MeOH, ethanol, and various combinations of these solvents concluding that a MeOH-ethanol (1:1) mix or MeOH-ACN-acetone (1:1:1) mix were preferable for improved intra/inter-day precision and protein removal respectively.[19] In summary, the literature suggests that ACN and acetone are the most efficient solvents for protein removal while MeOH and ethanol provide improved method precision and metabolome coverage.[14] Currently, MeOH or MeOH-ethanol mixture is the most common choice of PP prior to LC-MS analysis with ACN as the second most common.[11] In addition to solvent choice, there is also no consensus in the literature with regards to the ratio of sample volume to solvent volume, with studies using 1:2[17,20], 1:3[16], and 1:4.[19,20] Minimal sufficient solvent volumes are preferable as increased solvent volume results in diluted samples, decreasing the number of detected metabolites or requiring the addition of a concentration step.[18,20] Evaporation

followed by reconstitution can be added to sample preparation procedures to pre-concentrate and to change the solvent composition of the sample to improve compatibility with the chromatographic method.[14] The choice of reconstitution solvent varies and can affect the metabolome coverage depending on the solubility of metabolites in the chosen solvent.

Dilute-and-shoot is the simplest sample preparation technique where the sample is simply diluted with water before analysis.[21] This technique is most commonly used for urine samples since no protein is removed from the sample, and urine protein content is sufficiently low to not affect the performance of the chromatographic column. In contrast, plasma and serum contain between 6 and 8 g/dL of protein which must be removed prior to LC separation.[22] As an alternative to protein precipitation, ultrafiltration separates analytes from the sample matrix by applying pressure or centrifuging a sample to push analytes below a selected molecular weight threshold through a filter, leaving behind larger molecules including proteins.[23]

Solid-phase extraction (SPE) and liquid-liquid extraction (LLE) are both exhaustive sample preparation techniques. In LLE, analytes partition from the liquid sample into an immiscible solvent which is then analyzed. In comparison, in SPE analytes adsorb and/or absorb onto a solid sorbent and are then eluted from the solid sorbent using solvent, or pH. (Adsorption is a surface phenomenon compared to absorption which is a bulk phenomenon where the analyte penetrates the sorbent.) The selectivity of the method is influenced by the physico-chemical and physical properties of the solid sorbent.[24] The extraction process may be affected by the sample matrix due to factors such as competition for binding sites and the adsorption of macromolecules such as proteins.[24] Alternatively, solid-phase microextraction (SPME) is a non-exhaustive equilibrium-based sample preparation technique. Like SPE, the analytes adsorb and/or absorb onto a solid sorbent, however only a fraction of the analyte present in the sample partitions onto the sorbent. The total amount in the desorbed sample can then be determined using the partition co-efficient for each analyte.[25] Like SPE, SPME can be affected by the sample matrix. The theory of SPME will be discussed in more detail in Section 1.3.

When choosing a sample preparation technique, it is important to account for the limitations of each method such as ion suppression, analyte loss from co-precipitation with proteins, solubility, selectivity, ability to determine free or total concentration as well as the goals of the study.[14] Different sample preparation methods can lead to significant changes in the recovery, coverage, and data quality obtained.[26,27]

Table 1.1 Advantages and disadvantages of sample preparation techniques in the context of global metabolomics

Technique	Advantages	Disadvantages	References
Dilute-and-Shoot	• Simple and high-throughput • Minimal loss of metabolites	• No protein removal • High matrix effects are possible	14,21,28,29
Protein Precipitation by Organic Solvent	• Removes protein improving LC column lifetime • Disrupts protein binding allowing the measurement of total (free & bound) metabolite concentration • Simple and high-throughput • Cold solvent quenches enzymatic alteration of metabolites	• Prone to ionization suppression • Low selectivity produces complex samples that can hinder detection of low abundance metabolites • Co-precipitation of hydrophobic metabolites can occur	16,17,19,30–34
Ultrafiltration	• Good coverage of polar metabolome • Enables measurement of the free metabolite concentration	• Poor coverage of hydrophobic metabolome • Prone to ionization suppression	31,33,35
SPE	• Enables measurement of either free or total metabolite concentration • Increased sample clean-up decreases matrix effects • Can pre-concentrate samples • Can be adapted to high throughput formats • A large variety of sorbent chemistries are available	• Increased selectivity decreases metabolome coverage • Increased cost per sample • Possible matrix effects	14,16,36–38
SPME	• Enables measurement of free metabolite concentration • Decreased ionization suppression compared to exhaustive techniques • A large variety of sorbent chemistries are available • Decreased solvent consumption • Can be used for *in vivo* sampling and aid the detection of short-lived metabolites	• Lower sensitivity than exhaustive methods[39] • Lower metabolome coverage compared to solvent-extraction methods	33,39–43
LLE	• Good coverage of polar and non-polar metabolome with analysis of both the organic and aqueous phases • Simple	• High solvent consumption • More selective than solvent precipitation • Possible formation of an emulsion and splitting of metabolites between both phases can impact repeatability	32,35,44–46

1.1.4 Liquid Chromatography – Mass Spectrometry

1.1.4.1 Liquid Chromatography

High-performance liquid chromatography is used to separate samples before detection by MS to decrease ion suppression, increase sensitivity, increase selectivity, and increase data content.[2,4] The inclusion of a separation step decreases sample throughput by increasing total analysis time by several minutes to hours but is crucial when dealing with complex matrices like blood which can contain an average of three isomers for each monoisotopic mass[2] and in some cases many more. For example, a search of the METLIN[47] database for the molecular formula $C_9H_{11}NO_2$ returns 440 entries including the amino acid phenylalanine. Both HPLC[48] and ultra high-performance liquid chromatography (UHPLC)[27,49,50] have been used in metabolomics analyses. Ultra high-performance liquid chromatography uses smaller particle sizes (<2 µm) to increase chromatographic resolution, decrease analysis time, and increase peak capacity compared to HPLC but requires higher pressure.[51–53] Since becoming commercially available in 2004, UHPLC has become the preferred LC method over HPLC for metabolomics studies.[52]

Due to the wide physico-chemical character of metabolites, as illustrated by the logP distribution of blood metabolites in the HMDB shown in Figure 1.2, there is not one single chromatographic method capable of retaining the entire metabolome.[4] A combination of RPLC to separate non-polar metabolites and HILIC to separate polar metabolites is commonly used.[54,55] The most widely used RPLC stationary phase is octadecyl on a silica support, commonly referred to as C18. It is versatile, effectively retains hydrophobic compounds, and allows for the use of straightforward mobile phase compositions (namely ACN, MeOH, and water) and low concentrations of mobile phase additives, maintaining ESI compatibility.[4] Other RPLC stationary phases include, but are not limited to pentafluorophenyl[56], biphenyl[57], phenyl-hexyl[58], C4[59], and C8[60]. Each stationary phase has different retention characteristics providing for different selectivities in the separation of different classes of analytes. A biphenyl stationary phase, with trimethylsilyl endcapped core-shell silica particles, was used in this work for the analysis of aromatic metabolites. The stationary phase structure of the biphenyl column is shown in Figure 1.3. The ability to participate in π-π interactions with aromatic or conjugated analytes results in increased retention times and better separations of aromatic compounds. Biphenyl columns have been used to separate targeted groups of metabolites such as steroid hormones[61,62], thyroid hormones[57], and drugs/drug metabolites[63–65] since the large majority of these compounds have aromatic structures. Multiple studies[61,66] reported that the biphenyl stationary phase was able to separate isobaric analytes that were poorly resolved by other RPLC stationary phases, such as the C18.

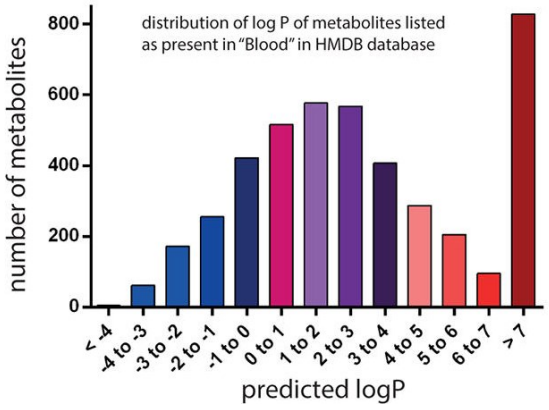

Figure 1.2 The distribution of predicted logP values for blood metabolites included in the HMDB as reported by Lindahl *et al*. Figure reproduced from reference[67] under ACS Author's Choice open access license for non-commercial use.

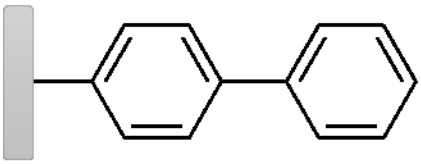

Figure 1.3 Biphenyl RPLC stationary phase chemistry.

Regrettably, hydrophilic compounds (logP approximately 1 or lower) in a sample elute in the solvent front when utilizing RPLC. This means that hydrophilic metabolites will undergo the greatest degree of interference and the greatest amount of ion suppression. Being able to detect and quantitate polar metabolites is key in metabolomics considering that many of the metabolites involved in important metabolic processes, for example amino acids, are polar.[4] To detect the polar portion of the metabolome, HILIC is used. A hydrophilic stationary phase and ACN/water mobile phase separates analytes by a combination of three retention mechanisms: liquid-liquid partitioning, electrostatic interactions, and hydrogen bonding.[68] The high organic content used for HILIC mobile phase is advantageous for its impact on ionization efficiency through quick desolvation of the droplets in the ESI source.[68,69] Unlike for RPLC, there is not one HILIC stationary phase that demonstrates the same versatility as C18. In conclusion, most global metabolomic analyses use both HILIC and RPLC separations to ensure as comprehensive metabolite coverage as possible. The details of HILIC will be discussed in depth in Section 1.2.

1.1.4.2 Electrospray Ionization: Matrix Effects and Ion Suppression

Electrospray ionization was initially introduced by Malcolm Dole in 1968[70] but was not used in conjunction with MS until 1984.[71,72] The coupling of an ESI source to a mass spectrometer by Yamashita and Fenn in

1984 allowed for the introduction of liquid samples, including from liquid chromatography systems, which revolutionized the use of MS and won Fenn the 2002 Nobel Prize in Chemistry.[73–75]

Electrospray ionization, a gentle ionization technique, converts samples solubilized in volatile, polar solvents into gas-phase ions. The sample is introduced into a needle that carries a high potential; either positive or negative depending on the ESI mode being implemented. The large electrical potential field between the needle and the nozzle, where the sample enters the mass analyzer, produces a Taylor Cone, as shown in Figure 1.4, and droplets of the liquid sample are expelled.[73] The newly formed droplets evaporate, with the aid of warmed nitrogen gas, by one of three proposed models: the charged residue model (CRM), the ion evaporation model (IEM), or the chain ejection model (CEM).[73,74,76] Which model occurs is dependent on the nature of the analyte, so that low molecular weight analytes are most likely to undergo IEM, globular analytes such as proteins are most likely to undergo CRM, and polymers are most likely to undergo CEM.[76] The ion evaporation model is the most applicable to metabolites, where solvated analyte ions are ejected from larger charged droplets. Any co-ejected solvent evaporates, eventually leaving a gas-phase analyte ion.[76] The newly formed gaseous ions then travel, propelled by the electrical field, from the atmospheric pressure of the ESI source to an intermediate vacuum region (7 to 14 torr), and then to the high vacuum region (1 to 3 torr) of the mass analyzer.[73,77]

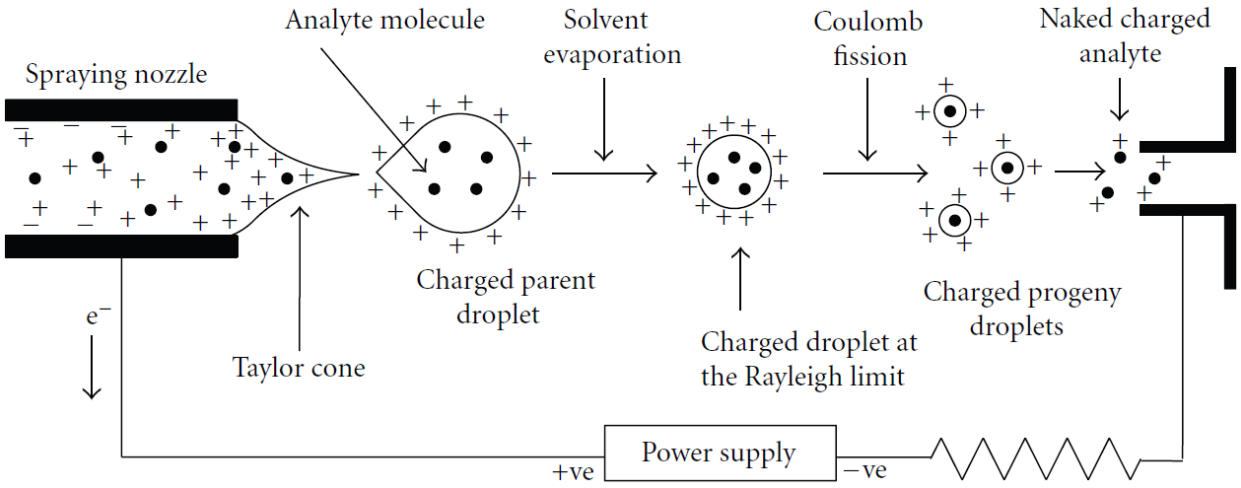

Figure 1.4 Schematic of an ESI source showing the ionization process in positive mode. Parent droplets, ejected from the Taylor Cone, evaporate until the repulsion between like charges in the droplet overcomes the droplet surface tension. This is known as the Rayleigh Limit. Coulomb fission occurs, splitting the parent droplet into multiple smaller droplets. The solvent in these droplets evaporates to produce gas phase ions. Figure reproduced from reference[78] under the Creative Commons Attribution License.

Key disadvantages of ESI are its incompatibility with non-polar solvents, which in turn prevents coupling with normal phase liquid chromatography (NPLC), its incompatibility with the use of non-volatile salts, plasticizers, detergents and ion pairing reagents, and signal suppression, a form of matrix effect.[73,74] Matrix effects are any influence the matrix components or co-eluting analytes of interest have on the quantitation of the analyte(s) of interest.[79]

Ionization suppression/enhancement is a common form of matrix effect when working with LC-ESI-MS. When the analyte of interest co-elutes with other matrix components, the ionization efficiency of the analyte can be affected. A combination of factors can contribute to ion suppression including the physical and chemical properties of the analyte and matrix components, the ratio of matrix component to analyte, the sample preparation technique which partially dictates the amount and type of matrix components in the analyzed sample, the chromatographic separation, and the ESI conditions used.[80] Ion suppression can vary between samples, is analyte dependent, impacted by the concentration, pKa, shape and size of the analyte as well as the sample/solvent pH, surface activity, and the presence of electrolytes.[74,80] Multiple possible mechanisms for ion suppression exist including competition for the limited amount of excess charge on the droplet surface, incomplete evaporation of the droplets, ion pairing with the analyte, gas-phase reactions, and charge neutralization.[79] These mechanisms are depicted in Figure 1.5. The ionization matrix effects for a given analyte can be calculated by Equation 1.1 where a value over 100% indicates signal enhancement and a value under 100% indicates signal suppression.[81] Within the range of 80% to 120% there is considered to be no significant matrix effects. Ion suppression can be addressed by altering the sample preparation method, to try and remove matrix components, altering the chromatographic conditions, to prevent co-elution of the analyte and matrix components, and by altering the MS parameters.[80] Ion suppression is especially problematic in metabolomics when attempting to detect low concentration metabolites that co-elute with high concentration metabolites or other matrix components, and when trying to quantitate metabolites.[82,83]

Equation 1.1 Analyte specific ionization matrix effects

$$Matrix\ Effect\ (\%) = \frac{Area_{Analyte\ spiked\ into\ matrix\ post\ extraction}}{Area_{Analyte\ in\ solvent}} \times 100$$

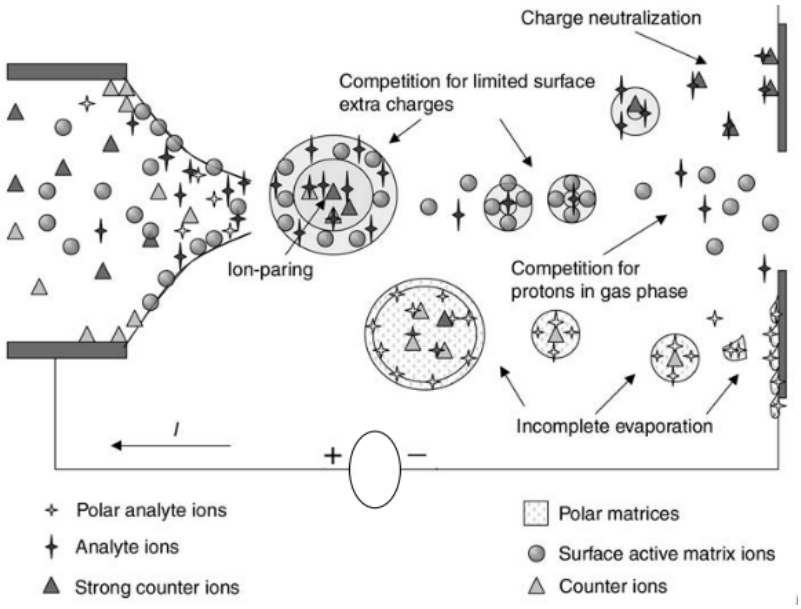

Figure 1.5 Mechanisms of ionization suppression in ESI including competition over a limited amount of droplet surface charge, incomplete solvent evaporation, ion pairing between strong acids and basic analytes, competition between gas phase matrix components and analytes over protons, and charge neutralization. Figure reproduced from reference[79] with permission from Taylor & Francis Group LLC.

1.1.4.3 Mass Spectrometry

Mass analyzers separate ions according to their mass-to-charge ratio (m/z) using the application of electromagnetic forces, or based on the kinetic energy and therefore velocity of the ions.[73] There are a large variety of mass analyzer technologies available, including but not limited to quadrupoles, time-of-flight (TOF), and Orbitrap instruments. Multiple mass analyzers can be coupled to each other to allow for tandem MS analyses.[73] When doing untargeted metabolomics of complex biological samples, high resolution mass analyzers such as the quadrupole-time-of-flight (Q-TOF) or Orbitrap are preferred for their ability to differentiate between metabolites with very close exact masses[84], allowing for the detection of more compounds[85], aiding metabolite identification, and facilitating increased accuracy in quantitation.[5] The faster acquisition rate of TOF mass analyzers, compared to the Orbitrap, allows for the collection of more data points over time facilitating hyphenation with UHPLC systems which produce narrower elution profiles. Since a Q-TOF instrument was used in this work, only these two types of mass analyzers will be discussed in depth.

The quadrupole mass analyzer consists of four rods, positioned parallel to each other and equal distance from each adjacent rod. Each pair, positioned opposite to one another, is connected electrically, with a

potential applied that is equal, yet oppositely charged to the other pair.[73] The application of alternating direct current (DC) and radio frequency (RF) potentials creates an electric field that oscillates, allowing only ions in a small m/z range to pass through, parallel with the rods, while all other ions collide with the rods, never reaching the detector.[73,74] By alternating the DC and RF potentials, yet keeping the ratio between the two constant, different m/z ions can pass through the mass analyzer, and a mass spectrum can be obtained.[73,74] Quadrupole mass analyzers are most commonly used with unit mass resolution because as the resolution of the mass analyzer is increased, the sensitivity drops.[73] The sensitivity of a quadrupole mass analyzer can be improved by using a smaller range of m/z values or by implementing selected ion monitoring, where only the ion abundances for specific m/z values are obtained.[86] Alternatively, applying RF only can be used to allow all ions to pass through the quadrupole towards a second mass analyzer, for example a TOF, when tandem MS is not required. Typically, MS mode is utilized for metabolomics studies with tandem MS being used in follow up analysis of metabolites of interest.

A TOF mass analyzer separates ions according to the duration of time they require to travel through the flight tube and impact the detector. An electric field is applied that accelerates ions down the field-free flight tube. Ions of the same charge carry the same kinetic energy, and ions with lower mass travel at a greater speed and reach the detector more quickly than ions of greater mass.[73,87] A time spectrum is produced and converted into a mass spectrum using time-of-flight data from calibrants with known masses.[73,74]

The resolving power, R, or resolution of a MS is an indicator of its ability to distinguish between two spectral peaks with similar m/z values. The smaller the m/z difference that is distinguishable, the greater the resolving power of the instrument. The resolving power of an instrument for a given m/z, R, can be calculated using Equation 1.2 where Δm is the difference in m/z between the two peaks.[73] The resolution of a TOF mass analyzer is affected by the range of velocities of ions at the start of the flight tube, and the time-resolving capability of the detector.[73,74]

Equation 1.2 Resolving power of a mass spectrometer for a given m/z

$$R = \frac{m}{\Delta m}$$

Not all ions of a given mass will have the same initial velocity, with accelerated ions travelling in different directions, which decreases the resolution.[88] This effect can be counteracted with the use of an electrostatic mirror or reflectron as was first proposed in 1973 by Mamyrin *et al.*[88] The Reflectron uses an electric field that repels the incoming ions, decreasing their velocity, and then re-accelerates them

towards the detector.[73,74] Since ions that were initially traveling at a greater velocity reside within the electrostatic mirror for longer time, the slower moving ions are allowed to catch up and the range of velocities for a given ion mass is decreased, improving the resolution.[73,74] This effect is independent of mass, making it simple to implement for a large m/z range of ions. Multiple electrostatic mirrors can be implemented in series to further improve the mass resolution of the instrument, however as the mass resolution improves the sensitivity of the instrument decreases.[73] Time-of-flight mass analyzers are capable of achieving resolution of up to 40,000.[89]

Orthogonal acceleration time-of-flight mass analyzers (Figure 1.6) direct ions into a flight tube that is perpendicular to the direction of ion flow from the ion source. By increasing the electric potential and accelerating the ions into the flight tube in bursts, this instrumental setup allows the pairing of continuous ion sources, such as ESI, with a TOF mass analyzer.[73] Each burst of ions that travels down the flight tube is in this way provided with a known start time, allowing its flight time to the detector to be calculated.[74]

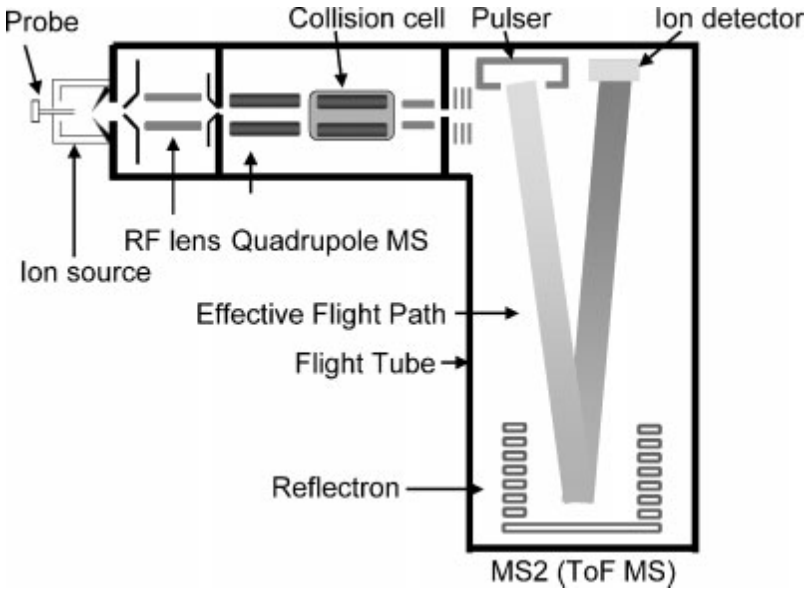

Figure 1.6 Schematic of quadrupole-orthogonal acceleration time-of-flight mass spectrometer. Liquid samples introduced into the ion source undergo ESI (Figure 1.4) producing gas phase ions which travel through the quadrupole mass analyzer, directed by an RF field, to enter the TOF mass analyzer. The ions are accelerated along the flight tube and enter the Reflectron where ions of the same mass but different velocity are focused and then accelerated towards the detector where the energy of their impact is converted into current and recorded by a computer.[90,91] Figure reproduced from reference[90] with permission from John Wiley and Sons.

The final major component of a mass spectrometer is the detector. Detectors are responsible for converting the impact energy of the arriving ion into electrical current which can be recorded by a computer.[73] Microchannel plates (MCP) are a collection of parallel continuous dynode electron multipliers that release as many as 10^4 electrons with each impact, amplifying the signal and improving the detection of ions present in low numbers.[73] The inside of each channel acts as a semiconductor, typically made of leaded glass or coated in beryllium, that releases electrons when impacted by an ion or electron.[73,74] Multiple MCP detectors can be combined in series to further increase gains.[73]

1.1.5 Data Processing

After LC-MS analysis, the collected data must be processed. Global processing involves chromatogram alignment, peak picking, subtraction of peaks also detected in the extraction blank, a comparison of signal intensities for each peak between sample groups using statistical analyses, and finally the identification of analytes determined to be of possible interest. Putative identification of these analytes is carried out using the determined accurate mass, product ion mass spectrum and metabolite databases, followed by a comparison of retention time and product ion mass spectrum with an authentic standard for confirmation.

1.1.6 Approaches for Improving Metabolite Coverage in Metabolomics

The discovery of a biological perturbation specific to a single physiological condition can be challenging given the interconnected nature of biological pathways within a biological system and that many metabolites are involved in more than a single pathway. For example, adenosine triphosphate is involved in glycolysis, the citric acid cycle, and fatty acid synthesis to name a few.[92] This means that altered levels of these metabolites are not good biomarker candidates as they cannot be linked to a single cause. In a biomarker search conducted by Lindahl *et al.*, 178 possible biomarkers were found in serum samples using RPLC-MS for non-Hodgkin lymphoma, congestive heart failure, or community acquired pneumonia by comparison with a control group.[93] They determined, by comparison, that 61% of these candidates were detected for more than one of the conditions studied and a literature search associated the remaining 39% with other diseases.[93] The lack of any perturbed metabolites unique to a single condition demonstrates the need for greater metabolome coverage in order to identify possible biomarkers or groups of biomarkers for a single biological condition or environmental exposure.

The metabolome coverage achieved in a study can be affected by any of the steps in the workflow presented in Figure 1.1. As previously discussed in 1.1.2, sample type selection can influence the number and type of metabolites detected by an untargeted metabolomics study. The combination of data from

multiple sample types from a single subject, for example plasma and urine, can improve metabolite coverage by detecting metabolites unique to each matrix.[94] The choice of sample preparation technique and exact extraction parameters can also impact metabolite coverage. For example, protein precipitation by organic solvent is a very common sample preparation technique in metabolomics. The choice of organic solvent to use for PP[15,19,95] and the choice of reconstitution solvent for the sample, post drying, will both impact the observed metabolite coverage.[67] Furthermore, Yang *et al.* showed that using multiple sample preparation techniques in series can help improve metabolite coverage by comparing MeOH PP to MeOH PP combined with methyl tert-butyl ether (MTBE) LLE and MeOH PP combined with MTBE LLE, MTBE extraction of the protein pellet, and SPE fractionation.[95] The final method produced five fractions containing enriched levels of different metabolite classes that were analyzed using either one or both of RPLC and HILIC coupled to MS. By combining the results of all five fractions, 3806 metabolites were detected compared to the 1851 detected using MeOH PP alone. The use of more complex sample preparation techniques, although characterized by decreased ion suppression, improved chromatographic separation and resolution, and longer column lifetime due to cleaner samples, also has disadvantages, such as increased sample preparation time, increased analysis time, and possible analyte loss.[95]

The type of analysis, both separation and detection, can also affect the metabolite coverage. LC-MS, GC-MS, capillary electrophoresis-mass spectrometry, supercritical fluid chromatography-mass spectrometry, and NMR can all be used. The use of multiple orthogonal separation techniques, which operate on differing separation mechanisms, can provide complementary data for a single sample.[94] This however can increase analysis time significantly. Additionally, global metabolomics workflows are, by default, better able to measure high abundance metabolites and metabolites that ionize efficiently in MS sources. Since many important metabolites are present endogenously at low concentrations, they are not detected.[8] Nano liquid chromatography-nano electrospray ionization (nLC-nESI) offers another alternative to traditional LC-ESI-MS. With increased sensitivity, nLC-nESI can allow for the detection and quantification of more low abundance metabolites.[96] Tugizimana *et al.* showed that optimizing ESI parameters to improve ionization efficiency can improve metabolome coverage.[97] Given that nanoelectrospray increases ionization efficiency, improvements should be observed for all analytes. Ionization behaviour and detection limits can also be improved with the implementation of chemical isotope labelling. For example, Li and colleagues have developed a series of derivatization methods to improve the analysis of phenol[98], organic acid[44], hydroxyl[99], and carbonyl[100] sub-metabolomes.

With many options for improving metabolome coverage, the key is to select one, or a combination, of approaches that maximize improvement while minimizing analysis time. With a 184% increase in metabolites included in the HMDB 4.0 compared to version 3.0 but only a 11% increase in metabolites that have actually been quantified, there is a clear need to advance the detection and quantitation of an increased number of metabolites.[3]

1.2 Hydrophilic Interaction Liquid Chromatography

Hydrophilic interaction chromatography (HILIC) was first utilized in 1975 by Linden *et al.* to separate saccharides.[101] This first foray utilized a hydrophilic amino silica stationary phase and an ACN and water gradient to separate sugars in samples collected during the refining of sugar beets.[101] In 1990, the name HILIC was proposed for this new chromatography technique that utilizes a hydrophilic stationary phase and a comparatively hydrophobic, highly organic mobile phase to separate both small and large molecules belonging to classes such as peptides, amino acids, sugars, and organic acids and bases.[68,102] Hydrophilic interaction liquid chromatography is complementary to RPLC and can be described as a combination of three common liquid chromatography techniques taking its adsorbent stationary phase from NPLC, mobile phase from RPLC, and its analytes from ion chromatography (IC).[68,69]

1.2.1 Retention Mechanism

The retention mechanism in HILIC is not completely understood to date. The prevailing theory states that HILIC retention is governed by three different mechanisms. In decreasing order of influence they are the water layer, electrostatic interactions, and hydrogen bonding.[68] The level of contribution for each mechanism is dependent on the type of stationary phase, mobile phase conditions, and the physical characteristics of the analyte.[69]

1.2.1.1 Water Layer

A water layer is formed on the surface of the polar stationary phase from the water content in the mobile phase. A minimum of 2% water in the mobile phase is required. This forms a liquid-liquid separation system and analytes partition into the water layer to varying degrees based on their polarity. As the water content in the mobile phase is increased and the difference in polarity between the water layer and the bulk decreases, the analytes leave the water layer in favour of the high organic bulk in order from least to most polar and are eluted.[68] Figure 1.7 demonstrates the retention of analytes by the water layer mechanism.

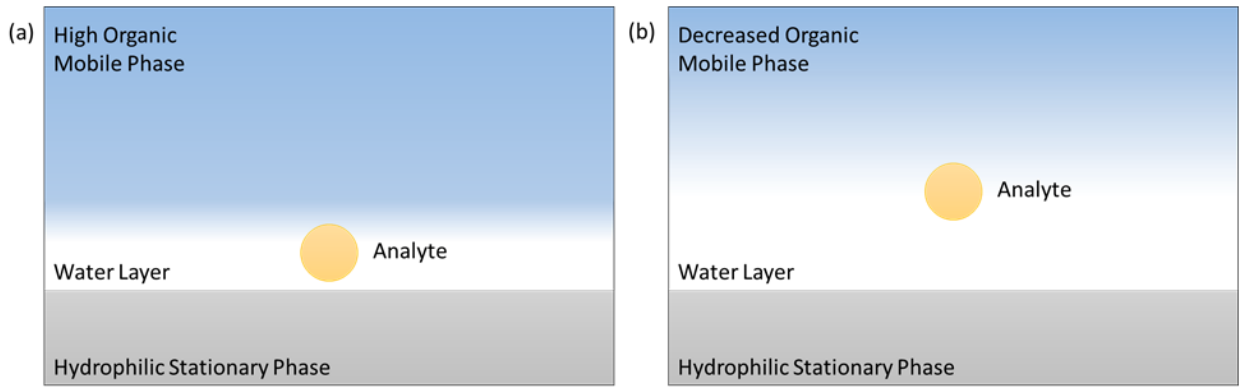

Figure 1.7 The water layer retention mechanism. (a) Water from the mobile phase adsorbs onto the surface of the stationary phase forming a liquid-liquid partition system that retains polar analytes. (b) As the water content of the mobile phase increases, the water layer grows until the difference in polarity between the water layer and the bulk mobile phase decreases and the retained analyte is eluted.[68]

1.2.1.2 Electrostatic Interactions

Electrostatic interactions between the charged or zwitterionic stationary phase and analyte increase or decrease the retention time of charged analytes depending on the nature of the interaction: attractive or repulsive, respectively. Electrostatic interactions have the greatest effect while the water layer is thin, providing easier access to the stationary phase for analyte interactions. Figure 1.8 (a) demonstrates the retention of analytes by the electrostatic interaction mechanism. Depending on the location of the charge on the analyte in reference to the stationary phase, hydrophilic interactions in the water layer can still retain analytes that undergo electrostatic repulsion.[68] This concept is shown in Figure 1.8 (b).

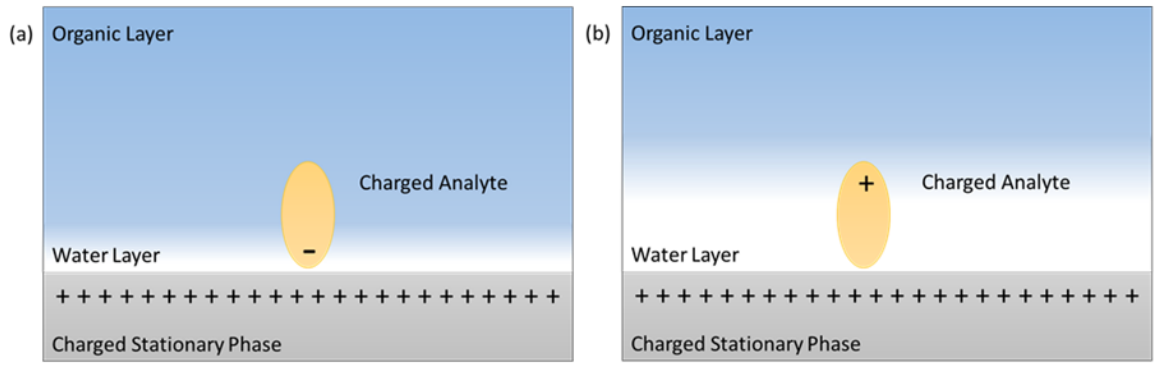

Figure 1.8 (a) Analytes carrying a charge opposite to the stationary phase can be retained through electrostatic interactions (b) Analytes repulsed by the stationary phase by electrostatic interactions can still be retained by the water layer if the charged portion of the analyte is oriented away from the stationary phase. [68]

1.2.1.3 Hydrogen Bonding

Hydrogen bonding can occur between the stationary phase and the analyte if a stationary phase with hydrogen bond donor or acceptor capability is used. Hydrogen bonding between the stationary phase and the analytes increases the retention time and is most influential for neutral analytes which are not involved in electrostatic interactions.[68] Figure 1.9 demonstrates the retention of analytes by the hydrogen bonding mechanism.

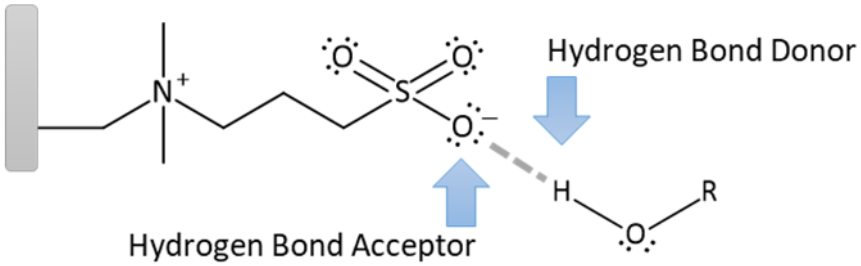

Figure 1.9 Hydrogen bonding retention mechanism for the hydrogen bond acceptor, zwitterionic sulfobetaine stationary phase.[68]

1.2.2 Stationary Phases

Hydrophilic interaction liquid chromatography stationary phases have polar, hydrophilic chemistries that can be classified as: neutral, charged, or zwitterionic.[68] While HILIC was originally undertaken using NPLC phases such as the amino silica used by Linden[101], there are currently a wide range of stationary phase chemistries available for HILIC. No one HILIC stationary phase is versatile enough to allow it to be the HILIC equivalent of the C18 stationary phase for RPLC as no stationary phase produces superior results over the others across the entire polar metabolome.[69,103] Table 1.2 shows the structure of several HILIC stationary phases along with some of their properties.

Table 1.2 Examples of HILIC stationary phases with their classifications and bonding characteristics.[68]

Example:	Amide	Silica	Sulfobetaine (ZIC-HILIC)
Class:	Neutral	Charged	Zwitterionic
	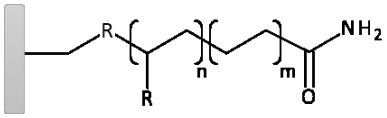	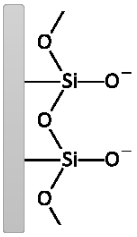	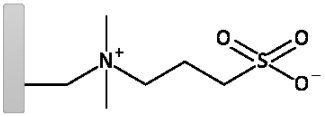
Hydrophilicity:	Very high	High	High
Electrostatic Interaction:	None	Strong	Weak
Hydrogen Bonding:	Donor & Acceptor	Acceptor (at pH>4-5)	Acceptor

1.2.2.1 Neutral Stationary Phases

Neutral HILIC stationary phases consist of polar functional groups, such as amides, diols, and cyanos, which are not charged between pH 3 and 8, corresponding to typical HILIC operating conditions. Because of the lack of charge, no ion exchange interactions occur between the stationary phase and analyte, simplifying the chromatographic retention mechanism. Silica phases can also be classified as neutral if used with mobile phase below pH 4 to 5. At this pH the silica is protonated, and therefore neutral.[68]

1.2.2.2 Charged Stationary Phases

Charged HILIC stationary phases contain polar functional groups with positive or negative charges. These phases include amino groups and silica, which carries a negative charge when deprotonated. Because of the charged nature of the stationary phase, ion exchange can play an important role in the retention mechanism of the chromatographic method, either increasing or decreasing retention time depending on the nature of the analyte. It is important to note that charged HILIC stationary phases are typically pH sensitive, therefore careful consideration must be given when choosing a mobile phase composition.[68]

1.2.2.3 Zwitterionic Stationary Phases

Zwitterionic stationary phases are made up of an equal number of strong acidic and strong basic functional groups in close proximity. The one-to-one ratio of positive and negative charges provides an overall net surface charge of zero while still allowing ionic interactions to occur between analyte and stationary

phase. Despite the net neutral charge, orientation plays a role in interactions and the distal charged group more strongly affects the electrostatic interactions. For example, the ZIC-HILIC column is composed of a sulfobetaine group where an alkyl group connects a quaternary ammonium group to a sulfonate group. The distal sulfonate provides the stationary phase with a net negative charge. Alternatively, the ZIC-cHILIC, with a distal phosphorylcholine group, presents a net positive charge.[68]

1.2.3 Mobile Phase

The mobile phase used in HILIC is a combination of water, an organic solvent, and a salt. When choosing an organic solvent for HILIC it is crucial to consider the following requirements; the solvent must be miscible and is preferably aprotic. Aprotic solvents are preferred owing to the fact that they cannot act as hydrogen bond donors or acceptors and therefore, do not compete with water to solvate the polar stationary phase, and do not hinder the formation of the water layer.[68] Acetonitrile is the most commonly used organic solvent in HILIC. In the event of extremely strong interactions between analyte and stationary phase that hinder elution, a protic solvent such as MeOH or isopropanol can be substituted.[68] The high organic composition of HILIC mobile phase makes HILIC highly compatible with mass spectrometry techniques that use atmospheric pressure ionization techniques such as ESI. The highly efficient ionization and desolvation processes provide high detection sensitivity, up to ten times higher than observed with RPLC.[68,69]

Various salts can be added to HILIC mobile phase to alter its ionic strength. The most commonly used salts are ammonium bicarbonate, ammonium formate, and ammonium acetate, as they are MS compatible and soluble in 95% organic solvent.[68,69] The effects of adding salt to HILIC mobile phase are threefold. First, increasing the salt concentration decreases the electrostatic interactions between the stationary phase and any charged analytes. This can either increase or decrease the retention time for the analyte depending on the nature of the interaction, either repulsive or attractive. Secondly, salt can be used to increase the thickness of the water layer. The salt in the mobile phase preferentially partitions into the water, out of the organic solvent, thickening the water layer. This thickening increases the retention of both the charged and neutral analytes by increasing partitioning into the adsorbed water layer. Third, salts are added to help produce reproducible, high quality peak shapes.[68] A salt gradient can also be used to aid the elution of charged analytes when using a stationary phase that incorporates ion exchange functionality.[102] The concentration of salt typically used in HILIC ranges from 5 to 100 mM with a maximum of 15 mM in 95% ACN mobile phase due to solubility issues.[68]

The pH of HILIC mobile phase can be adjusted using formic or acetic acid to alter the charged state of the analytes being separated. It is preferable to promote analyte charging as charged analytes are more hydrophilic than their neutral counterparts. Additionally, to achieve Gaussian peak shapes, free of tailing and asymmetry, and prevent poor recovery from the stationary phase, the analyte should be present in only one form.[68,69] Given the physico-chemical diversity of the metabolome, with a large range of pKa values, this is impossible to achieve for all of the metabolites in a sample at once, thus often resulting in poor peak shapes observed in HILIC for some metabolites

1.2.4 HILIC in Metabolomics

Hydrophilic interaction liquid chromatography has been used for many applications including studying the CSF metabolome[104], exposure studies[105,106], and studying changes in the metabolome associated with diseases.[107] In the context of metabolomics, the choice of which HILIC stationary phase to use can be a difficult. Several recent studies compared HILIC stationary phases using metabolite standards and various biological samples have been published. [103,108–110] For example, Contrepois *et al.* used 174 metabolite standards, plasma, and urine samples to evaluate five HILIC columns for global metabolomics.[110] They concluded that the sulfobetaine ZIC-HILIC stationary phase combined with a neutral pH mobile phase provided the best peak quality for standards and the best coverage for biological samples. Elmsjö *et al.* compared the performance of an amide column, a silica column, and a sulfobetaine column and concluded that the zwitterionic column outperformed the other two columns for the analysis of plasma, urine, and cell extract samples.[109] Wernisch and Pennathur completed the most extensive comparison of HILIC columns to date using 764 metabolite standards as well as plasma samples.[103] Of the five columns tested, they determined that stationary phases with hydrogen bond acceptors (HBAs), especially the zwitterionic phases, gave the best coverage of a diverse range of metabolites. All of these studies used water/acetonitrile mobile phases, however different salt/acid additives were used, indicating that while the choice of mobile phase additive is important, the selectivity of a method is strongly dictated by the choice of stationary phase. In addition to the polar ionic metabolome, HILIC has also been used to study amphiphilic compounds including phospholipids. Hydrophilic interaction liquid chromatography separates phospholipids by metabolite class and can be used to study these classes as a whole[111,112] or in combination with RPLC to further separate each individual phospholipid species.[54]

1.3 Solid-Phase Microextraction (SPME)

Solid-phase microextraction, first proposed by Arthur and Pawliszyn in 1990[113], is a non-exhaustive, equilibrium-based sample preparation method that combines the extraction and enrichment of

analytes.[114] The technique, in its simplest form, is governed by Equation 1.3 where the mass of analyte extracted (n) at equilibrium is related to the analyte concentration in the sample (C_o) according to the distribution coefficient between the fiber coating and sample matrix (K_{fs}), the volume of the fiber coating (V_f), and the volume of the sample (V_s).[25] Equation 1.3 can be modified to Equation 1.4 to account for an adsorptive. Here K_{Afs} is the adsorption equilibrium constant for the analyte, $C_{f\,max}$ indicates the maximum concentration of active sites available and C_f^{∞} is the equilibrium concentration for the analyte on the fiber.[115]

Equation 1.3 Amount of analyte extracted by SPME

$$n = \frac{K_{fs} V_f V_s C_o}{K_{fs} V_f + V_s}$$

Equation 1.4 Amount of analyte extracted by SPME with an adsorptive coating

$$n = \frac{K_{Afs} V_f V_s C_o (C_{f\,max} - C_f^{\infty})}{(C_{f\,max} - C_f^{\infty}) K_{Afs} V_f + V_s}$$

The SPME procedure can be divided into two steps; partitioning and desorption. In partitioning, the sorbent is exposed to the sample matrix and, depending on their respective distribution coefficients, the analyte(s) in the sample sorb to the sorbent. If the exposure time is greater than the time required to reach equilibrium between sorbent and sample, then longer exposure will not produce further increase in total amount of analyte sorbed and strict control of extraction time is not crucial. However, if the exposure time is less than that required to reach equilibrium, the amount of analyte sorbed is time-dependent and controlling the duration of exposure becomes critical to achieve the desirable level of repeatability. This control of timing is also required for the washing and desorption steps to achieve high repeatability.[25] The second step, desorption, involves removal of the analyte(s) from the sorbent either directly into an analytical instrument (e.g. mass spectrometer), thermal desorption for GC-MS analysis, or into a solvent which can then be analyzed (e.g. by LC-MS).[114]

Each step can be adjusted to optimize the overall extraction efficiency. This includes, but is not limited to, the choice of sorbent, coating thickness and volume, desorption solvent, desorption solvent pH, desorption solvent volume, extraction/desorption time and temperature, sample pH, sample volume, and overall format.[25] Solid-phase microextraction can be applied in multiple formats, shown in Figure 1.10, with the fiber format being the most common.[114]

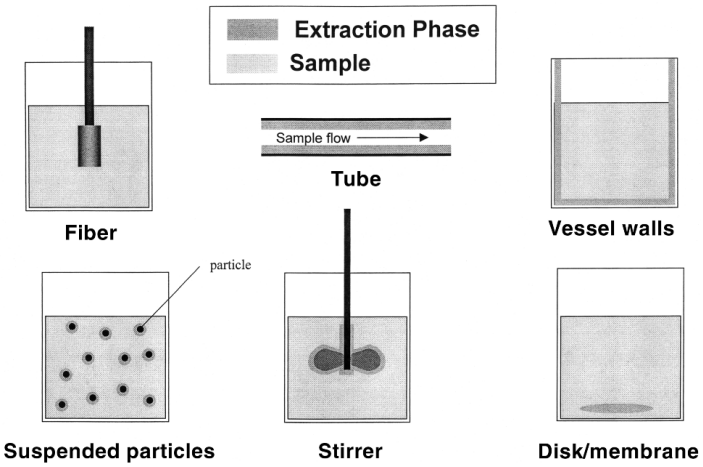

Figure 1.10 Various SPME configurations: fiber, suspended particle (ie. dispersive), sorbent coated tube, stirrer, and disk or membrane. Figure reproduced from reference[25] with permission from Oxford University Press.

Solid-phase microextraction is advantageous over the exhaustive SPE sample preparation technique for decreasing solvent consumption, decreasing ionization suppression, being compatible with *in vivo* sampling, and decreasing sample preparation time which can allow for high throughput analysis and automation. [25,114] Ionization suppression is decreased for SPME samples compared to exhaustive techniques since only a small fraction of the analytes in the original sample are injected into the MS, thus reducing the chance of introducing sufficient material to cause ionization suppression due to limited availability of charge.[114] The disadvantages of SPME include poor limits of detection, poor precision if extraction parameters are not controlled properly[25], and poor extraction of polar metabolites.[114]

1.3.1 Dispersive Solid-Phase Microextraction (D-SPME)

The dispersive format, D-SPME, is the simplest format of SPME, involving sorbent particles being added to and dispersed in the sample. Because the sorbent is evenly dispersed in the sample volume, analytes need only travel shorter distances to reach the sorbent compared to other SPME formats, facilitating diffusion. When increasing the sorbent volume in fiber format of SPME, the thickness of the sorbent coating increases, requiring a longer extraction time. With D-SPME the volume of sorbent used can be increased without having to increase the extraction time required to reach equilibrium.[25] Particles used in D-SPME vary in size but typically fall within the nm to µm range.[116–119] The disadvantage of D-SPME compared to other formats is the need to separate the sorbent particles from the sample. This is commonly achieved using centrifugation, filtration or by applying a magnetic field if magnetically functionalized particles are used as the sorbent.[120] In contrast, advantages of the dispersive format include

increased surface area and faster equilibration times. For these reasons, as well as easy testing of a new sorbent particle without the development of a more sophisticated format, the dispersive format was chosen to evaluate carbon nanoparticles for D-SPME of plasma.

1.3.2 Use of Solid-Phase Microextraction in Metabolomics

Solid-phase microextraction has been used to study both targeted[121] and untargeted[122] metabolomics using multiple formats, including but not limited to headspace[123], fiber[122], in-tube[121], and dispersive.[124] A variety of sorbents, each with its strengths and weaknesses, are available for SPME including commercially available sorbents such as divinylbenzene, C18, and polyacrylate[125], non-carbon sorbents such as metallic/metal oxide nanoparticles[118], and carbon nanoparticle sorbents such as buckminsterfullerenes[125], carbon nanotubes[118], and graphene.[118,126] A search of the literature yielded no previous work evaluating the use of carbon nanoparticles for SPME in the field of metabolomics prompting the evaluation of carbon nanopearls in this thesis.

1.4 Carbon Nanoparticles

Carbon nanoparticles are polymers composed solely of carbon atoms covalently bound to each other.[127] Many different forms (Figure 1.11) of carbon nanoparticles are available, including buckminsterfullerene, single (SWCNT) and multi-walled carbon nanotubes (MWCNT), and carbon nanopearls, all with at least one dimension in the nanometer range.[127–132]

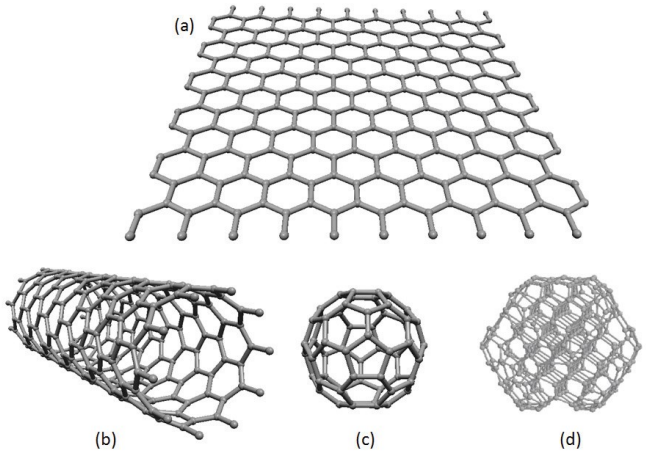

Figure 1.11 Nanoscale carbon allotropes: graphene (a), nanotubes (b), buckminsterfullerene (c), and nanodiamonds (d). Figure reproduced from reference[119] with permission of Future Science in the format Thesis/Dissertation via Copyright Clearance Center. Figure (d) originally from reference[133] and reprinted with permission from Elsevier.

1.4.1 Buckminsterfullerene

The buckminsterfullerene, C_{60}, discovered in 1985 and earning Robert F. Curl Jr., Sir Harold W. Kroto, and Richard E. Smalley the Nobel Prize in Chemistry in 1996, is a 0.7 nm wide truncated icosahedron of 60 carbon atoms, one at each vertex.[129,134] Each carbon in the molecule is covalently bound to three adjacent carbon atoms through two single bonds and one double bond allowing for a plethora of resonance structures, aromatic character, and a veneer of electrons on both the inner and outer surfaces.[129]

1.4.2 Carbon Nanotubes

Carbon nanotubes can be classified as either single wall or multiwall. The latter was discovered first in 1991 by Sumio Iijima and is composed of between two and fifty layers of graphene sheets which form concentric tubes with diameters between five and fifty nanometers.[130,135] MWCNTs often contain defects within their structure.[128] The SWCNT was concurrently discovered in 1993 by both Sumio Iijima and Toshinan Ichlashl, and Bethune *et al.*[127,131] Composed of a single graphene sheet, these structures have a diameter between one and two nanometers and a decreased surface area compared to MWCNTs.[135] Carbon nanotubes can possess fullerene like caps at either end, closing the internal cavity and eliminating any dangling bonds. This structure decreases the available surface area by closing off the internal cavity.[128]

1.4.3 Carbon Nanopearls

Carbon nanopearls (CNPs), named for their resemblance to a string of pearls, are solid spheres with an amorphous and nanocrystalline structure (shown in Figure 1.12a).[132,136] Each "pearl" is formed by layers of graphite like flakes approximately 16 nm^2 in area that themselves exhibit a wide range of structures thanks to the presence of both sp^2 and sp^3 hybridized carbon atoms. This variation in hybridization allows for the formation of five, six, and seven member rings. The edges of each flake present dangling bonds and the outer surface of each "pearl" is unsealed.[132] A proposed formation mechanism is shown in Figure 1.12.

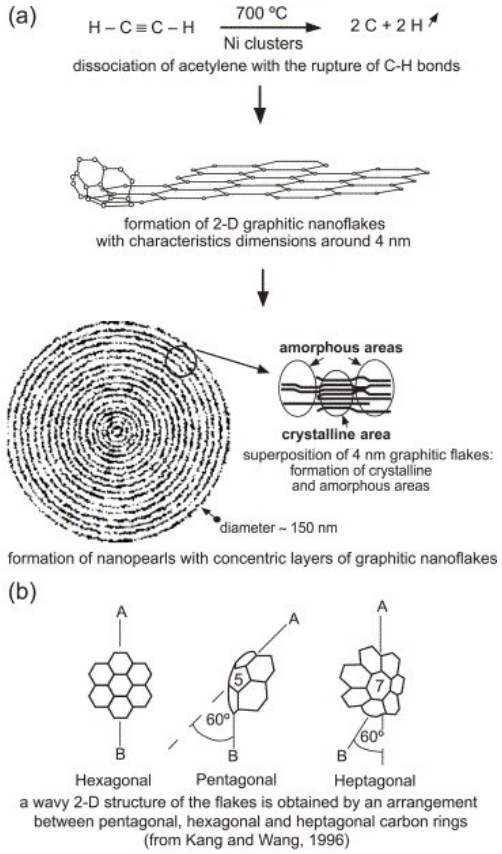

Figure 1.12 (a) The carbon nanopearl formation mechanism proposed by Levesque *et al.* This method provides an explanation for the amorphous structure and concentric layers of graphitic flakes observed. (b) The inclusion of five and seven member rings in the graphitic flakes produces the "wavy" structure observed. Figure reproduced from reference[132] with permission from Elsevier.

Energy dispersive x-ray spectroscopy testing performed by Levesque *et al.* concluded that carbon nanopearls are composed solely of carbon with traces of oxygen, silicon, and sulfur which they concluded were contamination due to handling rather than part of the carbon nanopearl composition.[132]

Each carbon nanopearl has a diameter of 150 nm (85% monodispersity) and groups together with other carbon nanopearls to form a three dimensional, foam like structure composed of "strings" of carbon nanopearls up to 10 µm in length.[132,136] The reason for this specific formation remains unknown. High resolution transmission electron microscopy (HRTEM) and scanning electron microscope (SEM) images of carbon nanopearls showing these structural characteristics are shown in Figure 1.13 and Figure 1.14 respectively.

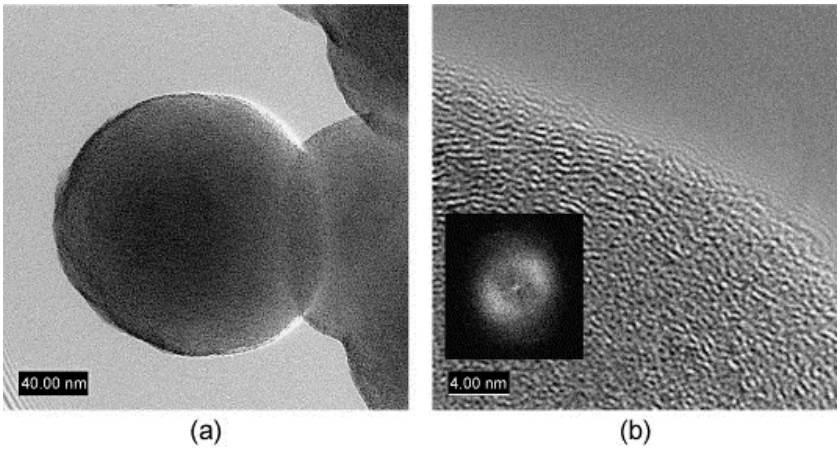

Figure 1.13 HRTEM image of a whole carbon nanopearl (a) and a close up of the surface of a carbon nanopearl (b). Figure reproduced from reference[132] with permission from Elsevier.

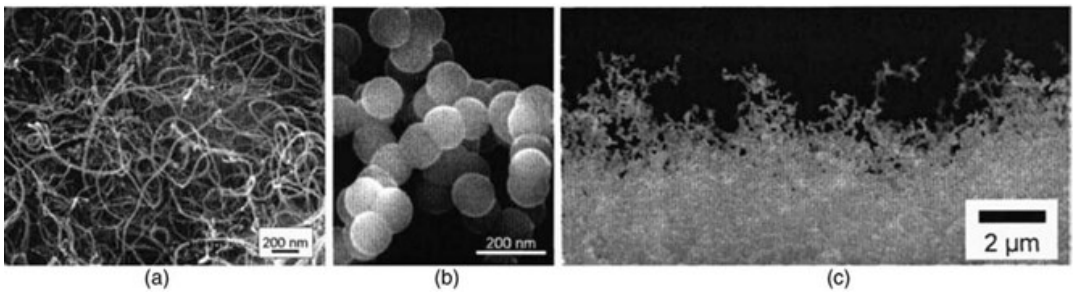

Figure 1.14 SEM images of carbon nanopearls showing the string like formation and foam like bulk of a layer of particles. Figure reproduced from reference[137] with permission from AIP Publishing.

1.4.4 Use of Carbon Nanoparticles in Solid-Phase Microextraction (SPME)

Thanks to their large surface area, allowing for fast mass transfer from sample to sorbent[118], chemical, mechanical and thermal stability[118,126], and the possibility of surface functionalization[118], allowing for customization of selectivity, carbon nanoparticles, in many forms, have been used in SPME to extract a variety of analytes from a range of sample types.[138] Single walled carbon nanotubes have been fixed to supports to perform SPME in the fiber format by Rastkari *et al.* to extract the toxic environmental pollutants monobutyltin, dibutyltin, and tributyltin from sea water samples[139] as well as to extract gasoline additives MTBE, ethyl tert-butyl ether, and tert-amyl methyl ether from human urine samples.[140] Additionally, Wu *et al.* used SWCNT-coated fibers to extract thirteen pesticides from samples of tea.[141] Carbon nanoparticles have also been used in the dispersive format of SPME. For example, Jiménez-Soto *et al.* used oxidized single walled carbon nanohorns (o-SWNHs) to extract polycyclic aromatic hydrocarbons (PAH) from tap, river, and bottled water samples[142] as well as to extract triazine herbicides

from water samples.[143] More recently, Hooshmand *et al.* used magnetic MWCNTs to extract the anticancer tyrosine kinase inhibitor sunitinib from a variety of human biological samples including plasma.[144] The results of these studies suggest that carbon nanoparticle sorbents have interesting selectivity that has not yet been investigated for applications in global metabolomics. Considering their ability to participate in π-π interactions, it is possible that carbon nanoparticles may interact preferentially with aromatic compounds and improve the coverage of the aromatic sub-metabolome. This possibility merits further investigation.

1.5 Research Objectives

Global metabolomics studies require the selection of the appropriate and complementary chromatographic separation and sample preparation techniques to achieve adequate coverage of the highly complex metabolome. Hydrophilic interaction liquid chromatography is often used to chromatographically separate the polar metabolome before MS detection however there is a lack of consensus in the literature on which HILIC column is preferable. Thus, the first objective of this thesis is to evaluate in detail two HILIC stationary phases, the charged underivatized silica and zwitterionic sulfobetaine, using both metabolite standards and methanol-precipitated human plasma. The main evaluation criteria included the retention time, peak quality, and metabolite coverage achieved with each column. Adequate retention and chromatographic resolution of analytes is crucial to avoid ionization suppression caused by a large number of co-eluting compounds. Good peak quality, including width and symmetry, is required to obtain high quality data through quantitative or global data processing. Metabolite coverage is important to gather as comprehensive a picture as possible of the metabolome at a given time. The effect of salt concentration in the mobile phase on the retention of standards on the ZIC-HILIC column will be evaluated and the effect of adding trace amounts of ammonium phosphate to samples will be evaluated to determine if peak shape is improved.

Dispersive solid-phase microextraction may possibly be useful as a sample preparation technique in global metabolomics for its low cost and the ability to improve detection of low abundance metabolites and decrease ionization suppression. Interest in carbon nanoparticles, in their many forms, as sorbents for sample preparation has grown recently. To further investigate their potential in global metabolomics, the second objective of this thesis is to develop a carbon nanopearl based D-SPME protocol for human plasma sample preparation. The performance of these particles as a sorbent will be evaluated using both a mixture of aromatic metabolite standards as well as human plasma samples, in an attempt to determine the selectivity and overall performance of these particles.

Chapter 2: A Comparison of an Underivatized Silica and Zwitterionic Sulfobetaine HILIC Stationary Phases for Global Metabolomics of Human Plasma

2.1 Abstract

Chromatographic separation, both reversed phase liquid chromatography (RPLC) and hydrophilic interaction liquid chromatography (HILIC), of samples is implemented before detection by mass spectrometry to increase metabolome coverage. A variety of stationary phases are available for HILIC and each of these stationary phases varies in terms of relative hydrophobicity, hydrogen bonding ability, and electrostatic interaction capabilities. A lack of consensus in the literature on HILIC stationary phase performance prompted this study to compare zwitterionic ZIC-HILIC stationary phase to a charged HILIC stationary phase, specifically the Ascentis Si Express. During method development, the salt concentration in the mobile phase and the mobile phase gradient were both investigated. The quality of the peak shapes, analyte retention time, peak separation capability, and metabolite coverage were used to compare the results from each stationary phase. The methods were initially evaluated using a mixture of 37 standards covering a range of logP values (-10 to 3.73), molecular weights (59 to 776 Da), charges (15 anions, 11 cations, and 11 neutral) and multiple classes of metabolites including but not limited to vitamins, amino acids, hormones, and neurotransmitters. The results suggest that the zwitterionic ZIC-HILIC column provides improved peak shape quality over the silica stationary phase with 14 standards achieving good quality peaks compared to the 7 with the silica column. Only 2 standards were undetected with the ZIC-HILIC column compared to the 14 undetected with the silica column. Additionally, it has been shown that the addition of trace amounts of ammonium phosphate to samples can improve peak shape on the ZIC-pHILIC. To investigate whether similar results could be obtained on other HILIC columns such as the ZIC-HILIC or Ascentis Silica Express, the results for standards and plasma samples both with and without the addition of ammonium phosphate were compared. Improved peak quality for standards was observed however plasma data showed no conclusive evidence that ammonium phosphate addition was beneficial. In a subsequent experiment, phospholipid standards were also investigated using optimized conditions. Phospholipids are separated by HILIC based on the polarity of their head group, regardless of fatty acyl chain length or degree of saturation. Given that lipids can cause ion suppression, lipid standards were analyzed to determine their retention times for both HILIC methods and aid in the interpretation of plasma analysis results.

2.2 Introduction

Metabolomics is the comprehensive analytical study of the metabolome, broadly defined as the collection of all of the low molecular weight species in a biological system.[2] Chromatographic separation of samples in combination with mass spectrometry (MS) is routinely used in metabolomics in order to provide the highest metabolome coverage. Although a large portion of the metabolome can be adequately separated by RPLC, there is a significant portion that is too polar, and often charged, that is not amenable to reversed phase separation.[145] Implementing normal phase liquid chromatography (NPLC) to separate the polar metabolome may be the obvious alternative to RPLC. However, NPLC is incompatible with MS and it may be difficult to solubilize ionic analytes in the highly non-polar solvent. These two disadvantages severely limit its application in metabolomics. Alternately, HILIC uses MS-compatible solvents to separate polar analytes and is therefore commonly employed to separate the polar metabolome and improve metabolome coverage.[103,110,146–148]

Hydrophilic interaction liquid chromatography uses a hydrophilic stationary phase and acetonitrile-rich mobile phases to separate polar analytes by three mechanisms.[69] Firstly, water from the mobile phase is adsorbed onto the stationary phase to form a liquid-liquid partitioning system where polar analytes are retained in the water layer while less polar analytes are eluted in the bulk of the mobile phase. As the water content of the mobile phase is increased, decreasing the polarity gradient between the water layer and bulk, analytes are eluted from the least to most polar. Secondly, electrostatic interactions, both attractive and repulsive, between the charged analyte and charged stationary phase increase or decrease retention time, respectively. The strength of these interactions can be mitigated by the addition of salts, such as ammonium acetate, to the mobile phase. Finally, hydrogen bonding between the stationary phase and analytes can occur, increasing retention.

A variety of stationary phases are available for HILIC and can be grouped into three categories: neutral, charged, and zwitterionic.[68] Each stationary phase differs in relative hydrophobicity, hydrogen bonding ability (presence of hydrogen bond donor (HBD) and/or acceptor (HBA) groups), and electrostatic interaction capability. The ability to participate in electrostatic interactions, and to what extent, is of particular interest for metabolomics because numerous polar charged analytes are poorly retained by RPLC. For this reason, no neutral stationary phase was tested in this work, and charged and zwitterionic phases were selected for further study and comparison. There is currently no consensus in the literature as to which stationary phase provides the best results for global metabolomics applications, however there is growing interest in the newer zwitterionic stationary phases.[103,108–110] Wernisch and Pennathur

evaluated five HILIC columns using 764 metabolite standards and human plasma to conclude that stationary phases with HBAs, especially those that are zwitterionic, provided the best coverage for a diverse range of analytes.[103] Elmsjö *et al.* evaluated amide, silica, and sulfobetaine HILIC columns using plasma, urine, and cell extract samples to conclude that the zwitterionic sulfobetaine column provided the best separation.[109] Contrepois *et al.* evaluated five HILIC columns using 174 metabolite standards, plasma, and urine samples to conclude that the sulfobetaine ZIC-HILIC column performed best for both standards and biological samples.[110]

To further investigate the performance of charged and zwitterionic phases in global metabolomics, a zwitterionic sulfobetaine stationary phase was compared to a charged silica stationary phase using selected metabolite standards and methanol-precipitated plasma samples. Standard metabolite results were evaluated individually to determine peak quality and the influence of salt concentration in mobile phase, as well as to evaluate the extent of chromatographic separation. Plasma sample results were compared by evaluating the extent of co-elution as well as the total number of compounds detected by each column. Phospholipid standards were analyzed to determine the retention time for each class to aid in the interpretation of plasma results, looking at areas of high co-elution and possibly high ionization suppression. Spalding *et al.*[149] recently demonstrated that trace amounts of ammonium phosphate added to either the mobile phase or directly to the samples analyzed using a ZIC-pHILIC column improved both peak shape and coverage of the polar metabolome. The ZIC-pHILIC column utilizes a polymeric support[150] rather than the silica support used in the ZIC-HILIC.[151] To investigate whether trace phosphate can also improve performance of the ZIC-HILIC and silica stationary phases, results for standard metabolites and plasma samples with and without phosphate were compared. The overall objective of this study was to select the most complementary HILIC method for global metabolomics of human plasma to use in combination with standard RPLC method.

2.3 Experimental

2.3.1 Chemicals and Materials

Acetonitrile, methanol, and water, all LC-MS grade, were purchased from Fisher Scientific Inc. (Ottawa, ON, Canada). All metabolite standards, ammonium phosphate, and the mobile phase additive ammonium acetate were purchased from Millipore Sigma (Oakville, ON, Canada). Phospholipid standards were purchased from Avanti Polar Lipids (Alabaster, AL, USA). Pooled human citrated plasma (lot# BRH1317314) was purchased from Bioreclamation IVT (Baltimore, MD, USA).

2.3.2 Preparation of Standard Metabolite Mixture

Individual stock standard solutions were prepared at 1 mg/mL in the appropriate solvent, as indicated in Table 2.1. A stock standard mixture of all 37 standards was prepared at 10 µg/mL using water as a diluent. A working standard mixture for analysis was prepared at 200 ng/mL in 80% ACN/20% water. A second working standard mixture was prepared at 200 ng/mL in 80% ACN/20% water with an ammonium phosphate concentration of 10 mM.

Table 2.1 Main physico-chemical properties of polar metabolite standards selected for evaluation.[3] The adduct used is indicated by * for $[M+H]^+$ and ‡ for $[M-H]^-$.

Metabolite Standard	log P	Formula	Monoisotopic Mass	Physiological Charge	No. HBD	No. HBA	Stock Solution Solvent
Adenosine triphosphate (ATP)*	-6	$C_{10}H_{16}N_5O_{13}P_3$	506.9957	-3	7	14	H_2O
Maleic Acid‡	-0.04	$C_4H_4O_4$	116.0109	-2	2	4	H_2O
D-Ribose 5-phosphate‡	-2.4	$C_5H_{11}O_8P$	230.0191	-2	5	7	H_2O
D-Glucose 6-phosphate‡	-3.1	$C_6H_{13}O_9P$	260.0297	-2	6	8	H_2O
Adenosine monophosphate (AMP)*	-4.8	$C_{10}H_{14}N_5O_7P$	347.0630	-2	5	10	H_2O
Adenosine diphosphate (ADP)*	-5.3	$C_{10}H_{15}N_5O_{10}P_2$	427.0294	-2	6	12	H_2O
3-Hydroxybutyric Acid‡	-0.39	$C_4H_8O_3$	104.0473	-1	2	3	H_2O
L-Glutamic Acid‡	-3.2	$C_5H_9NO_4$	147.0531	-1	3	5	MeOH/H_2O (1/1)
Biotin‡	0.32	$C_{10}H_{16}N_2O_3S$	244.0881	-1	3	3	MeOH/H_2O (1/1)
Glutathione*	-4.9	$C_{10}H_{17}N_3O_6S$	307.0838	-1	6	7	H_2O
Riboflavin*	-0.92	$C_{17}H_{20}N_4O_6$	376.1382	-1	5	9	H_2O
Cholic Acid‡	2.48	$C_{24}H_{40}O_5$	408.2875	-1	4	5	MeOH
Estrone Glucuronide‡	2.36	$C_{24}H_{30}O_8$	446.1940	-1	4	8	MeOH
Taurocholic Acid‡	-0.24	$C_{26}H_{45}NO_7S$	515.2916	-1	5	7	H_2O
Nicotinamide adenine dinucleotide (β-NAD)*	-10	$C_{21}H_{28}N_7O_{14}P_2$	664.1169	-1	8	15	H_2O
Gamma-aminobutyric acid (GABA)*	-2.9	$C_4H_9NO_2$	103.0633	0	2	3	H_2O
Creatinine*	-1.1	$C_4H_7N_3O$	113.0589	0	2	3	H_2O
Nicotinamide*	-0.39	$C_6H_6N_2O$	122.0480	0	1	2	H_2O

Adenine*	-0.57	$C_5H_5N_5$	135.0544	0	2	4	H_2O
L-Histidine*	-3.6	$C_6H_9N_3O_2$	155.0694	0	3	4	H_2O
L-Phenylalanine‡	-1.2	$C_9H_{11}NO_2$	165.0789	0	2	3	MeOH/H_2O (1/1)
D-Glucose*	-2.9	$C_6H_{12}O_6$	180.0633	0	5	6	H_2O
L-Tryptophan*	-1.1	$C_{11}H_{12}N_2O_2$	204.0898	0	3	3	MeOH/H_2O (1/1)
Adenosine*	-2.1	$C_{10}H_{13}N_5O_4$	267.0967	0	4	8	H_2O
Cortisol*	1.28	$C_{21}H_{30}O_5$	362.2093	0	3	5	MeOH
Thyroxine‡	3.73	$C_{15}H_{11}I_4NO_4$	776.6866	0	3	4	Dimethyl Sulfoxide
Guanidine*	-1.2	CH_5N_3	59.0483	1	3	3	H_2O
Choline*	-4.7	$C_5H_{14}NO$	104.1075	1	1	1	H_2O
Histamine*	-0.7	$C_5H_9N_3$	111.0796	1	2	2	H_2O
Ornithine*	-3.7	$C_5H_{12}N_2O_2$	132.0898	1	3	4	H_2O
L-Lysine*	-3.2	$C_6H_{14}N_2O_2$	146.1055	1	3	4	H_2O
Dopamine*	0.03	$C_8H_{11}NO_2$	153.0789	1	3	3	H_2O
Tryptamine*	1.49	$C_{10}H_{12}N_2$	160.1000	1	2	1	H_2O
L-Arginine*	-3.2	$C_6H_{14}N_4O_2$	174.1116	1	5	6	H_2O
Serotonin*	0.48	$C_{10}H_{12}N_2O$	176.0949	1	3	2	H_2O
Epinephrine*	-0.43	$C_9H_{13}NO_3$	183.0895	1	4	4	H_2O
5-Methoxytryptamine*	1.33	$C_{11}H_{14}N_2O$	190.1106	1	2	2	MeOH/H_2O (1/1)

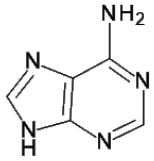

Adenine

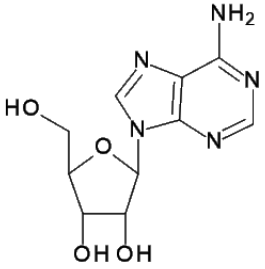

Adenosine

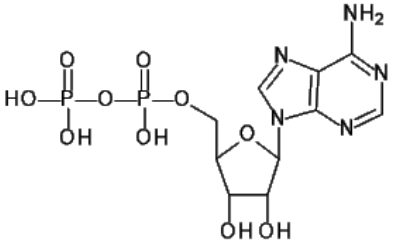

ADP

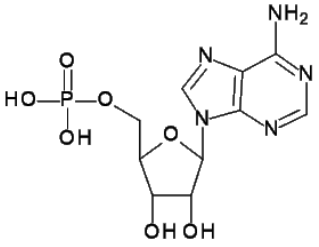

AMP

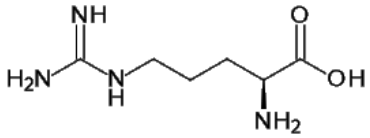

L-Arginine

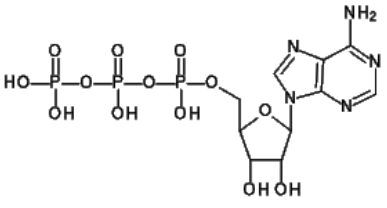

ATP

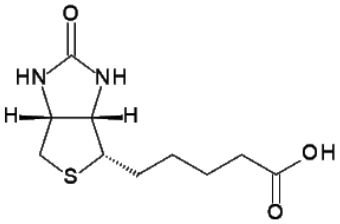 Biotin	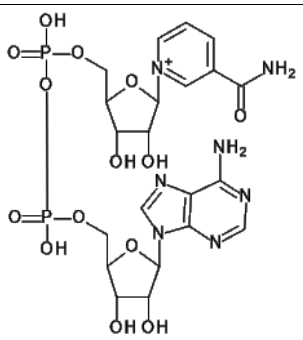 B-NAD	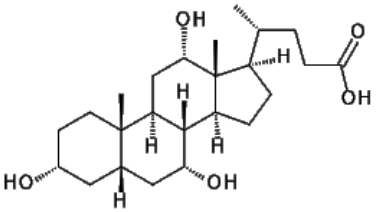 Cholic Acid
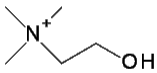 Choline	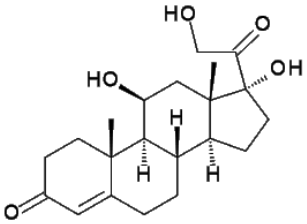 Cortisol	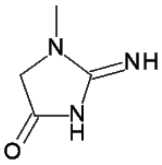 Creatinine
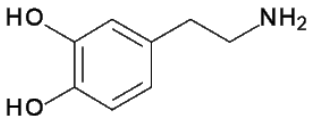 Dopamine	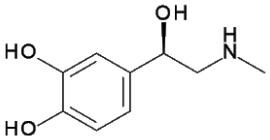 Epinephrine	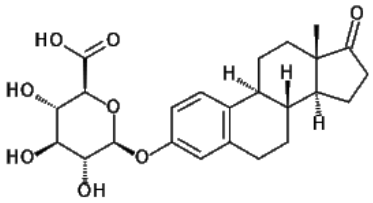 Estrone Glucuronide
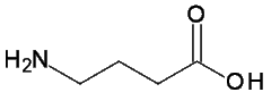 GABA	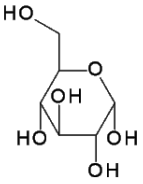 D-Glucose	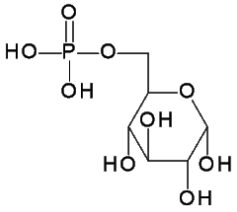 D-Glucose 6-phosphate
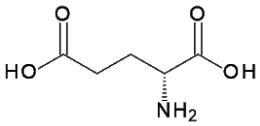 L-Glutamic Acid	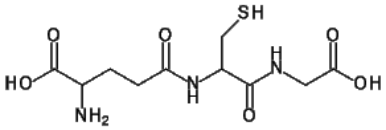 Glutathione	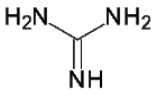 Guanidine
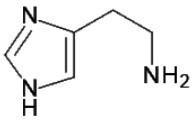 Histamine	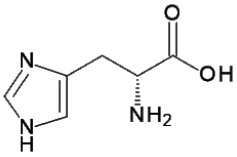 L-Histidine	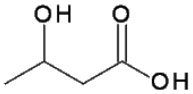 3-Hydroxybutyric Acid

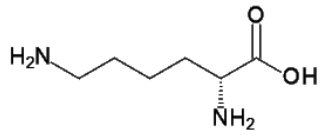 L-Lysine	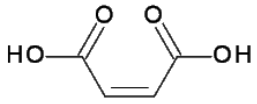 Maleic Acid	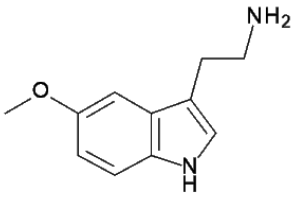 5-Methoxytryptamine
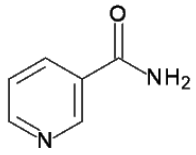 Nicotinamide	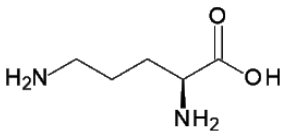 Ornithine	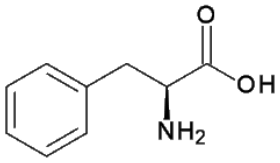 L-Phenylalanine
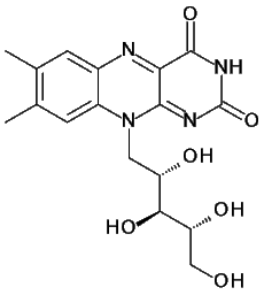 Riboflavin	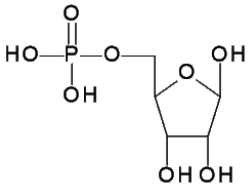 D-Ribose 5-phosphate	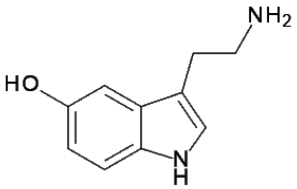 Serotonin
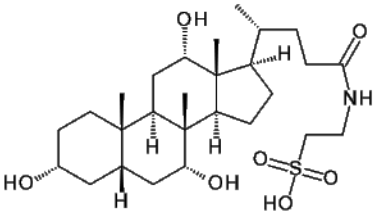 Taurocholic Acid	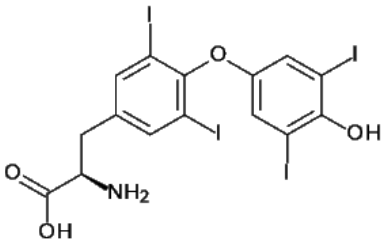 Thyroxine	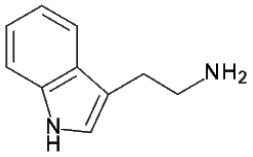 Tryptamine
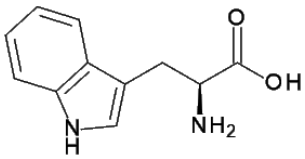 L-Tryptophan		

Figure 2.1 Polar standard metabolite structures[3]

2.3.3 Preparation of Phospholipid Standards

Phospholipid stock standard solutions in methanol were diluted to either 100 ng/mL or 500 ng/mL in 90% acetonitrile/10% methanol, as indicated in Table 2.2.

Table 2.2 Main physico-chemical properties of phospholipid standards[152]

Phospholipid Standard		Formula	Monoisotopic Mass	LogP	Physiological Charge	Polar Surface Area (Å²)	Concentration Analyzed (ng/mL)
Class	Fatty Acyl Chain						
PE	(15:0/15:0)	$C_{35}H_{70}NO_8P$	663.4839	11.31	0	134.38	500
	(12:0/13:0)	$C_{30}H_{60}NO_8P$	593.4057	9.36	0		
	(16:0/16:0)	$C_{37}H_{74}NO_8P$	691.5152	12.09	0		
PS	(12:0/13:0)	$C_{31}H_{60}NO_{10}P$	637.3955	8.82	-1	171.68	500
	(17:0/17:0)	$C_{40}H_{78}NO_{10}P$	763.5363	12.33	-1		
LPE	(13:0)	$C_{18}H_{38}NO_7P$	411.2386	4.89	0	128.31	500
PC	(17:0/17:0)	$C_{42}H_{84}NO_8P$	761.5935	12.82	0	111.19	100
	(16:0/16:0)	$C_{40}H_{80}NO_8P$	733.5622	12.04	0		
LPC	(16:0)	$C_{24}H_{50}NO_7P$	495.3325	6.01	0	105.12	500
	(17:0)	$C_{25}H_{52}NO_7P$	509.3481	6.40	0		
PI	(17:0/20:4)	$C_{46}H_{81}O_{13}P$	872.5415	11.52	-1	209.51	500
	(16:0/16:0)	$C_{41}H_{79}O_{13}P$	810.5258	10.47	-1		
PA	(17:0/17:0)	$C_{37}H_{73}O_8P$	676.5043	12.49	-2	119.36	500
	(18:0/18:0)	$C_{39}H_{77}O_8P$	704.5356	13.27	-2		
PG	(17:0/17:0)	$C_{40}H_{79}O_{10}P$	750.5411	12.55	-1	148.82	100
	(18:0/18:0)	$C_{42}H_{83}O_{10}P$	778.5724	13.33	-1		
LPS	(17:1)	$C_{23}H_{44}NO_9P$	509.2754	5.68	-1	165.61	500

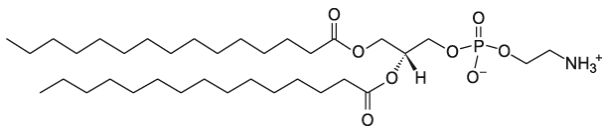

PE (15:0/15:0)
1,2-dipentadecanoyl-sn-glycero-3-phosphoethanolamine

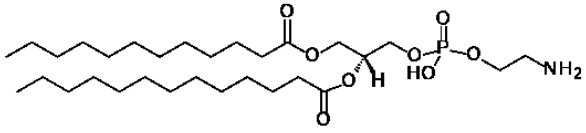

PE (12:0/13:0)
1-dodecanoyl-2-tridecanoyl-sn-glycero-3-phosphoethanolamine

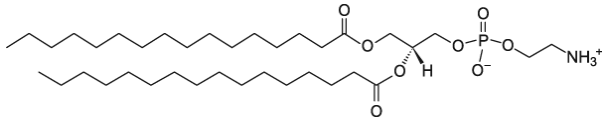

PE (16:0/16:0)
1,2-dipalmitoyl-sn-glycero-3-phosphoethanolamine

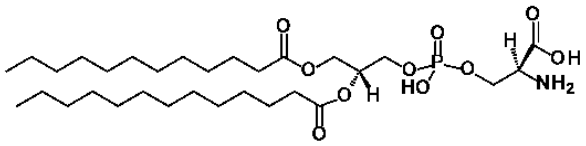

PS (12:0/13:0)
1-dodecanoyl-2-tridecanoyl-sn-glycero-3-phospho-L-serine

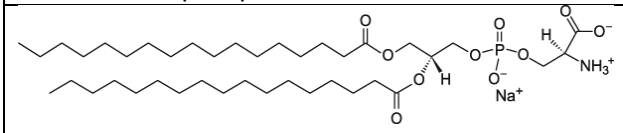

PS (17:0/17:0)
1,2-diheptadecanoyl-sn-glycero-3-phospho-L-serine

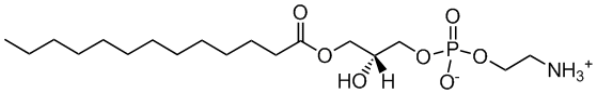

LPE (13:0)
1-tridecanoyl-sn-glycero-3-phosphoethanolamine

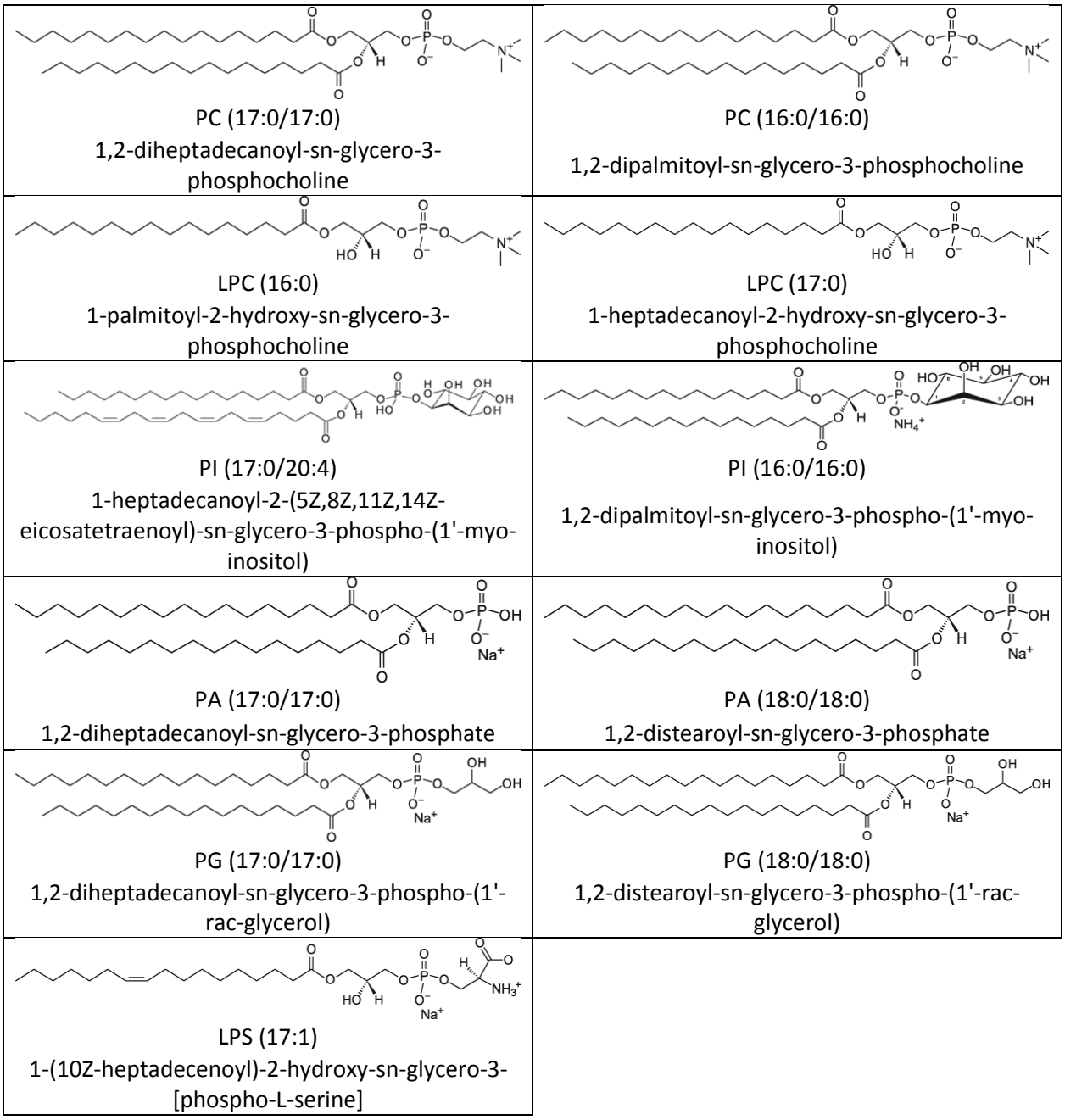

Figure 2.2 Phospholipid standard structures

2.3.4 Preparation of Methanol-Precipitated Plasma Samples

Frozen citrated pooled human plasma was thawed on ice. Thawed plasma (200 µL) was mixed for 30 seconds with 600 µL of cold methanol, using a vortex and then stored at -80°C for 30 minutes. The samples were then centrifuged for 20 minutes at 25000 g to separate the precipitated protein in the samples. The supernatant (300 µL) was transferred into a new vial and evaporated to dryness in a Savant Speedvac SPD111V (Thermo Scientific, Ottawa, ON, Canada). The dried samples were then reconstituted in 300 µL of 80% ACN/20% H_2O using sonication for 5 minutes followed by vortexing for 30 minutes. Six replicates

were prepared. A single extraction blank was prepared in the same way, substituting 200 µL of methanol for the 200 µL of plasma. Samples with trace phosphate were prepared by substituting 80% ACN/20% H_2O with 10 mM ammonium phosphate in place of 80% ACN/20% H_2O as the reconstitution solvent.

2.3.5 LC-MS Analysis

All of the chromatographic separations included in this work were performed on an Agilent 1290 Infinity II UHPLC system (Agilent Technologies, Santa Clara, CA, USA) equipped with a G4226A autosampler, G4220A binary pump, and G1330B thermal column compartment. The autosampler was set at 4°C for all analyses. Two columns were used in this work: the 100 mm x 2.1 mm Ascentis Si Express (Millipore Sigma, Oakville, ON, Canada) with a 2.7 µm particle size, 90 Å pore size and, and the 100 mm x 2.1 mm SeQuant ZIC-HILIC (Millipore Sigma, Oakville, ON, Canada) with a 3.5 µm particle size, 100 Å pore size. Appropriate guard columns were used with both columns: Ascentis Si Express (2.1 mm x 5 mm, 2.7 µm) and SeQuant ZIC-HILIC (2.1 mm x 2 mm, 3.5 µm) respectively. Samples were analyzed using the gradient method as described in Table 2.3. The concentration of ammonium acetate in mobile phase was varied to evaluate its effect, as discussed in 2.4.1.

Table 2.3 Summary of LC conditions used in this study

LC Parameter	Conditions
Mobile Phase A	acetonitrile/water (5/95, v/v) 5 mM ammonium acetate
Mobile Phase B	acetonitrile/water (95/5, v/v) 5 mM ammonium acetate
Flow Rate	400 µL/min
Run Time	40 min
Injection Volume	10 µL
Mobile Phase Gradient	0-2 min 0% A 2-25 min linear gradient to 20% A 25-35 min linear gradient to 50% A 35.1-40 min 0% A
Column Temperature	35°C

All MS analyses were performed with an Agilent 6550 iFunnel Quadrupole-Time-of-Flight (Q-TOF) instrument with an ESI source and Dual Agilent Jet Stream (AJS) technology (Agilent Technologies, Santa Clara, CA, USA). An Agilent G1310B isocratic pump was used to introduce a reference solution into the ESI source to perform internal mass calibration and maintain mass accuracy throughout all the analyses. The reference solution contained purine (m/z 112.050873 in positive ESI, 199.036320 in negative ESI) and HP-0921 (m/z 922.009798 in positive ESI, 980.016375 in negative ESI). The MS conditions used in this work

are listed in Table 2.4. MassHunter data acquisition software for the 6200 series TOF/6500 series QTOF (version B.06.01, build 6.01.6157) was used to control LC-MS acquisition.

Table 2.4 Q-TOF conditions used in this study

N_2 drying gas temperature	250°C	**Nozzle voltage**	400V
N_2 drying gas flow	15 L/min	**Fragmentor voltage**	175 V
Nebulizer pressure	35 psig	**Acquisition rate**	2 spectra/s
Capillary voltage	3500 V	**Mass range**	50-1100 m/z

2.3.6 Data Processing

Data processing for standard metabolites was completed using Agilent Mass Hunter TOF Qualitative Analysis software (version B.07.00, build 7.0.7024.29). Extraction of the selected ion m/z, obtained from METLIN[47] for standard metabolites and LIPID MAPS[152] for phospholipids, was performed with a 10 ppm window. All peak integrations were manually checked. The m/z used for phospholipid standards are listed in Table 2.8. The $[M+H]^+$ or $[M-H]^-$ adduct, as indicated in Table 2.1, was used for all other standards. For standards detected in both positive and negative ESI modes, the m/z ion with the greater signal intensity was used.

Data processing for methanol-precipitated plasma samples was completed using Agilent MassHunter Profinder Software (version B.09.00, build 8.0.8137.0). The software finds compounds through chromatographic deconvolution and then performs peak alignment using compound retention time and mass. The software also performs de-isotoping and de-adducting so that all ions belonging to a single metabolite are combined into a single entry. Global processing was applied between chromatographic run times of 1 minutes and 35 minutes. The applied processing parameters are presented in Table 2.5. The list of detected compounds was then further refined by (i) removing any compounds not found in the sample with the signal intensity at least 5 times the intensity of the extraction blank, (ii) removing any compounds not found in all replicates, and (iii) removing all compounds with a mass greater than 1100 Da.

Table 2.5 Global data processing parameters applied to plasma samples using Agilent MassHunter Profinder Software

Use peaks with height	≥250 counts	**Mass window**	±20 ppm +2.0 mDa
m/z range	50-1100	**Retention time window**	2% ±0.3
Allowed adducts (+ESI)	$[M+H]^+$, $[M+Na]^+$, $[M+K]^+$, $[M+NH_4]^+$	**Minimum number of required ions**	2
Allowed adducts (-ESI)	$[M-H]^-$, $[M+Cl]^-$, $[M+Br]^-$, $[M+HCOO]^-$, $[M+CH_3COO]^-$, $[M+CF_3COO]^-$	**Absolute height**	2500 counts
Charge state limit	1-3	**MFE score**	70

2.4 Results and Discussion

2.4.1 Effect of Mobile Phase Salt Concentration on Analyte Retention in ZIC-HILIC

Volatile salts, such as ammonium acetate, are added to HILIC mobile phases to alter the selectivity of a chromatographic method. The effects of adding salt are two-fold: increasing retention times by increasing the thickness of the water layer adsorbed onto the stationary phase, and decreasing the effect of electrostatic interactions between the charged stationary phase and charged analytes. The results of increasing the ammonium acetate from 2 mM to 5 mM to 10 mM are shown in Figure 2.3 and Figure 2.4. Figure 2.3 shows an example of cation, anion, and neutral molecules to illustrate the general trends for retention time shifts with increased salt concentration: decreased retention for cations, increased retention for anions, and a minimal increase in retention time for neutrals.

The standard metabolites in Figure 2.4 are grouped by their net charge at physiological pH. The effect of altering mobile phase concentration on uncharged species is minimal (<1 min). The increase in water layer thickness with increased salt concentration should theoretically increase the retention time which is most clearly seen in the comparison of 2 mM and 5 mM ammonium acetate (Figure 2.4c). For example, adenine shows a less than half minute increase in retention time for all three comparisons made in Figure 2.4. Four standards, GABA, histidine, L-tryptophan, and L-phenylalanine, are in fact zwitterionic, so while they demonstrate no net charge, they are still able to participate in electrostatic interactions. These four appear to act similarly to cations with increased salt resulting in decreased retention time due to decreased attraction between the distal negative charge of the sulfonate group and the positive charge on the analyte. This effect is minimal for all except L-phenylalanine. One possible explanation for this is that the aromatic ring which is hydrophobic may orient into the less polar bulk of the mobile phase, thus directing the charged end of the molecule towards the stationary phase, facilitating electrostatic interactions. The same trend is not seen with the aromatic amino acid L-tryptophan. This discrepancy is

possibly due to the amine in the R group of L-tryptophan which increases its polar surface area to 79.11 Å^2 compared to the 63.32 Å^2 of L-phenylalanine, allowing the aromatic R group to penetrate the water layer further than that of L-phenylalanine. Figure 2.4 also shows that no trend can be observed corresponding to the number of HBDs.

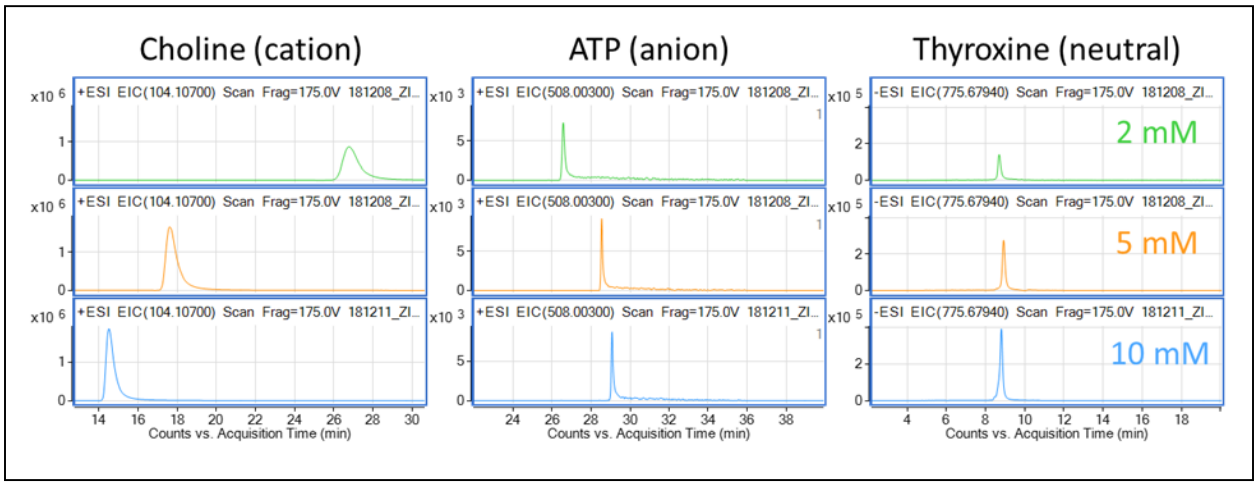

Figure 2.3 Example EICs for standard metabolites (200 ng/mL) showing the effect on retention time and peak shape with increasing ammonium acetate concentration (2 mM, 5 mM, 10 mM) in mobile phase on the ZIC-HILIC column.

The effect of altering mobile phase salt concentration on species with a net positive or negative charge is more distinct. Given that the negative charge of the sulfonate group of the stationary phase, Figure 2.5, is dominant in electrostatic interactions over the positive charge of the quaternary amine, cations are attracted to the stationary phase while anions are repelled. These interactions are weakened with increasing salt concentration resulting in decreased retention time for cations and increased retention time for anions. This is what is observed in the data with the exception of L-arginine. L-arginine carries two positive charges and one negative charge so it is possible that despite the net positive charge, it interacts with the stationary phase as an anion. The EICs for L-arginine with the three ammonium acetate concentrations are shown in Figure 2.6. Ornithine and L-lysine, both carrying a net positive charge, were not observed with the 2 mM ammonium acetate mobile phase concentration. The EICs for ornithine, shown in Figure 2.6, show that at the lower salt concentration, it is likely that ornithine is too strongly retained and does not elute. Glutathione was also not observed with 2 mM ammonium acetate mobile phase concentration.

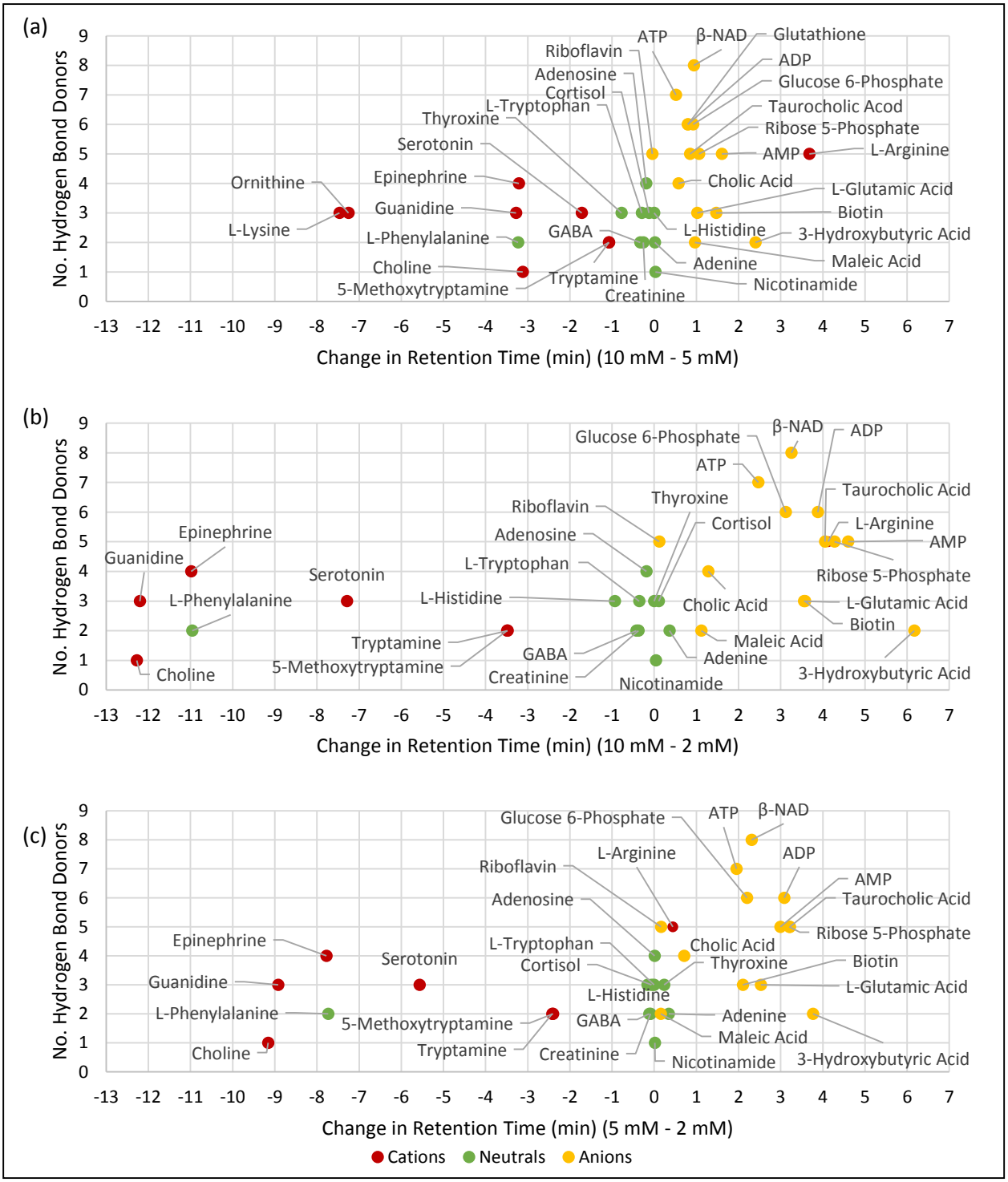

Figure 2.4 Retention time changes observed for standard metabolites by increasing ammonium acetate concentration in mobile phase between (a) 5 mM and 10 mM, (b) 2 mM and 10 mM, and (c) 2 mM and 5 mM, plotted against the number of hydrogen bond donors for each standard metabolite. Obtained using the ZIC-HILIC column.

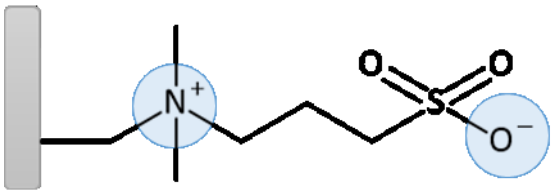

Figure 2.5 ZIC-HILIC stationary phase with charges on the quaternary amine and sulfonate groups highlighted. The distal negative charge is dominant in electrostatic interactions due to accessibility.

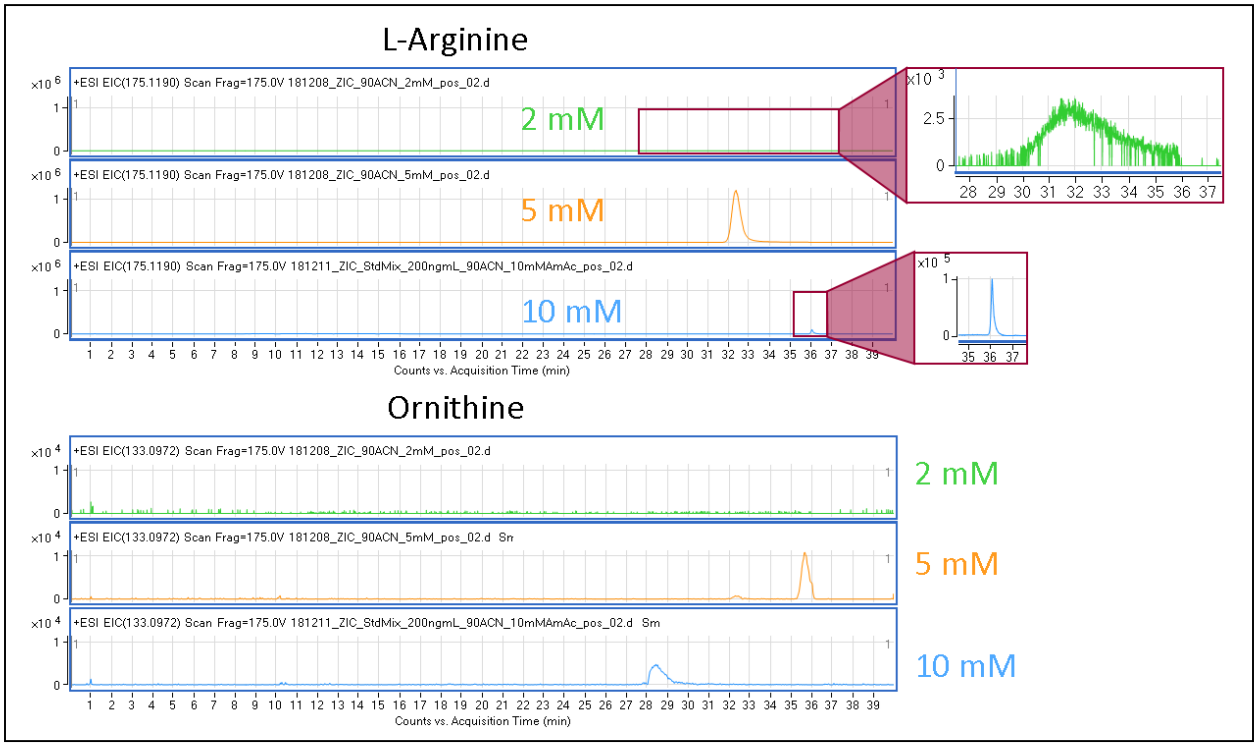

Figure 2.6 EICs of L-arginine and ornithine analyzed using mobile phase ammonium acetate concentrations of 2 mM, 5 mM, and 10 mM on the ZIC-HILIC column.

A greater difference in retention time is observed between 2 mM and 5 mM ammonium acetate than 5 mM and 10 mM suggesting that the effect of mobile phase salt concentration is not linear and there is a limit to its effect. This non-linear effect is consistent with results shown by Alpert[153] and may be the result of the contributions from multiple competing retention mechanisms. As salt concentration is increased, it acts as counter ions titrating the charges on the stationary phase.[153] As 10 mM ammonium acetate was the highest concentration soluble in 5/95 water/ACN, there is also a practical limit to the use of salt to alter column selectivity. The salt concentration is also limited by the compatibility with the method of

detection. In case of MS detection, increasing the concentration of mobile phase additives may start to suppress ionization of analytes and lower MS signal.

In summary, 5 mM ammonium acetate was determined to be the best choice for mobile phase concentration, providing adequate separation of the standard mixture and allowing for the detection of the most number of the tested metabolite standards (35 of 37). Estrone glucuronide was not detectable with 10 mM ammonium acetate. This concentration is lower than used in other key studies that compared HILIC stationary phase performance for metabolomics, such as Contrepois *et al.*[110] who used 10 mM ammonium acetate and Wernisch and Pennathur[103] who used 20 mM ammonium carbonate in the aqueous phase only.

2.4.2 Comparing Silica and Sulfobetaine Stationary Phases Using Polar Standard Metabolites

The distribution of standard metabolites along the chromatographic run time for each column is shown in Figure 2.7. Based on the number of standards eluting in each minute of the chromatographic run, the silica HILIC column shows fewer instances of co-elution. The ZIC-HILIC column however shows more even use of the chromatographic space and the increased co-elution is due to the increase in number of standards detected from 23 with the silica HILIC column to 35 with the ZIC-HILIC column. Looking at the distribution of standards, the two stationary phases clearly show different selectivity. Figure 2.8 shows a comparison of the retention time for each metabolite standard detected on both columns. When grouped into standards carrying a negative, zero, or positive net charge, the effect of the difference in electrostatic interactions between the two columns becomes evident. Uncharged and neutral standards, unaffected by the charge of the two stationary phases, had very similar retention times on both columns. Theoretically, cationic analytes should show increased retention time on the silica column due to the stronger electrostatic attraction with the negatively charged silica, while anionic analytes should show increased retention time on the ZIC-HILIC column due to the weaker repulsion with the negative charge of the sulfonate and the added attractive electrostatic interaction with the positively charged quaternary amine. This was observed in Figure 2.8 with the exception of guanidine and serotonin for the positively charged analytes and biotin and cholic acid for the negatively charged analytes. These outliers could be due to the influence of retention mechanisms other than electrostatic interactions. In addition, the charged groups on serotonin, biotin, and cholic acid are located at the end of alkyl chains with multiple rotatable bonds which could allow them greater access to the positive charge of the stationary phase quaternary amine. Guanidine is the smallest

of the standards and carries its charge at the end of the molecule which could also facilitate greater access to the positive charge of the ZIC-HILIC stationary phase allowing it greater influence on retention.

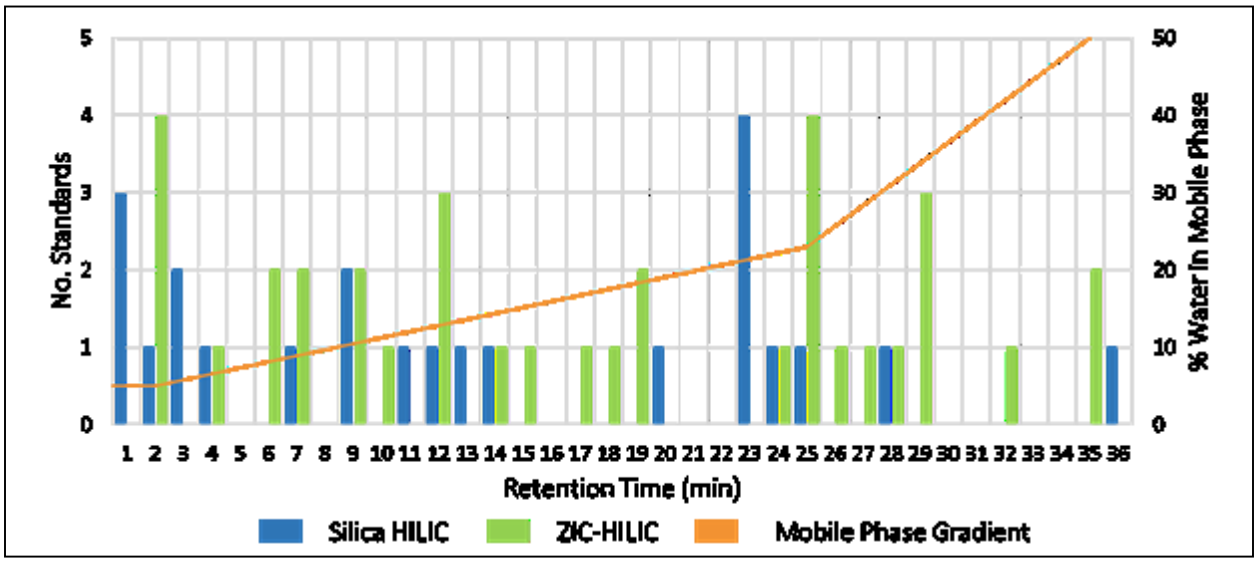

Figure 2.7 Distribution of standard metabolites across the method run time on the ZIC-HILIC column (green), and on the silica HILIC column (blue). Combined results for positive and negative ESI. Obtained using 5 mM mobile phase ammonium acetate concentration.

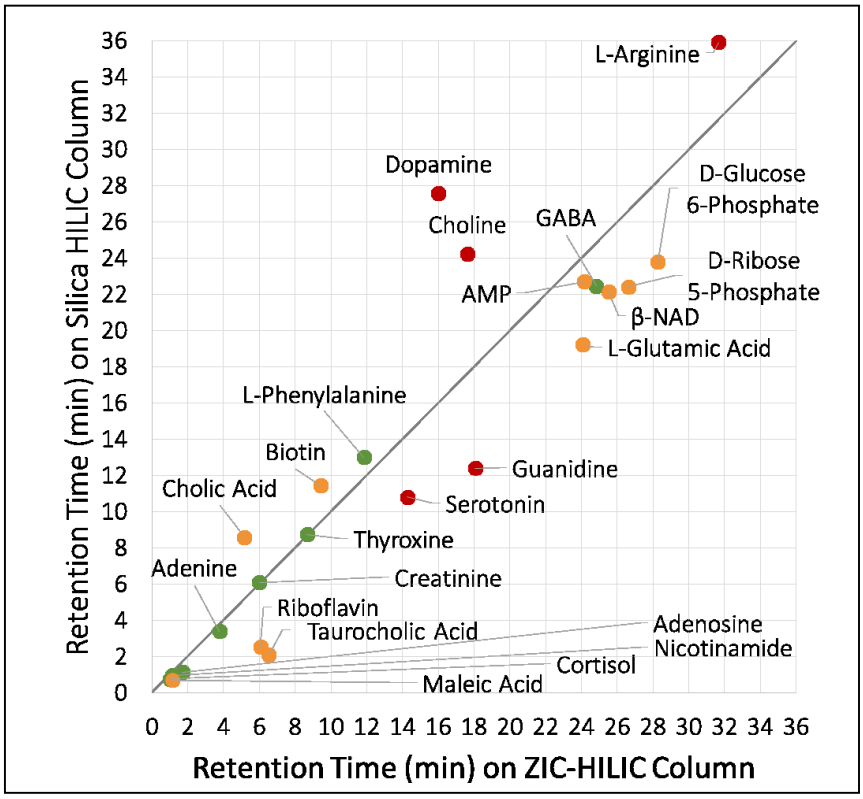

Figure 2.8 A comparison of retention times for standard metabolites between the ZIC-HILIC column and the Silica HILIC column. Obtained using 5 mM mobile phase ammonium acetate concentration.

A scoring system, summarized in Table 2.6, was devised to aid in the evaluation of the performance of each column for each metabolite standard. The scoring scheme included capacity factor, k', to account for adequate retention, baseline peak width and peak symmetry to account for peak quality, and a visual inspection of each peak as a secondary check of peak quality.

Adequate retention of each standard metabolite is crucial to avoid elution at or near the void volume of the column where a large number of unretained compounds elute leading to ionization suppression in the ESI source. Capacity factor was calculated according to Equation 2.1 where t_R is the retention time of the peak in minutes and t_O is the void volume of the column in minutes.

Equation 2.1 Capacity factor

$$k' = \frac{t_R - t_O}{t_O}$$

Peaks with a capacity factor of less than one were automatically given a final classification of unacceptable. Peaks with a capacity factor greater than one but less than two, indicating a retention time between the void volume and twice the void volume, were scored as acceptable while those with a capacity factor greater than or equal to two were scored as good.

Peak width was used as an indicator of peak quality given that a narrower elution profile provides a greater signal improving the limits of detection of a LC-MS method. Additionally, narrower peaks improve chromatographic resolution and facilitate peak detection and integration by data analysis software.

Peak symmetry was used as an indicator of peak shape quality where an ideal peak would have a Gaussian shape, absent of any peak fronting or tailing. Peak symmetry was calculated for each standard metabolite peak by the Agilent MassHunter TOF Qualitative Analysis software using Equation 2.2 through Equation 2.6 as shown in Figure 2.9 where a is the area of each slice of the peak, t is the time of each slice of the peak, H_f and H_r are the height of the front and rear inflection points respectively, and H is the height of the peak. In this data set, symmetry values ranged from 0.09 to 13.28.

Equation 2.2 First preliminary peak symmetry calculation

$$m_1 = a_1(t_2 + \frac{a_1}{1.5H_f})$$

Equation 2.3 Second preliminary peak symmetry calculation

$$m_2 = \frac{a_2^2}{0.5H_f + 1.5H}$$

Equation 2.4 Third preliminary peak symmetry calculation

$$m_3 = \frac{a_3^2}{0.5H_r + 1.5H}$$

Equation 2.5 Fourth preliminary peak symmetry calculation

$$m_4 = a_4(t_3 + \frac{a_4}{1.5H_r})$$

Equation 2.6 Peak symmetry

$$Peak\ Symmetry = \sqrt{\frac{m_1 + m_2}{m_3 + m_4}}$$

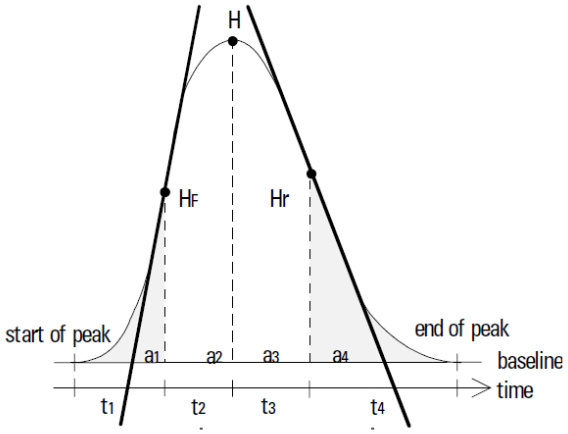

Figure 2.9 Schematic demonstrating peak symmetry calculation by Agilent MassHunter Qualitative Analysis software.[154]

Finally, a visual inspection of each standard metabolite peak was performed to check for irregular peak shapes, multiple peaks, and to discern any subtleties missed by the software. The individual score for each category was summed for each peak to provide a final classification of good, acceptable, or unacceptable as shown in Table 2.7.

Table 2.6 Breakdown of the scoring system used in the evaluation of standard metabolite peaks

Attribute	Scoring			
	Good	Acceptable	Unacceptable	No Peak
	"+1"	"0"	"-1"	NA
k'	≥2	2<k'≤1	<1 *	NA
Baseline Peak Width (min)	<1.0	1.0≤Width<2.5	≥2.5	NA
Peak Symmetry	0.5≤Symmetry<1.5	Symmetry<0.5 or 1.5≤Symmetry<2.5	≥2.5	NA
Visual Inspection	Good	Acceptable	Unacceptable	No Peak

Table 2.7 Determination of the final assignment of peak quality for standard metabolites

Final Score	
Good	≥3
Acceptable	2
Unacceptable*	1
No Peak	NA
*Compounds with an unacceptable k' score were automatically defined as unacceptable.	

The results of scoring each standard metabolite are shown in Figure 2.10 and example EICs of different quality peaks are shown in Figure 2.11. In total, the ZIC-HILIC column provided good, acceptable, and unacceptable peaks for 14, 5, and 16 of the standards respectively. Two standard metabolites could not be detected using this column. Overall, this represents a 53% increase in good/acceptable peaks over the silica column which provided good, acceptable, and unacceptable peaks for 7, 2, and 14 of the standards respectively and no detectable peaks for 14 standard metabolites. The two columns show a large amount of overlap, with only one standard, biotin, with good/acceptable peak quality being detected with the silica column that was not detected with good/acceptable peak quality with the ZIC-HILIC column. This indicates that there would be little benefit in using both columns to analyze a sample, especially given the increased analysis time.

The ZIC-HILIC is a weaker electrostatic interactor than the silica column, decreasing its effect on retention, lessening the effect of multiple competing retention mechanisms, decreasing peak width and improving peak symmetry. The four standards that showed improved performance on the ZIC-HILIC column compared to the silica column all carry a net negative charge. L-glutamic acid, AMP, and β-NAD had

improved peak symmetry while taurocholic acid had increased retention on the ZIC-HILIC to achieve a capacity factor greater than two. This is attributable to the decreased repulsion from the negative charge of the ZIC-HILIC compared to the silica as well as the added attractive interaction with the positive charge of the ZIC-HILIC column. Of the eleven standards seen with the ZIC-HILIC but not the silica, seven achieved good/acceptable scores, all of which carry a charge. While stationary phases with electrostatic interaction capability were chosen over a neutral stationary phase to aid with the separation of charged polar species, these results suggest that the weaker electrostatic interactions of the ZIC-HILIC column provide improved results over a stronger electrostatic interactor such as the silica column. Nine standards were observed with unacceptable peak quality on both columns. Three, cortisol, maleic acid, and nicotinamide, were poorly retained with capacity factors less than one. Cortisol was included in the standard mixture as a hydrophobic marker and was not expected to be retained. The remaining six all showed poor peak symmetry. L-phenylalanine, adenosine, and choline had large baseline peak widths and adenosine also had a capacity factor of 0.61 on the silica column and 1.43 on the ZIC-HILIC column.

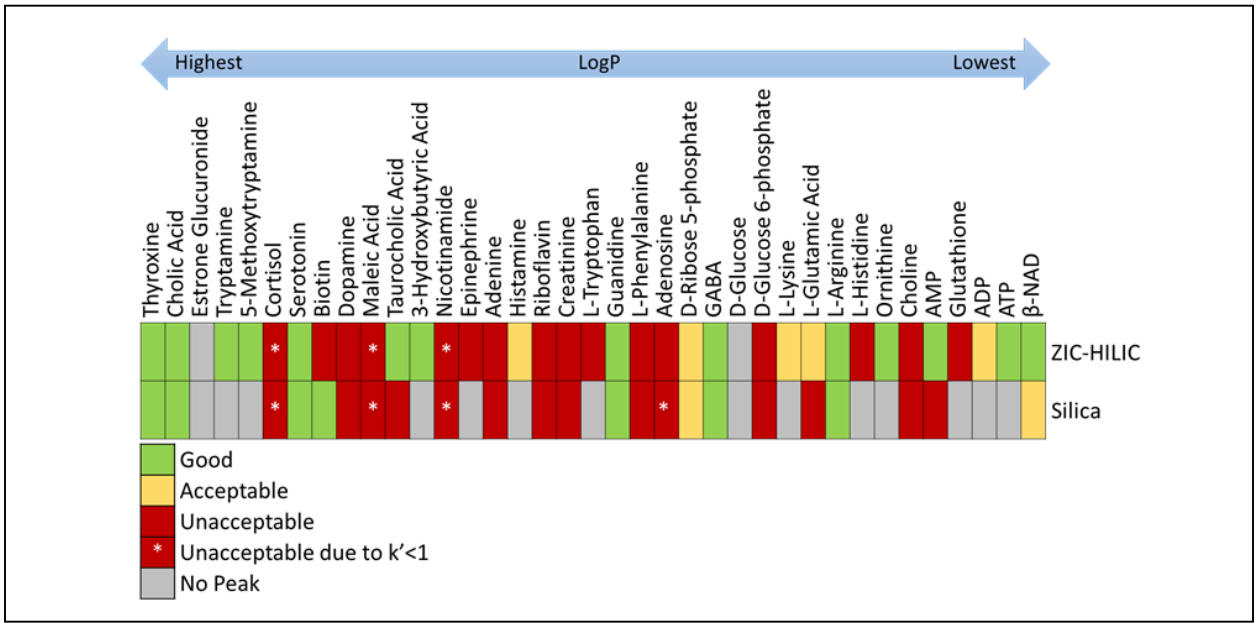

Figure 2.10 Peak quality assignment for standard metabolites analyzed on both the silica HILIC and ZIC-HILIC columns using 5 mM mobile phase ammonium acetate concentration.

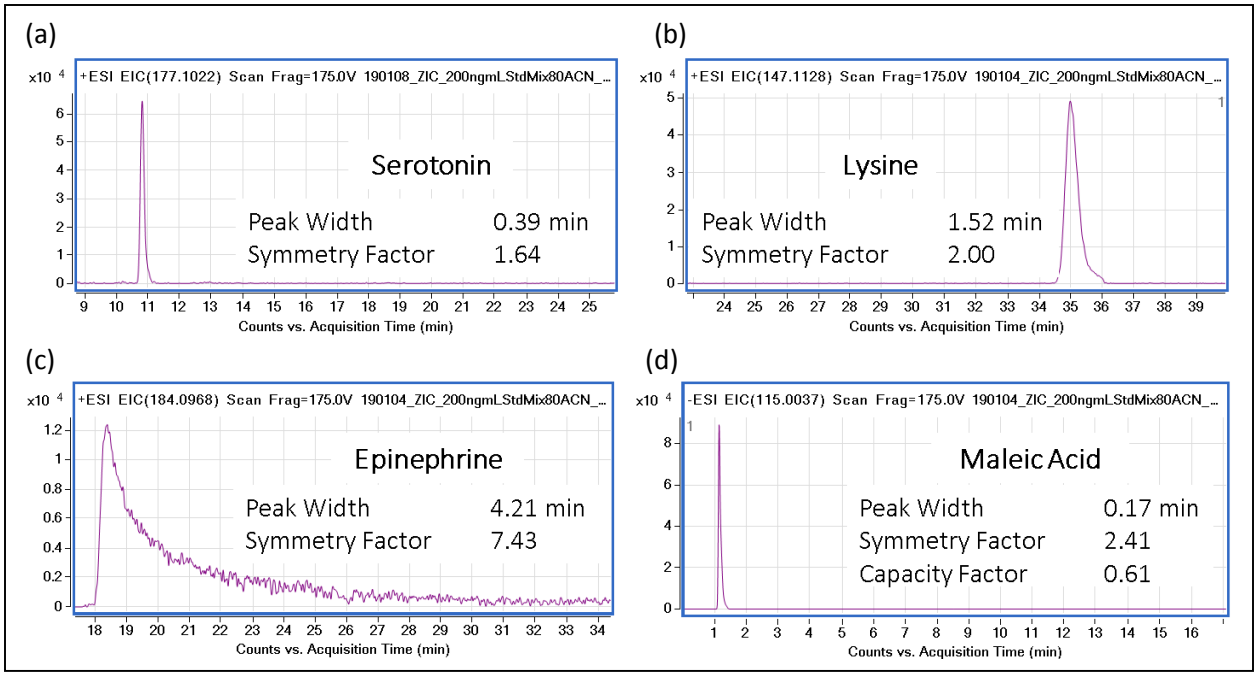

Figure 2.11 Example EICs showing (a) good quality peak for serotonin on the Silica HILIC column, (b) acceptable quality peak for L-lysine on the ZIC-HILIC column, (c) unacceptable quality peak for epinephrine on the ZIC-HILIC column, and (d) unacceptable quality peak for maleic acid on the ZIC-HILIC column due to an unacceptable capacity factor value. All standards analyzed at 200 ng/mL. Obtained using 5 mM mobile phase ammonium acetate concentration.

2.4.3 Comparing Silica and Sulfobetaine Stationary Phases Using Human Plasma Samples

The distribution of compounds detected in methanol-precipitated plasma for each column are shown in Figure 2.12. Metabolite maps of the detected compounds are shown in Figure 2.13. The compounds shown were detected in all 12 plasma replicates, 6 without ammonium phosphate added to the sample, and 6 with ammonium phosphate added. The data sets were not curated, however visual inspection confirmed that the majority of peaks were correctly picked by the software. A total of 1612 compounds were detected on the ZIC-HILIC column with positive ESI and 1643 compounds with negative ESI. A total of 3520 compounds were detected on the silica column with positive ESI and 2734 compounds with negative ESI, which represents a 118% and 66% increase in coverage respectively. While more compounds were detected with the silica column, the ZIC-HILIC column made better use of the chromatographic space, especially in negative ESI, and provided superior peak shapes. Improved use of the chromatographic space could possibly be achieved through further optimization of the gradient specific to each stationary phase. The distribution of compounds detected shows areas of high co-elution. To

investigate whether these regions of co-elution belong to phospholipids, the chromatographic behavior of a series of phospholipid standards was investigated in the next section.

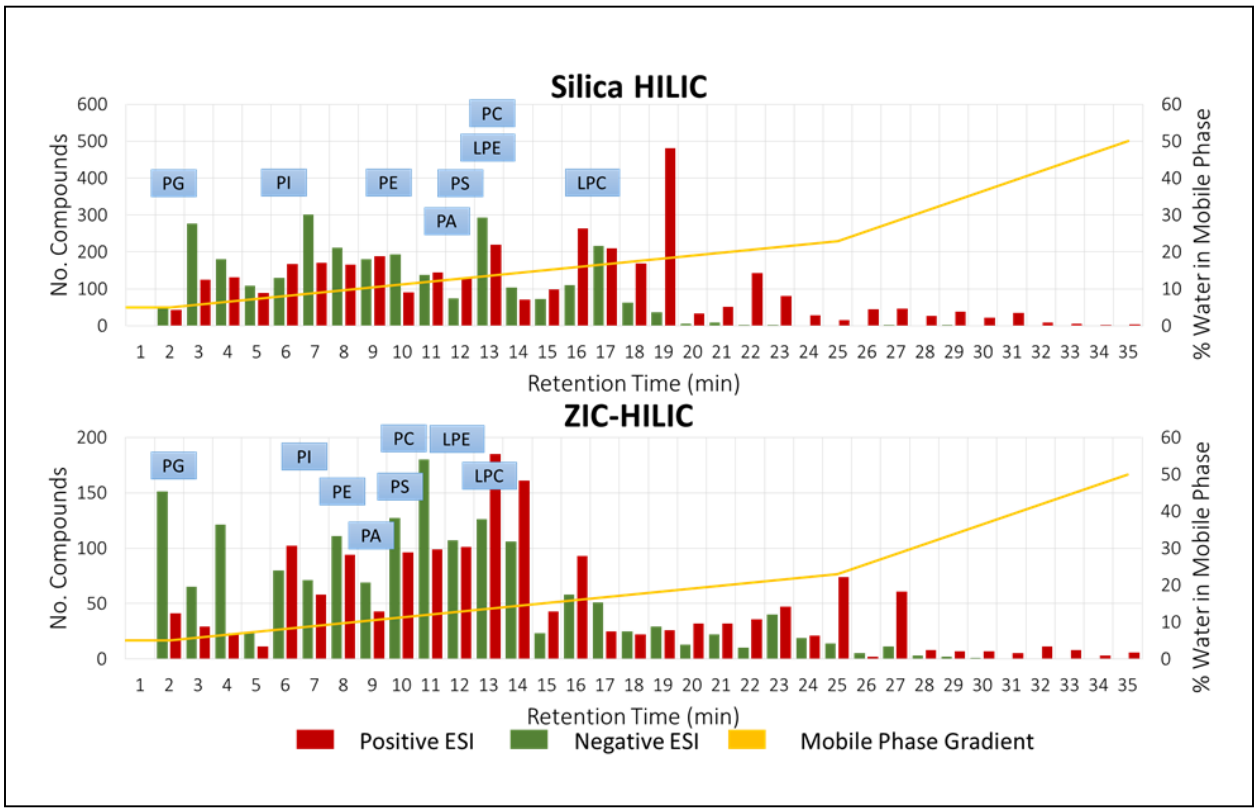

Figure 2.12 Distribution of compounds detected in 12/12 methanol-precipitated plasma samples using positive and negative ESI by analysis with the silica HILIC and ZIC-HILIC columns. Global data analysis was performed between run times of 1 and 35 min and all compounds with a mass greater than 1100 Da were removed.

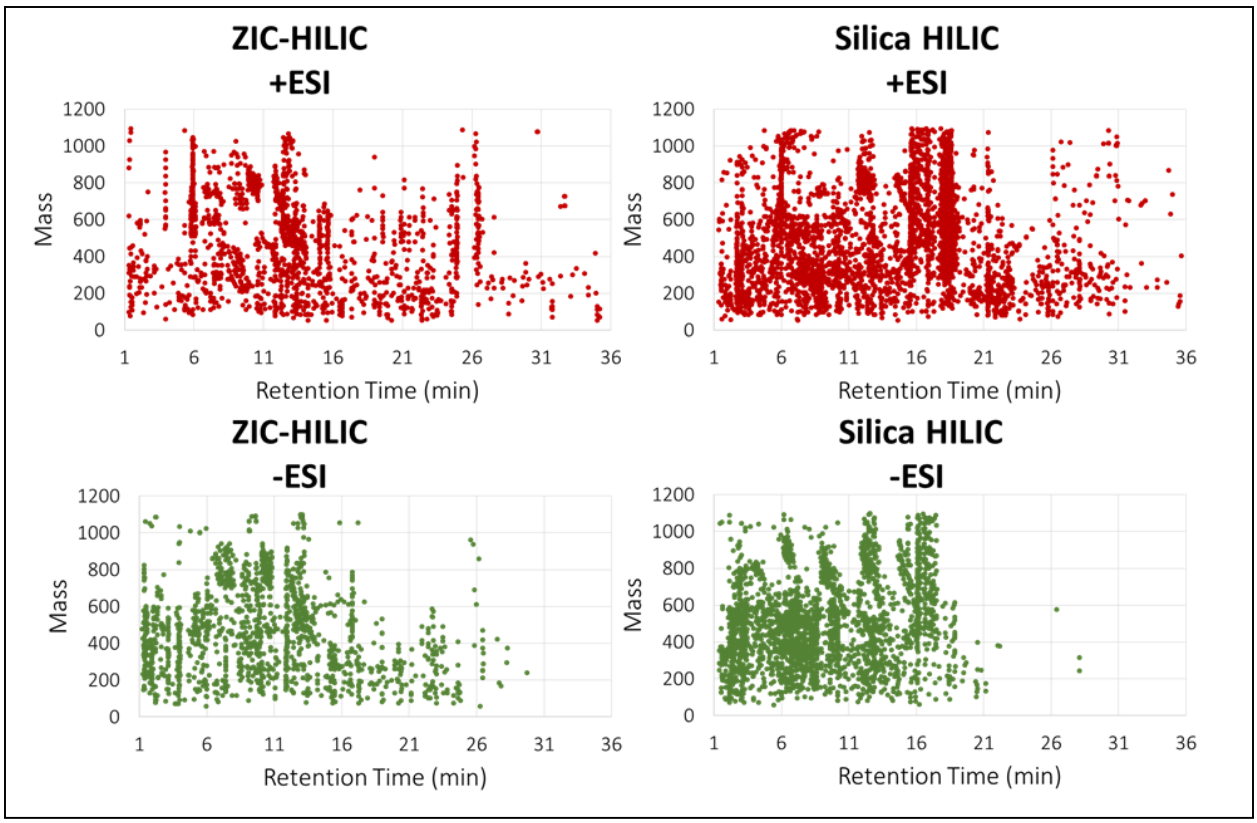

Figure 2.13 Metabolite maps of compounds detected in 12/12 methanol-precipitated plasma samples using positive and negative ESI by analysis with the silica HILIC and ZIC-HILIC columns. Global data analysis was performed for 1 to 35 min retention time range and all compounds with a mass greater than 1100 Da were removed.

2.4.4 Analysis of Phospholipid Standards on Silica and Sulfobetaine Stationary Phases

As amphiphilic compounds, phospholipids are separated by HILIC according to the hydrophilicity of their polar head groups, and not by their fatty acyl chain length and degree of unsaturation as they are by RPLC. Phospholipids make up the majority of biological membranes, and are therefore present in biological samples in significant concentrations.[111,155] Phospholipids are also known to be a source of matrix effects, especially the phosphatidylcholines (PC) and lyso phosphatidylcholines (LPC).[155] To determine the retention times for phospholipid classes, standards were analyzed on the silica and ZIC HILIC columns. The results of this analysis are summarized in Table 2.8. The EICs shown in Figure 2.14 demonstrate that phospholipids of the same class, yet with different carbon chain lengths and degrees of unsaturation elute within a narrow retention time window. Longer-chain lipids elute with slightly shorter retention times than shorter lipids, but may not be fully chromatographically separated as is well-known for lipid analysis by HILIC. The EICs of phospholipids also demonstrate that the peak shapes for phospholipids were narrower and of better

quality on the ZIC-HILIC column. Figure 2.15a shows that the elution order for phospholipid classes is the same on both columns. This elution order is consistent with elution orders reported in literature on silica stationary phases.[156,157] When looking at the effect of phospholipid physico-chemical properties with respect to the observed retention times, no trend was observed for the logP values or charge. A comparison of polar surface area to retention time, as shown in Figure 2.15b, shows that retention time increases with decreasing polar surface area. This result is unexpected since more polar compounds are typically more retained with HILIC. When comparing the retention times of phospholipid classes to the methanol-precipitated plasma results, the retention times for all phospholipid classes do not align with the areas of high co-elution, however some correlation between areas of high o-elution and phospholipid classes can be observed. For example, phosphatidylcholines elute in areas of high co-elution with both the silica and ZIC-HILIC columns.

Table 2.8 A summary of retention times and extracted m/z for phospholipid analysis on the silica HILIC and ZIC-HILIC columns.

Lipid Standard	Adduct	m/z	Retention Time (min)	
			Silica HILIC	ZIC-HILIC
PE (12:0/13:0)	$[M-H]^-$	592.39782	10.13	8.56
PE (15:0/15:0)		662.47607	9.79	8.28
PE (16:0/16:0)		690.50737	9.67	8.21
PS (12:0/13:0)	$[M-H]^-$	636.38765	12.18	10.08
PS (17:0/17:0)		762.52850	11.71	9.36
LPE (13:0)	$[M-H]^-$	410.23076	13.45	11.78
PC (16:0/16:0)	$[M+CH_3COO]^-$	792.57545	13.00	10.88
PC (17:0/17:0)		820.60675	12.93	10.85
LPC (16:0)	$[M+CH_3COO]^-$	554.34579	16.90	13.42
LPC (17:0)		568.36144	16.66	13.34
PI (16:0/16:0)	$[M-H]^-$	809.51850	6.45	7.44
PI (17:0/20:4)		871.53365	5.83	6.85
PA (17:0/17:0)	$[M-H]^-$	675.49648	12.32	9.65
PA (18:0/18:0)		703.52778	12.34	9.52
PG (17:0/17:0)	$[M-H]^-$	749.53326	2.59	2.32
PG (18:0/18:0)		777.56456	2.56	2.30

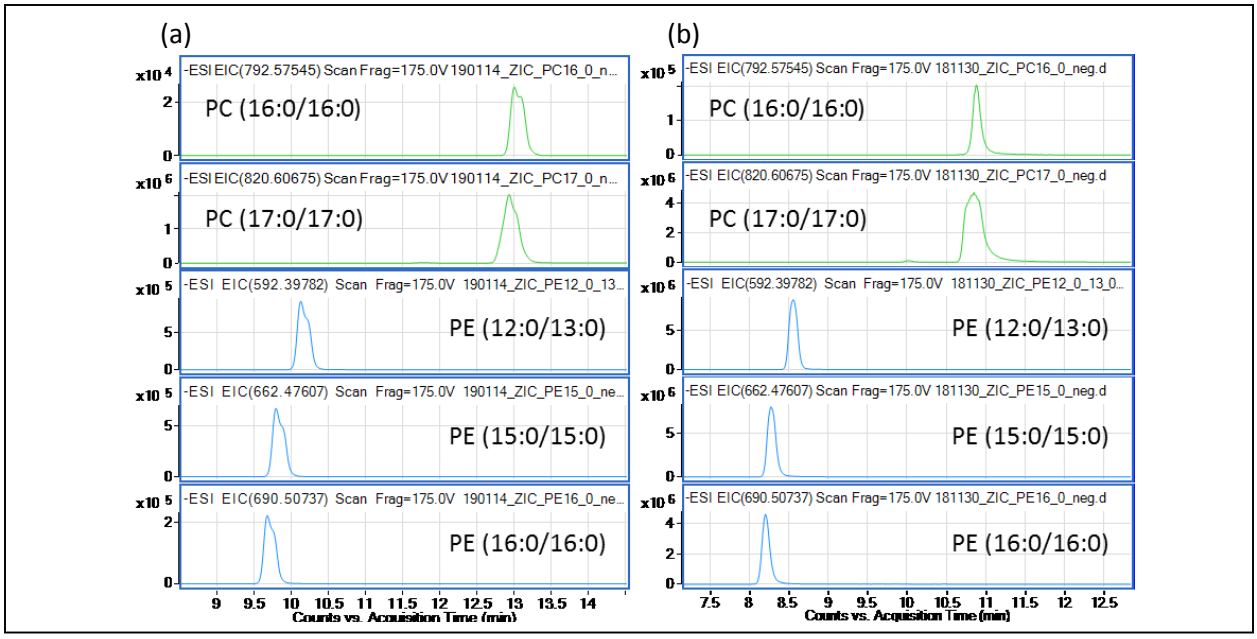

Figure 2.14 Sample EICs for phospholipid standards analyzed on (a) the silica HILIC column and (b) the ZIC-HILIC method demonstrating the co-elution or elution in narrow retention time window of phospholipids of the same class: phosphatidylcholines (PC) (100 ng/mL) in green and phosphatidylethanolamines (PE) (500 ng/mL) in blue.

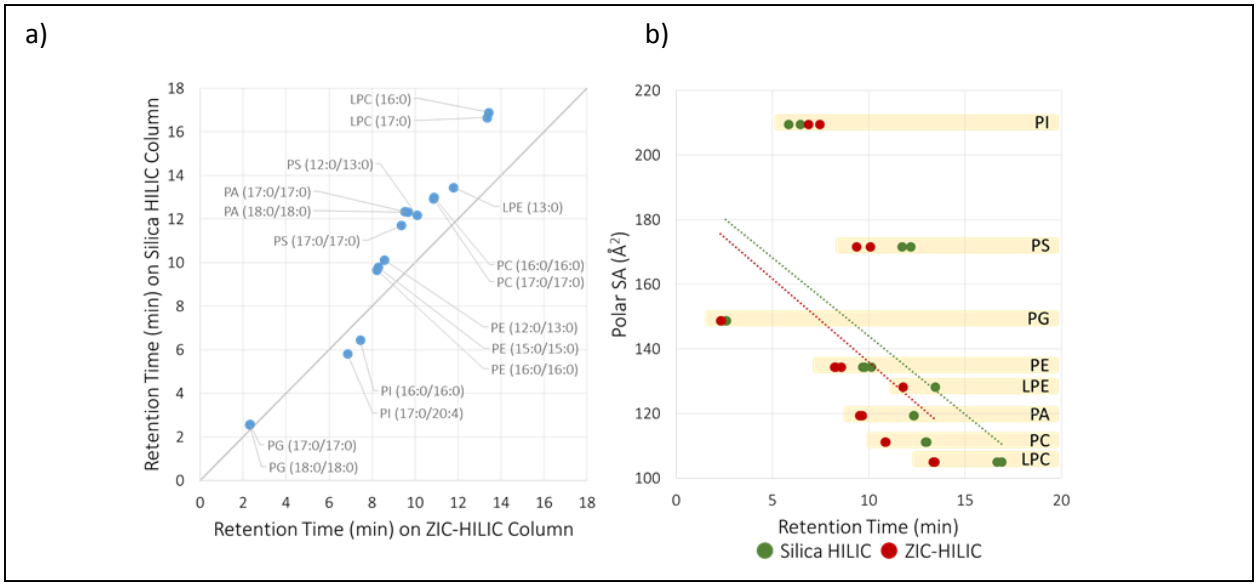

Figure 2.15 a) A comparison of phospholipid standard retention times between the ZIC-HILIC and silica HILIC columns with line showing where retention times would fall if retention was identical on both columns. b) A plot of phospholipid polar surface area vs. retention time with trendlines showing the relationship between the two. (Silica HILIC: SA = $-4.8372t_R + 192.37$, $R^2 = 0.3804$ ZIC-HILIC: SA = $-5.1504t_R + 187.41$, $R^2 = 0.2389$) Obtained using 5 mM mobile phase ammonium acetate concentration.

2.4.5 Effect of Addition of 10 mM Ammonium Phosphate on Analyte Peak Shape and Metabolite Coverage

2.4.5.1 Addition of 10 mM Ammonium Phosphate to Standards

Spalding *et al.*[149] recently reported that the addition of millimolar ammonium phosphate to samples or micromolar ammonium phosphate to the mobile phase improves peak shape, MS signal intensity, and coverage for metabolomics analysis executed on the ZIC-pHILIC column. They found that both approaches were equivalent in terms of improvement achieved. Addition to the sample was chosen for this work to facilitate side-by-side comparison of the two conditions. It was proposed that these effects are due to the shielding, by the phosphate ions, of electrostatic interactions that cause poor peak shapes. A decrease in electrostatic interactions decreases the competition between retention mechanisms, resulting in narrower peaks with improved symmetry. Figure 2.16 shows the peak quality scores for each standard on each column both with and without ammonium phosphate added to the sample. This effect was observed for all of the ten standards with improved scores on the ZIC-HILIC column and five standards with improved scores on the silica HILIC column. For example, L-tryptophan displayed decreased baseline peak width and improved symmetry as shown in Figure 2.17.

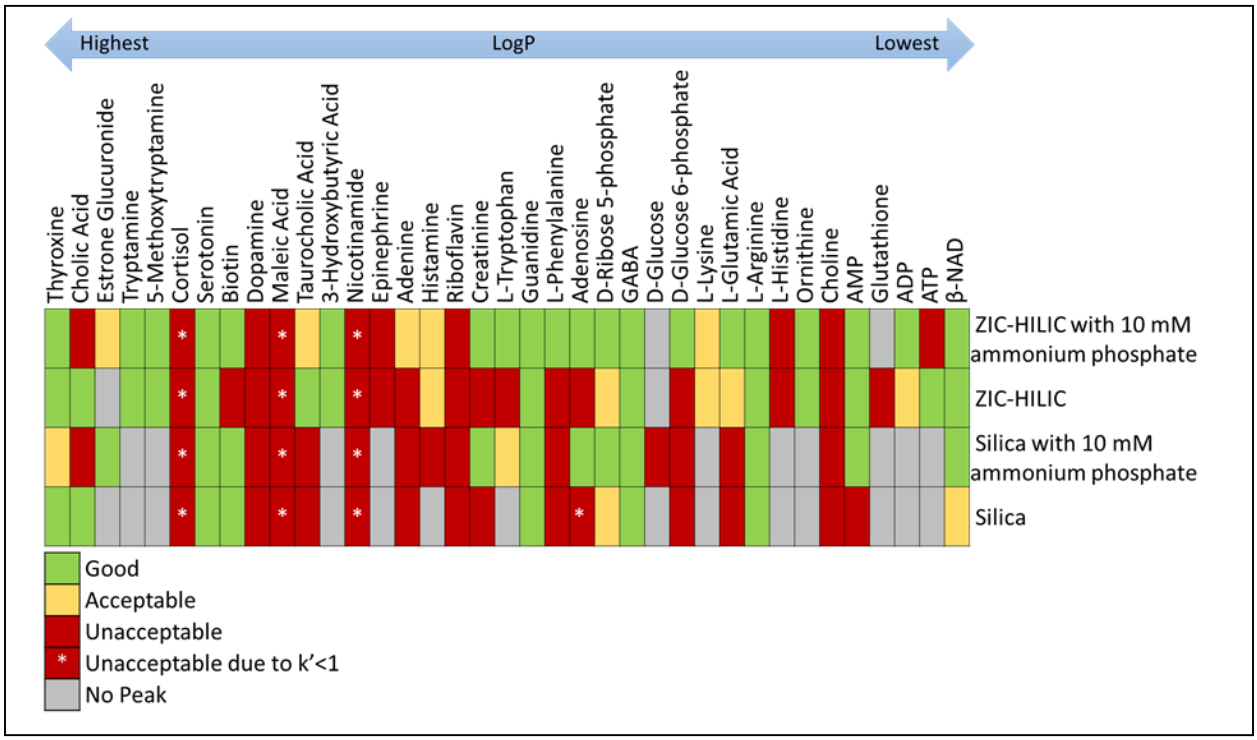

Figure 2.16 Peak quality assignment for standard metabolites analyzed on both the silica HILIC and ZIC-HILIC columns with and without 10 mM ammonium phosphate added to the sample.

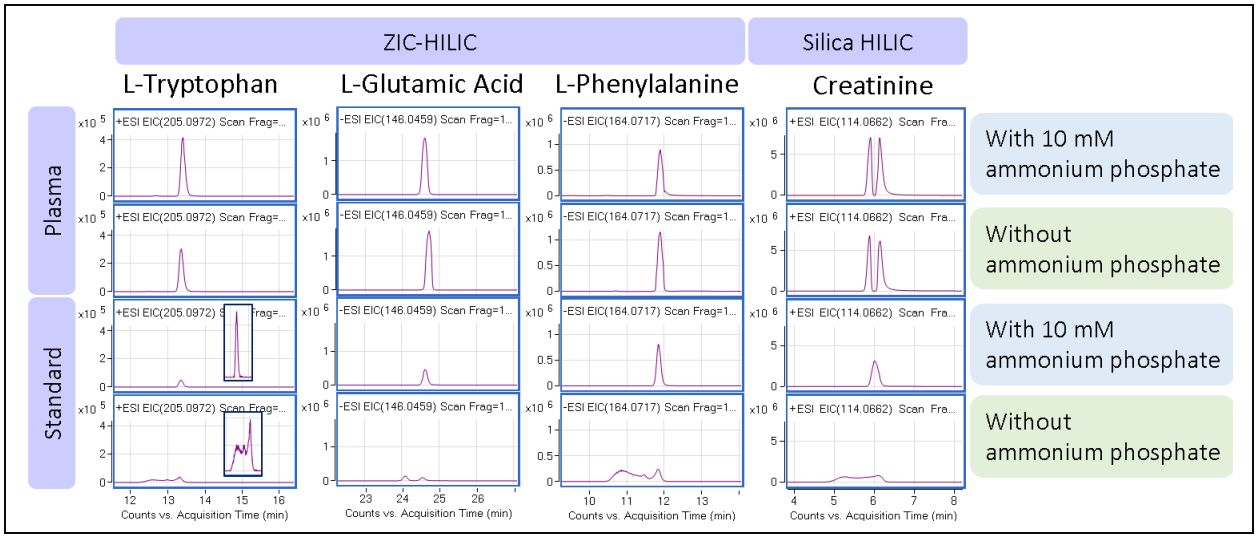

Figure 2.17 EICs for standards in solvent (200 ng/mL) and plasma showing the effect of adding 10 mM ammonium phosphate to the sample. Samples were analyzed using either the ZIC-HILIC column or Silica HILIC column and using 5 mM mobile phase ammonium acetate concentration.

2.4.5.2 Addition of 10 mM Ammonium Phosphate to Human Plasma

The effect of ammonium phosphate addition on plasma analysis was evaluated by analyzing six replicates of each with all twelve samples analyzed in a randomized order. Methanol-precipitated plasma results show that the addition of 10 mM ammonium phosphate to the reconstitution solvent increased the number of compounds detected for the ZIC-HILIC column in positive ionization mode only. The number of compounds unique to each sample and shared between the two for each column and each ionization mode are displayed in Figure 2.18. The results indicate that the addition of phosphate to the sample improves the detection of many compounds, it is also detrimental to the detection of many others. The metabolite maps in Figure 2.19 show that the effects of ammonium phosphate in the sample are not more distinct at any given retention time or mass range.

The addition of ammonium phosphate to plasma samples allowed for the detection of new compounds at the expense of others. There is not clear cut evidence for the benefit of ammonium phosphate to plasma samples. This difference in results compared to that seen on the ZIC-pHILIC could be due to the difference in support material, specifically the type and number of electrostatic sites. Additionally, the discrepancy between peak shape improvement of standards in solvent compared to the lack of peak shape change for plasma samples could be due to the matrix which contains a large concentration of ions such as sodium (endogenous concentration in blood of 140 mM), potassium (4.2 mM), chloride (100 mM), and phosphate (1.1 mM) which could serve the same function as the added ammonium phosphate making

it redundant. It is also possible that the use of sodium citrate as an anticoagulant during plasma collection contributes a sufficient number of ions to negate the need to add ammonium phosphate to samples.

Table 2.9 Number of compounds detected in methanol-precipitated plasma for each column with and without 10 mM ammonium phosphate added to the samples

	ZIC-HILIC Column		Silica Column	
	+ESI	-ESI	+ESI	-ESI
Without ammonium phosphate	1755	2195	4165	3142
With 10 mM ammonium phosphate	1923	2033	3963	3111

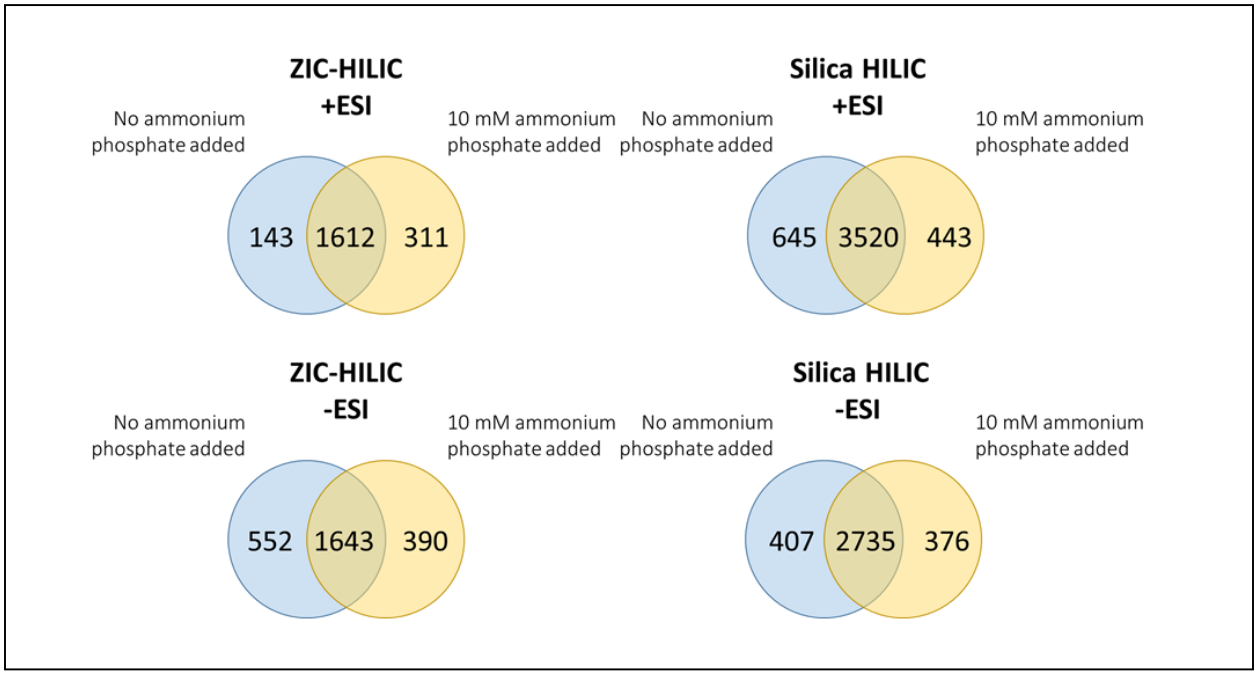

Figure 2.18 Venn diagrams comparing the number of compounds detected in methanol-precipitated human plasma samples with and without 10 mM ammonium phosphate added to the reconstitution solvent using positive and negative ESI by analysis with the silica HILIC and ZIC-HILIC columns. Global data analysis was performed in the retention time window of 1 to 35 min and all compounds with a mass greater than 1100 Da were removed. The reported compounds were detected in 6/6 replicates for each condition.

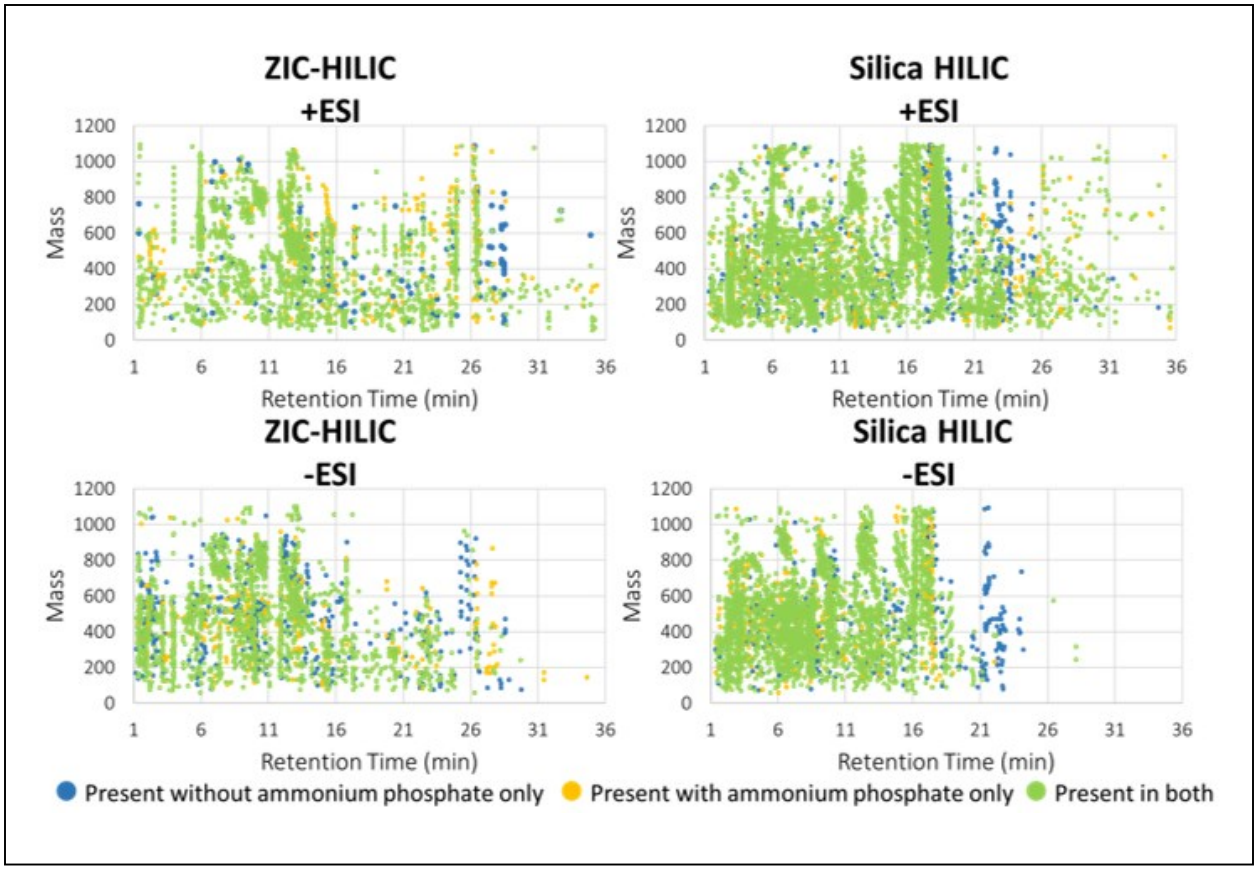

Figure 2.19 Metabolite maps comparing compounds detected in methanol-precipitated human plasma samples with and without 10 mM ammonium phosphate added to the reconstitution solvent using positive and negative ESI by analysis with the silica HILIC and ZIC-HILIC columns. Global data analysis was performed in the retention time window of 1 to 35 min and all compounds with a mass greater than 1100 Da were removed. The reported compounds were detected in 6/6 replicates for each condition.

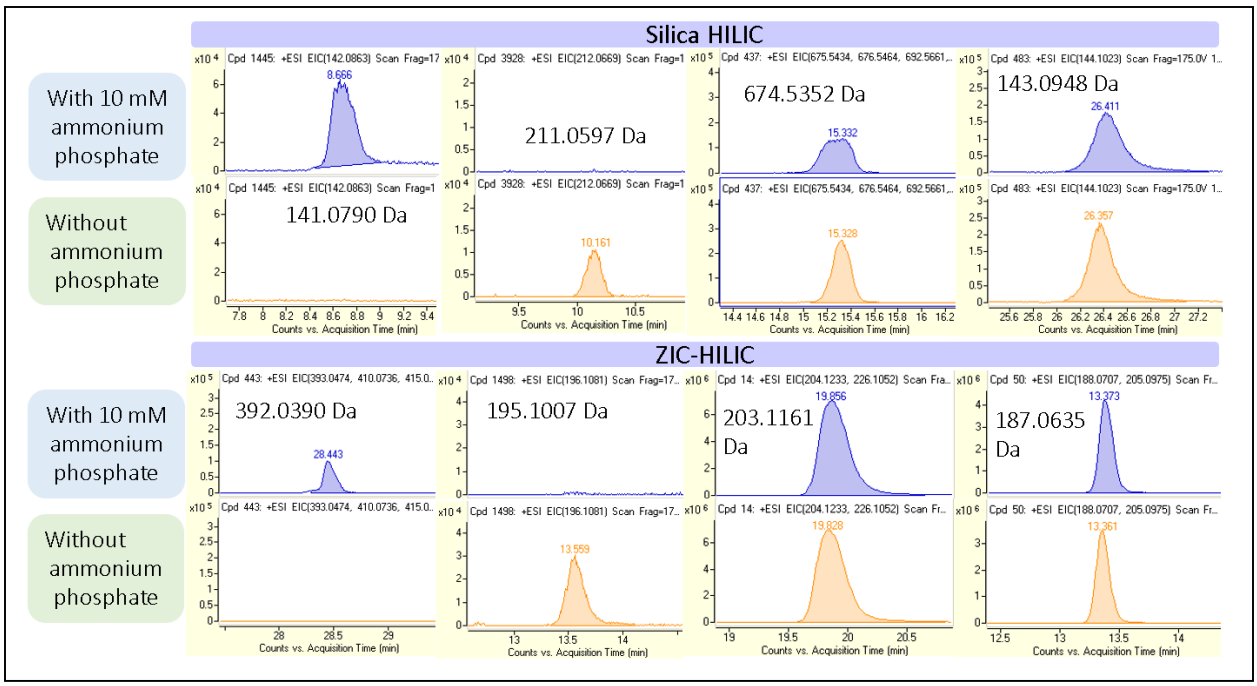

Figure 2.20 Examples of compounds detected by global processing of human plasma samples for the comparison of 10 mM ammonium phosphate addition. Peaks shown in blue were detected in samples with 10 mM ammonium phosphate added to the reconstitution solvent while peaks shown in yellow were detected in samples with no ammonium phosphate in the reconstitution solvent. Pairs of peaks demonstrate the effect on ammonium phosphate inclusion.

2.5 Conclusions

Hydrophilic interaction liquid chromatography is used in metabolomics to separate the polar metabolome before detection by MS. A multitude of polar stationary phases are available for HILIC applications and while there is no consensus in the literature on which is the best performing, a growing interest in zwitterionic phases prompted this comparison of the ZIC-HILIC column against an underivatized silica column. During method development, the effect of mobile phase salt concentration was evaluated with the ZIC-HILIC column, showing its different effects on analytes carrying different charges, and it was determined that 5 mM ammonium acetate was optimal. Analysis of a mixture of metabolite standards showed an increase in the number of standards detected as well as the quality of the peaks with the ZIC-HILIC column. Surprisingly, the analysis of human plasma samples showed that more compounds were detected with the silica HILIC column however the peak shapes obtained using the ZIC-HILIC column were of a higher caliber which could improve the performance of peak picking performed by data analysis software. Further investigation of the plasma results for each column, including curation of the plasma

data sets is required to compare the number of compounds with high quality results detectable using each column. The addition of 10 mM ammonium phosphate to samples improved peak shape, both decreasing baseline peak width and improving symmetry, for several standards on both columns, however, for plasma samples, the addition of ammonium phosphate to the reconstitution solvent showed no clear advantage over solvent alone. One hypothesis to explain this discrepancy between the results for standards and plasma is that plasma samples already contain large concentrations of endogenous ions, for example sodium, potassium, and carbonate, and sodium citrate anticoagulant which act similar to the phosphate, modulating electrostatic interactions between the analytes and stationary phase. Multiple hypotheses are possible to explain the discrepancy in results between those obtained here using the ZIC-HILIC column and those obtained by Splading *et al.*[149]. First, the ZIC-pHILIC uses a polymeric support which may carry positively charged electrostatic binding sites for the phosphate ions to interact with, while the ZIC-HILIC column uses a silica support which should carry negatively charged electrostatic binding sites. This could indicate that the improved performance for standards with the addition of ammonium phosphate was the result of the ammonium ions blocking electrostatic interactions rather than the phosphate ions. Second, the improvement in polar metabolome coverage observed by Spalding *et al*.[149] was for *E. coli* samples rather than plasma which would have contained different matrix components capable of influencing chromatographic separation. And third, since preliminary studies showed that greater that 20% in samples resulted in poor peak shape quality, the use of higher water content (33%) in samples by Spalding *et al*.[149] compared to the 20% water used in this study could have produced poorer initial peak shapes, leaving more room for improvement. These results indicate that for global metabolomics studies there is no clear benefit to adding trace levels of ammonium phosphate to methanol-precipitated plasma samples before HILIC analysis on either the silica or ZIC-HILIC columns. Targeted studies may observe improvements on an analyte specific basis.

Chapter 3: Evaluation of Carbon Nanopearls as Dispersive Solid-phase Microextraction Sorbent for Global Metabolomics of Human Plasma

3.1. Abstract

The goal of global metabolomics is the comprehensive study of all metabolites in a biological system. A variety of sample preparation methods have been developed in an attempt to achieve this goal including SPME. This technique has been implemented in multiple formats and using a large variety of sorbent materials, including carbon nanoparticles. In this study, a preliminary evaluation of the use of carbon nanopearls (CNPs) as a sorbent in the dispersive format of SPME was completed. A mixture of aromatic metabolite standards in both PBS and human plasma samples was used to evaluate the effect of varying extraction parameters. Aromatic metabolites were chosen given the hypothesized ability of the CNPs to interact with analytes through π-π interactions. The 24 metabolite standards covered a range of molecular weights (122 to 777 Da), and polarities (logP -4.8 to 3.73). The extraction efficiency and effect on extraction efficiency of varying extraction parameters such as extraction time, extraction temperature, and desorption solvent were evaluated. Results showed that equilibrium was achieved between sample and sorbent for standards in PBS within 2 minutes, however in the presence of the more complex matrix, plasma, equilibrium was not reached as quickly. The extraction of standards in PBS indicated higher selectivity of CNPs was for more hydrophobic analytes in the mixture, specifically flavonoids such as diosmin and diosmetin and iodo metabolites such as thyroxine and triiodothyronine. Similar selectivity for more hydrophobic compounds was also observed for plasma extracts. Additionally, it was determined that the evaporation of extracts followed by reconstitution in 90% water/10% MeOH prior to LC-MS analysis provided improved metabolome coverage and improved peak shapes for early eluting compounds.

3.2. Introduction

Metabolomics is the comprehensive study of all of the metabolites (low molecular weight compounds) in a biological system.[2] Sample preparation plays a key role in obtaining high quality data in metabolomics studies. The ideal sample preparation method for global metabolomics studies is non-selective, easy to implement, reproducible, quenches the metabolome, and produces an LC-MS compatible sample with the same metabolite content as the original sample.[14] Additionally it is beneficial if the sample preparation method improves the detection of low abundance metabolites by enrichment and/or removal of interferences to improve metabolome coverage.[6] Solid phase microextraction (SPME) is a non-exhaustive, equilibrium-based technique[25] that has been implemented in metabolomics studies in many forms[121,122],

using a wide variety of sorbents including commercially available sorbents[125], non-carbon sorbents (ex. metal oxide nanoparticles[118]), and carbon nanoparticle sorbents (ex. buckminsterfullerenes[125,158], carbon nanotubes[118,159,160], and graphene.[118,126]). Interest in carbon nanoparticles as sorbent has grown owing to their favourable physical and chemical characteristics which include large surface area[118], chemical stability, mechanical stability, thermal stability[118,126], and the possibility of surface functionalization[118]. The interest in these sorbents extends beyond metabolomics and they have been used to extract a variety of analytes, often with aromatic character, from a variety of sample types.[117,139–141,143,144] For example, Xiao *et al.* used buckminsterfullerenes immobilized on a fiber to extract polyaromatic hydrocarbons and showed that compared to commercial polydimethylsiloxane fibers, the ability to interact through π-π interaction favoured interactions between the sorbent and aromatic analytes, increasing extraction efficiency, selectivity, and sensitivity of the extraction.[158] Multi-walled carbon nanotubes have been shown to improve the enrichment of polybrominated diphenyl ethers from water and milk samples compared to commercial fibers[159] and it has been demonstrated that the surface of CNTs can be functionalized, through oxidation, to improve the extraction of more polar analytes such as phenols.[160]

Carbon nanopearls (CNPs) are solid spheres, with a diameter of 150 nm, composed of concentric layers of graphitic flakes (2 to 6 nm diameter) that form both amorphous and nanocrystalline structures in approximately 2 nm repeats.[132] Initially developed for use as cold cathodes in low vacuum conditions[132], CNPs have not, to date, been used as a sorbent for sample preparation. The overall objective of this study was to develop a protocol for the use of CNPs as a sorbent for D-SPME of human plasma for global metabolomics. To investigate the application of CNPs for this application, a standard mixture of 24 metabolites was chosen based on (1) commercial availability, (2) to cover a range of molecular weights, (3) to cover a range of polarities, (4) to include both high and low abundance metabolites, and (5) aromaticity. Samples were analyzed by LC-MS using a biphenyl RP column and Q-TOF mass spectrometer in both positive and negative mode ESI to maximize metabolome coverage and to provide good separation and retention of aromatic metabolites.

3.3. Experimental

3.3.1. Chemicals and Materials

Acetonitrile, methanol, water, and acetic acid, all LC-MS grade, were purchased from Fisher Scientific Inc. (Ottawa, ON, Canada). All metabolite standards and salts were purchased from Millipore Sigma (Oakville, ON, Canada). All lipid standards were purchased from Avanti Polar Lipids (Alabaster, AL, USA). Pooled human citrated plasma (lot# BRH1317314) was purchased from Bioreclamation IVT (Baltimore, MD, USA).

Carbon nanopearls were provided by Prof. Truong Vo-Van from the Department of Physics, Concordia University.

3.3.2. Preparation of Standard Mixture, Phosphate Buffered Saline, and Spiked Plasma Samples

Individual stock standard solutions of each metabolite were prepared at 1 mg/mL in the appropriate solvent, as indicated in Table 2.1. A stock standard mixture of all 24 standards was prepared at 10 µg/mL using methanol as a diluent. A working standard mixture for analysis was prepared at 100 ng/mL in 10% methanol/90% water. A calibration curve was constructed by 2x serial dilution of the working standard mixture with 10% methanol/90% water to a minimum concentration of 0.39 ng/mL.

Ten milliliters of 10x phosphate buffered saline (PBS) was prepared by dissolving 0.8 g of sodium chloride, 0.02 g of potassium chloride, 0.024 g of potassium phosphate monobasic, and 0.144 g of sodium phosphate dibasic in water. PBS (1x) was prepared by diluting 10x PBS one in ten with water and then adjusting the pH to 7.4 with sodium hydroxide or hydrochloric acid.

Standards in PBS and plasma was prepared by combining equal volumes of each individual stock standard solution, evaporating to dryness using a Savant Speedvac SPD111V (Thermo Scientific, Ottawa, ON, Canada) and then reconstituting to 10 µg/mL in PBS or plasma with 1% MeOH.

Table 3.1 Main physico-chemical properties of aromatic metabolite standards[3]

Metabolite Standard	log P	Formula	Monoisotopic Mass	Stock Solution Solvent
Adenosine monophosphate (AMP)	-4.8	$C_{10}H_{14}N_5O_7P$	347.0630	H_2O
L-Histidine	-3.6	$C_6H_9N_3O_2$	155.0694	H_2O
Folic Acid	-2.5	$C_{19}H_{19}N_7O_6$	441.1396	MeOH/H_2O (1/1) 0.1% NH_4OH
L-Tyrosine	-2.26	$C_9H_{11}NO_3$	181.0738	MeOH/H_2O (1/1) 0.1% FA
Adenosine	-2.1	$C_{10}H_{13}N_5O_4$	267.0967	H_2O
Inosine	-2.1	$C_{10}H_{12}N_4O_5$	268.0807	H_2O
Thiamine (Vitamin B1)	-2.1	$C_{12}H_{16}N_4OS$	265.1123	H_2O
Guanosine	-1.9	$C_{10}H_{13}N_5O_5$	283.0916	MeOH/H_2O (1/1)
Kynurenine	-1.9	$C_{10}H_{12}N_2O_3$	208.0847	H_2O
L-Phenylalanine	-1.2	$C_9H_{11}NO_2$	165.0789	MeOH/Water H_2O (1/1)
L-Tryptophan	-1.1	$C_{11}H_{12}N_2O_2$	204.0898	MeOH/H_2O (1/1)

Riboflavin	-0.92	$C_{17}H_{20}N_4O_6$	376.1382	Water/DMSO (1/1) 0.1% FA
Guanine	-0.91	$C_5H_5N_5O$	151.0494	H_2O 0.1 M NaOH
Pyridoxine (Vitamin B6)	-0.77	$C_8H_{11}NO_3$	169.0738	H_2O
Thymine	-0.62	$C_5H_6N_2O_2$	126.0429	H_2O
Adenine	-0.57	$C_5H_5N_5$	135.0544	H_2O
Diosmin	-0.44	$C_{28}H_{32}O_{15}$	608.1741	MeOH/DMSO (1/1)
Nicotinamide	-0.39	$C_6H_6N_2O$	122.0480	H_2O
Homovanillic Acid	0.473	$C_9H_{10}O_4$	182.0579	H_2O
5-methoxytryptamine	1.33	$C_{11}H_{14}N_2O$	190.1106	MeOH/H_2O (1/1)
Melatonin	1.6	$C_{13}H_{16}N_2O_2$	232.1211	H_2O
Diosmetin	2.55	$C_{16}H_{12}O_6$	300.0633	MeOH/DMSO (1/1)
Triiodothyronine	2.9	$C_{15}H_{12}I_3NO_4$	650.7900	DMSO
Thyroxine	3.73	$C_{15}H_{11}I_4NO_4$	776.6866	DMSO

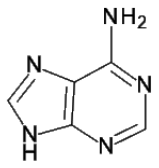

Adenine

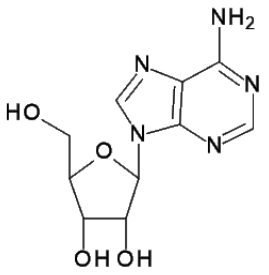

Adenosine

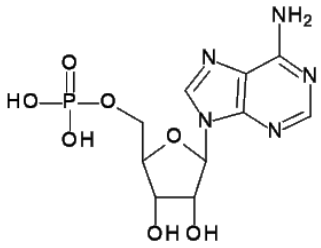

AMP

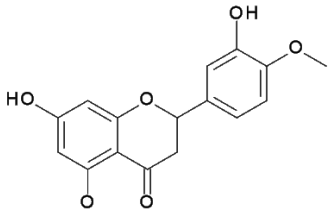

Diosmetin

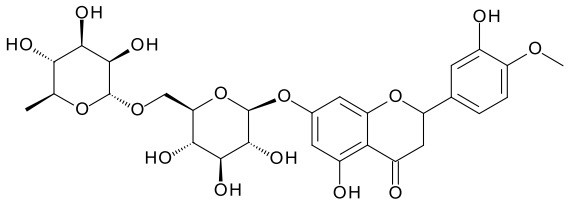

Diosmin

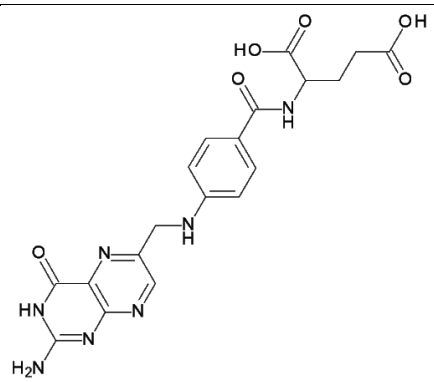 Folic Aid	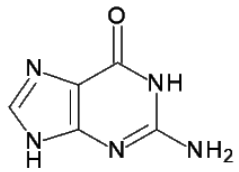 Guanine	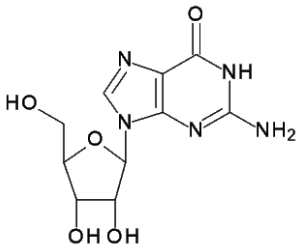 Guanosine
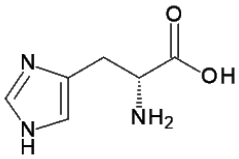 L-Histidine	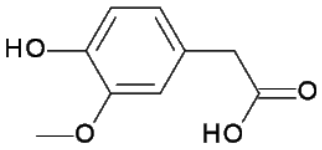 Homovanillic Acid	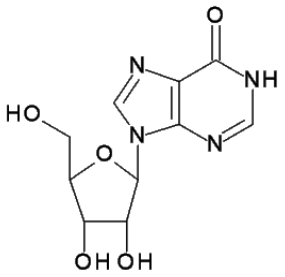 Inosine
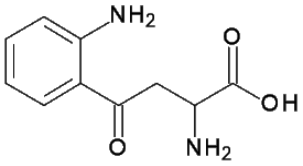 Kynurenine	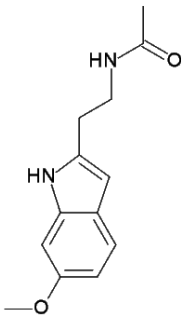 Melatonin	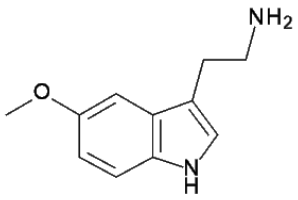 5-methoxytryptamine
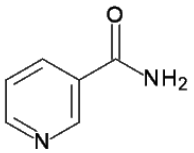 Nicotinamide	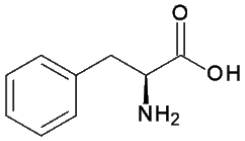 L-Phenylalanine	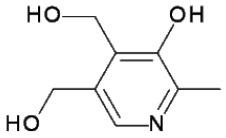 Pyridoxine (Vitamin B6)
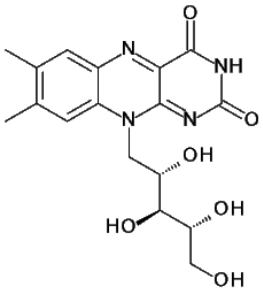 Riboflavin	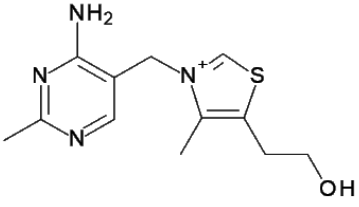 Thiamine (Vitamin B1)	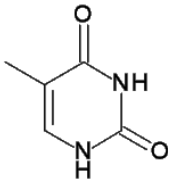 Thymine

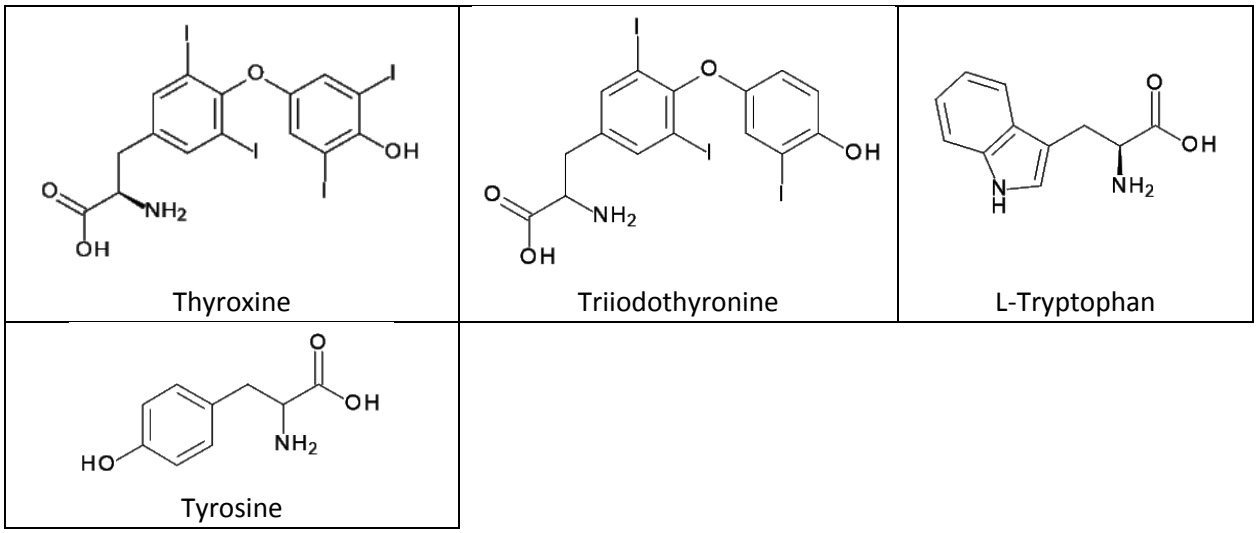

Figure 3.1 Aromatic metabolite standard structures[3]

3.3.3. General Workflow for CNP-Based D-SPME

The general workflow for D-SPME using CNPs used in this work is presented in Figure 3.2. All incubations steps were at 4°C, all centrifugation steps were 30 min at 25000 g (Thermo Scientific Sorvall ST 16R Centrifuge, Ottawa, ON, Canada). Prior to making the CNP suspension, the particles were washed four times with 1.5 mL of methanol to remove any contaminants. This was done since yellow contaminants were observed when the particles were first suspended in methanol. 60 µL of CNPs suspended in methanol (0.01 g/mL) were deposited into an Eppendorf tube and centrifuged. 40 µL of the methanol supernatant was removed to minimize the amount of this solvent in the sample during the extraction. The sample (1.5 mL) was then added to the tube, vortexed for 10 seconds to re-disperse the CNPs, mixed at 450 rpm for 30 minutes at room temperature to extract, and then centrifuged to separate the CNPs from the sample. To wash the CNPs after the sample was removed, 200 µL of 20% MeOH/80% water was added, vortexed for 10 seconds, and centrifuged. After the wash solution was removed, 25 µL of ACN was added, vortexed for 10 seconds to re-disperse the CNPs, mixed at 450 rpm for 30 minutes, and then centrifuged to separate the desorbed sample from the CNPs. Initial experiments then included a 1/10 dilution with water to achieve sample composition compatible with the initial LC mobile phase conditions in an attempt to avoid an evaporation/reconstitution step. However, the resulting samples were very dilute. The final protocol incorporated evaporation of the extracted sample to dryness and reconstitution in 25 µL of 90% water/10% MeOH.

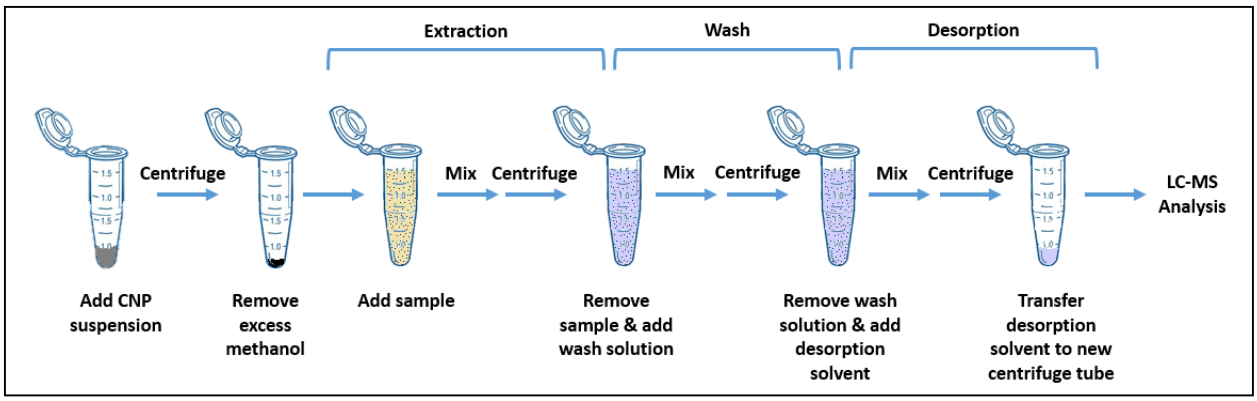

Figure 3.2 General workflow for D-SPME using CNPs as a sorbent highlighting the extraction, wash, and desorption steps.

3.3.4. LC-MS Analysis

All of the chromatographic separations included in this work were performed on an Agilent 1290 Infinity II UHPLC system (Agilent Technologies, Santa Clara, CA, USA) equipped with a G4226A autosampler, G4220A binary pump, and G1330B thermal column compartment. The autosampler was set at 4°C for all analyses. A Kinetex Biphenyl column (Phenomenex, Torrence, CA, USA) with a 1.7 µm particle size, 100 Å pore size, and 100 mm x 2.1 mm dimensions was used in this work accompanied by a Kinetex C18 Biphenyl guard column (Phenomenex) for 2.1 mm internal diameter columns. Samples were separated using the method described in Table 2.3. The RPLC method for the separation of aromatic metabolites was initially developed using acetonitrile as the strong solvent. A change to methanol was made to improve separation of the 24 metabolite standards. Increased retention was observed for all of the standards with methanol. There are two possible causes for the increased retention, and it is likely that both contributed. Firstly, methanol is a weaker solvent in the context of RPLC and a greater percentage in the mobile phase is required to have an equivalent polarity index and therefore elute analytes compared to acetonitrile.[161] Secondly, acetonitrile is known to interact, through its unsaturated triple bond, with aromatic moieties, inhibiting π-π interactions between the stationary phase and the analytes, decreasing retention.[162] In future, switching to acetic acid as mobile phase additive may further improve method sensitivity with negative ESI.

Table 3.2 Summary of LC parameters

LC Parameter	
Mobile Phase A	Water 0.1% formic acid
Mobile Phase B	Methanol 0.1% formic acid
Flow Rate	0.3 mL/min
Run Time	33 min
Injection Volume	10 µL
Mobile Phase Gradient	0-4 min 3% B 4-22 min linear gradient to 57% B 22-27 min linear gradient to 93% B 27-29 min 93% B 29.10-33 min 3% B
Column Temperature	35°C

MS analysis was performed with an Agilent 6550 iFunnel Quadrupole-Time-of-Flight (Q-TOF) instrument equipped with an ESI source and Dual Agilent Jet Stream (AJS) technology (Agilent Technologies, Santa Clara, CA, USA). An Agilent G1310B isocratic pump was used to introduce a reference solution into the ESI source to maintain mass accuracy throughout the analyses. The reference solution contained purine (m/z 112.050873 in positive ESI, 199.036320 in negative ESI) and HP-0921 (m/z 922.009798 in positive ESI, 966.000725 in negative ESI). The MS conditions used in this work are listed in Table 2.4. MassHunter data acquisition software for the 6200 series TOF/6500 series QTOF (version B.06.01, build 6.01.6157) was used to control LC-MS acquisition.

Table 3.3 Summary of Q-TOF parameters

N_2 drying gas temperature	250°C	**Nozzle voltage**	400 V
N_2 drying gas flow	15 L/min	**Fragmentor voltage**	250 V
Nebulizer pressure	35 psig	**Acquisition rate**	2 spectra/s
Capillary voltage	3500 V	**Mass range**	50-1100 m/z

3.3.5. Data Processing

Quantitative processing for standard metabolites was completed using Agilent Mass Hunter TOF Quantitative Analysis software (version B.07.00, build 7.0.457.0). Extraction of the adduct mass, obtained from METLIN, was performed using a 10 ppm window. All peak integrations were manually checked. The $[M+H]^+$ or $[M-H]^-$ adduct was used for all standards. Calibration curves with a 1/x weighted regression were used.

Data processing for plasma samples was completed using Agilent MassHunter Profinder Software (version B.08.00, build 8.0.8137.0). The software finds compounds through chromatographic deconvolution and then performs peak alignment using compound retention time and mass. The software also performs de-isotoping and de-adducting so that all ions belonging to a single metabolite are combined into a single entry. Global processing was applied for the 2 - 29 min retention time window in order to exclude metabolites eluting in the solvent front or during column re-equilibration. The applied processing parameters are presented in Table 2.5. The list of detected compounds was then further refined by (i) removing any compounds not found in the sample with a signal intensity at least 5 times the intensity of the extraction blank (ii) removing any compounds not found in all replicates, and (iii) removing any compounds with a mass greater than 1100 Da.

Table 3.4 Global data processing parameters applied to plasma samples using Agilent MassHunter Profinder Software

Use peaks with height	≥250 counts	**Mass window**	±20 ppm +2.0 mDa
m/z range	50-1100	**Retention time window**	2% ±0.3
Allowed adducts (+ESI)	$[M+H]^+$, $[M+Na]^+$, $[M+K]^+$, $[M+NH_4]^+$	**Minimum number of required ions**	2
Allowed adducts (-ESI)	$[M-H]^-$, $[M+Cl]^-$, $[M+Br]^-$, $[M+HCOO]^-$, $[M+CH_3COO]^-$, $[M+CF_3COO]^-$	**Absolute height**	2500 counts
Charge state limit	1-3	**MFE score**	70

3.4. Results and Discussion

Various sample preparation parameters, presented in Figure 3.3, that could affect the performance of the method were evaluated for their influence on extraction efficiency.

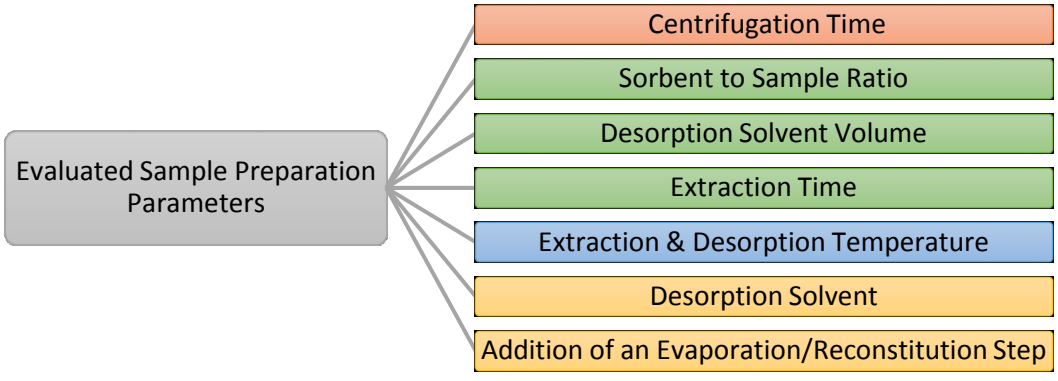

Figure 3.3 Outline of sample preparation parameters evaluated in this work. Parameters were evaluated for CNPs in solvent (orange), standards in PBS (blue), standards spiked in plasma (yellow), or standards in PBS and plasma. Plasma experiments were also evaluated for global metabolite coverage.

3.4.1. LC Method Using Biphenyl Chromatography

Thanks to the ability to participate in π-π interactions with aromatic or conjugated analytes, biphenyl stationary phases have been used to chromatographically separate targeted groups of metabolites including steroid hormones[61,62], thyroid hormones[57], and drug metabolites.[63–65] Given the hypothesis that CNPs will be able to extract aromatic metabolites, a liquid chromatography method for the aromatic metabolite standards was developed using a biphenyl column. The separation of standards achieved is shown in Figure 3.4. L-Histidine, guanine, thiamine, AMP, and adenine were not adequately retained and eluted close to the solvent front.

L-Histidine $[M-H]^-$ 0.80 min	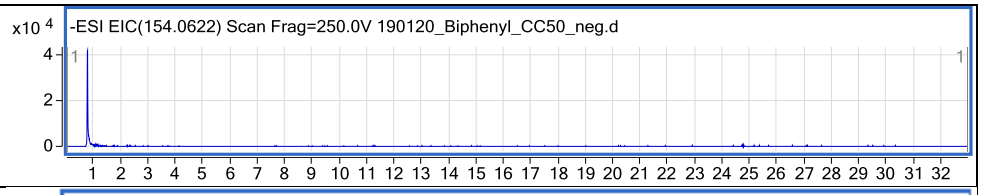
Guanine $[M+H]^+$ 1.07 min	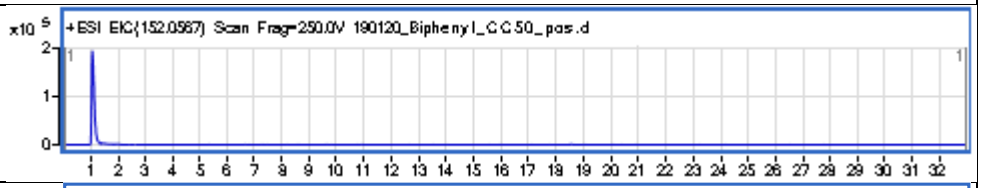
Thiamine $[M+H]^+$ 1.09 min	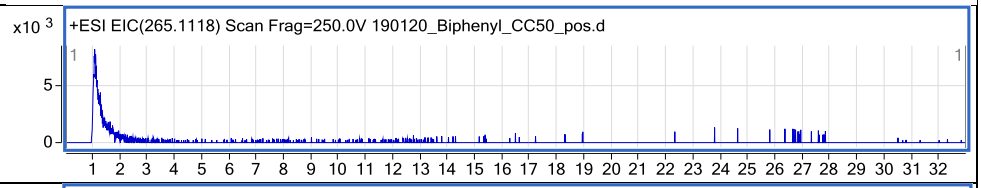
AMP $[M-H]^-$ 1.12 min	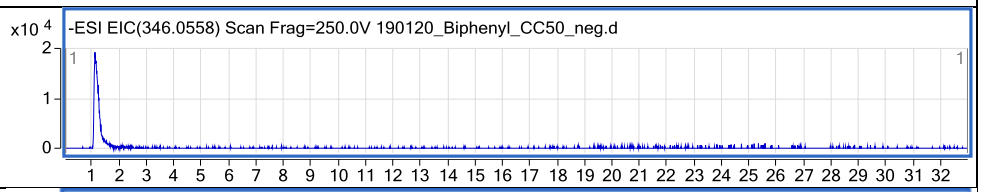
Adenine $[M-H]^-$ 1.14 min	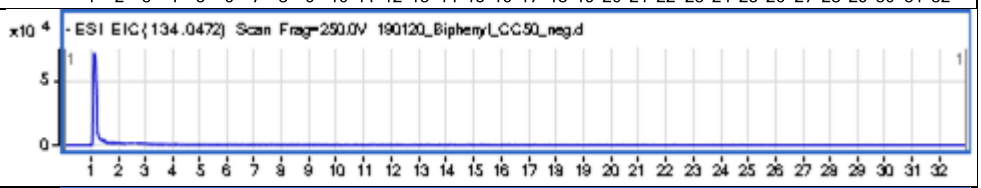
L-Tyrosine $[M+H]^+$ 1.48 min	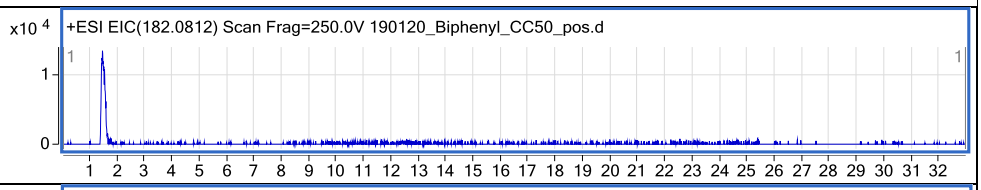
Nicotinamide $[M+H]^+$ 1.65 min	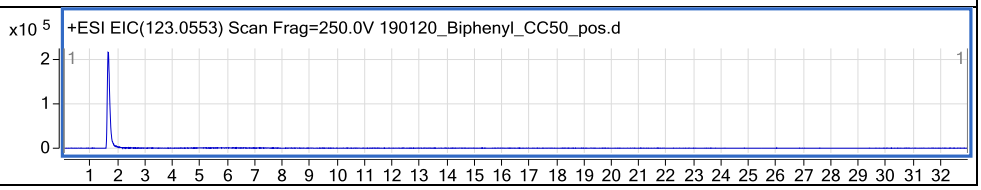

Pyridoxine $[M-H]^-$ 2.17 min	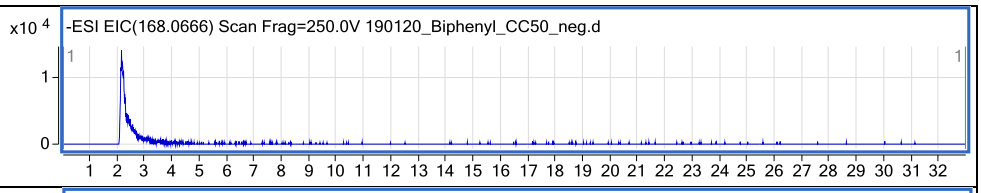
Adenosine $[M+H]^+$ 2.45 min	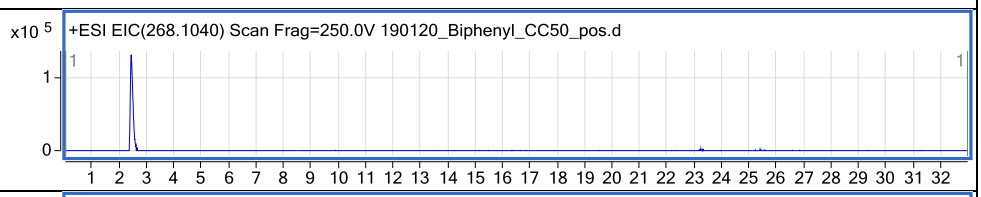
Guanosine $[M+H]^+$ 2.47 min	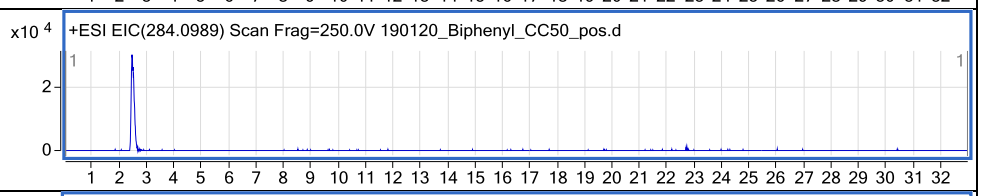
Inosine $[M-H]^-$ 2.57 min	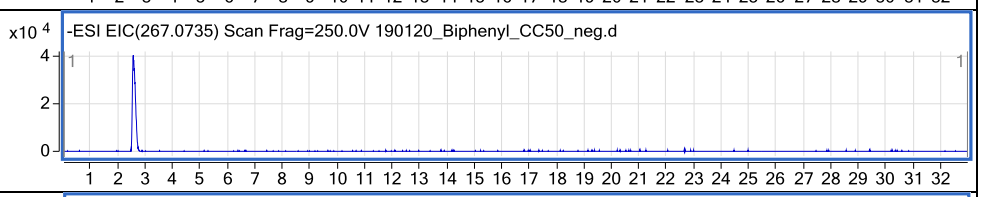
Thymine $[M+H]^+$ 2.63 min	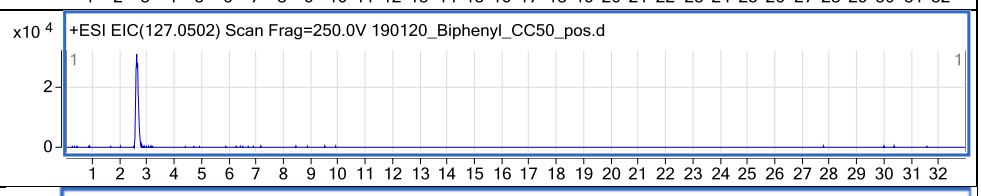
L-Phenylalanine $[M+H]^+$ 3.67 min	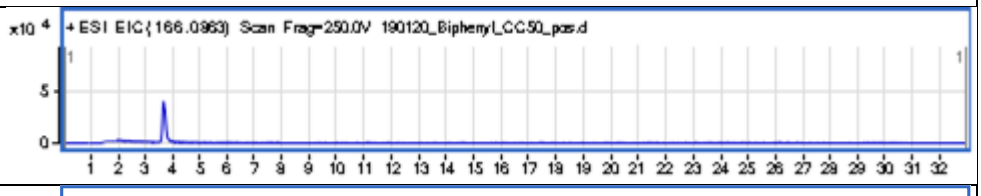
Kynurenine $[M+H]^+$ 6.13 min	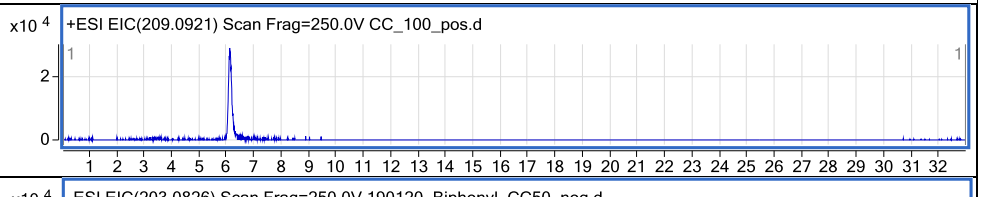
L-Tryptophan $[M-H]^-$ 7.59 min	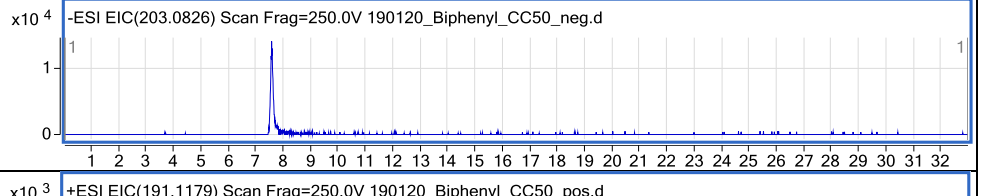
5-methoxytryptamine $[M+H]^+$ 10.96 min	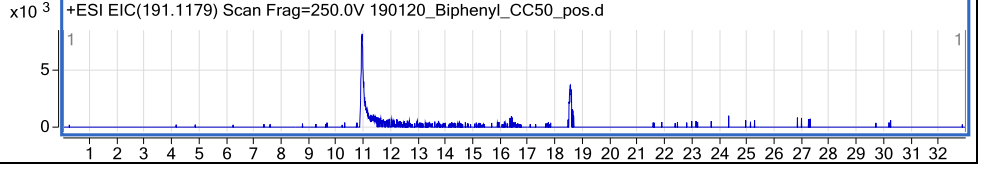

Homovanillic Acid $[M-H]^-$ 12.18 min	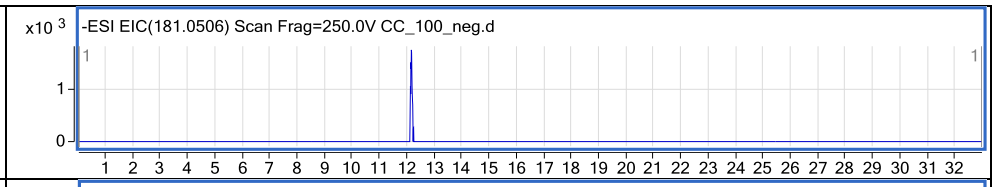
Folic Acid $[M-H]^-$ 14.25 min	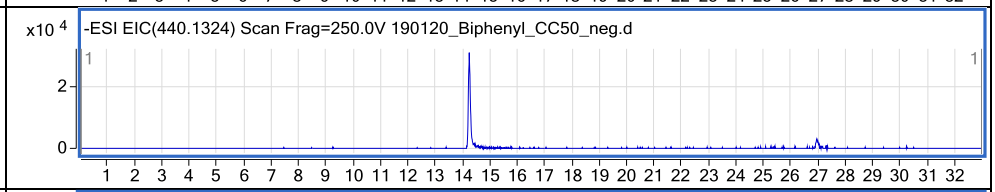
Riboflavin $[M-H]^-$ 17.90 min	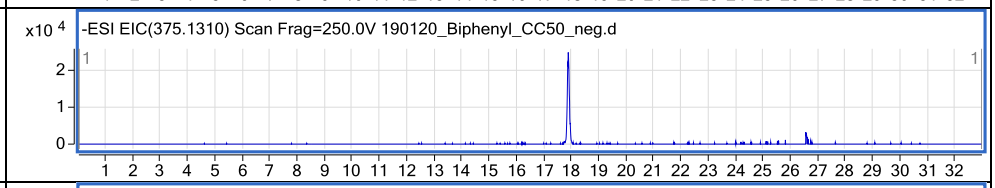
Melatonin $[M+H]^+$ 18.56 min	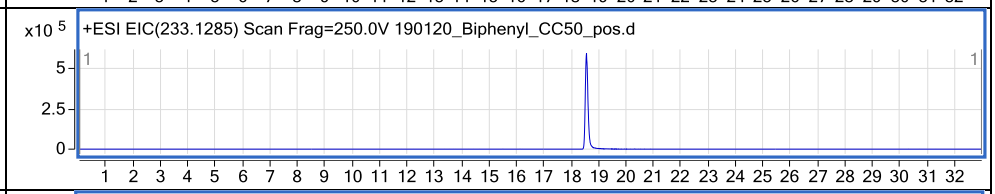
Diosmin $[M+H]^+$ 21.46 min	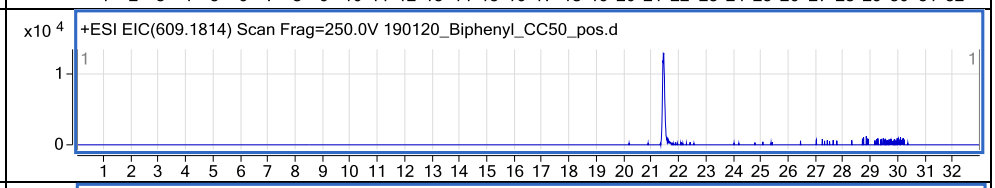
Triiodothyronine $[M-H]^-$ 24.08 min	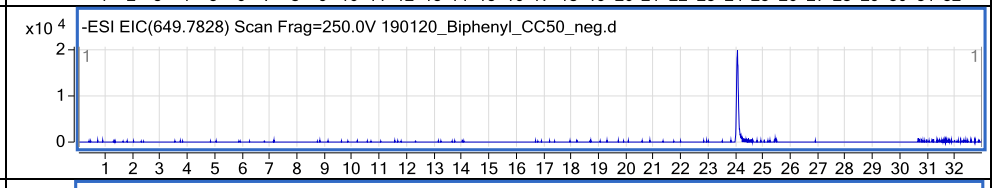
Diosmetin $[M+H]^+$ 24.57 min	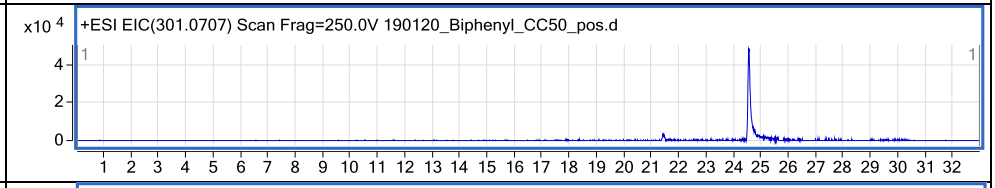
Thyroxine $[M-H]^-$ 25.44 min	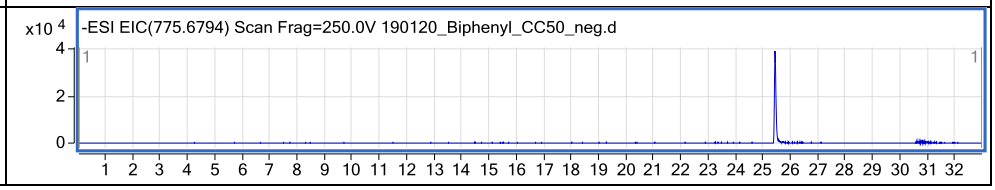

Figure 3.4 EICs of aromatic metabolite standards indicating the retention time and adduct used for each. Shown for all standards at 50 ng/mL except for kynurenine and homovanillic acid which are shown at 100 ng/mL.

3.4.2. Evaluation of CNP Dispersion and Centrifugation Time

Before D-SPME method development, it was necessary to disperse the CNPs in solvent to allow for the sorbent to be dispensed into each sample. It was determined that the CNPs were dispersible in methanol at 0.01 g/mL with no visually evident aggregation of the particles.

The efficiency of separation by centrifugation, for a given solvent, is dependent on four factors: time, the relative centrifugal force (RCF), temperature, and the length of the sample tubes.[163] The temperature was maintained at 4°C to ensure the stability of the biological samples. The RCF is governed by the technical specifications of the centrifuge, therefore the maximum achievable force, 25000 g was used. Sample tube length was fixed by the experimental design. With the other variables fixed, centrifugation time was the only factor to be optimized. Given that centrifugation time adds to the total sample preparation time and adds to the extraction, wash, and desorption times, use of the minimal required centrifugation time is preferable. To determine the minimum time to separate the CNPs from the sample, wash solution, or desorption solvent, a series of centrifugation times were tested at 25000 g. The results of this test are shown in Figure 3.5(b-d). A 30-minute centrifugation time was determined to be the minimum required, and was used for all subsequent experiments.

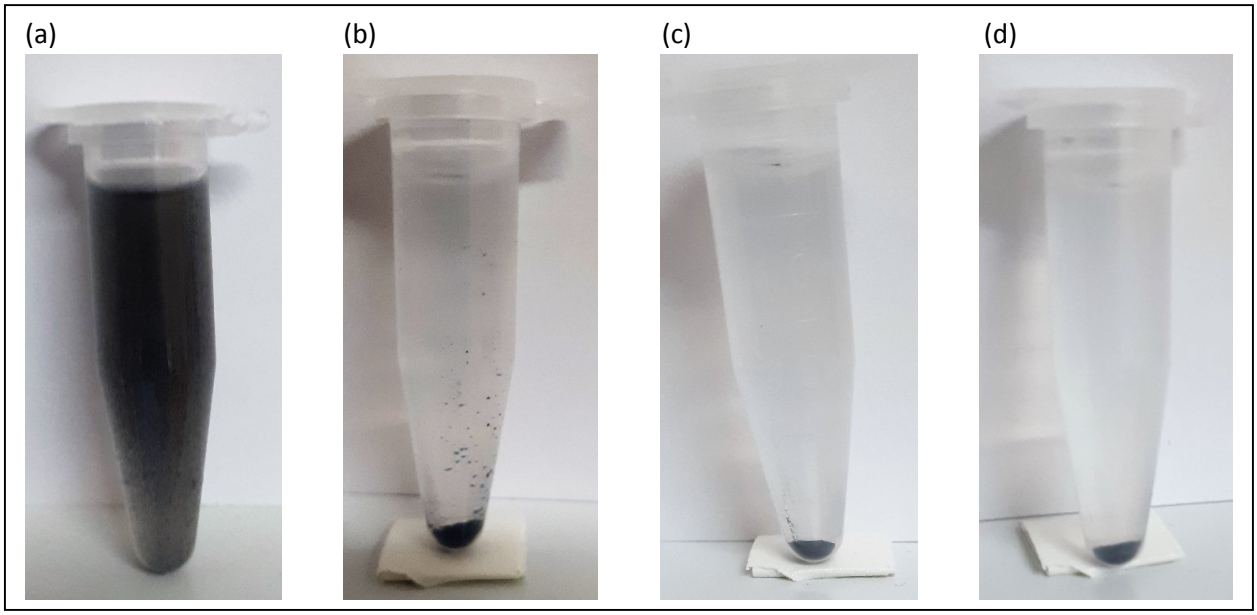

Figure 3.5 Effect of centrifugation time on the separation of CNPs from supernatant. Showing 30 µL of carbon nanopearl suspension (0.01 g/mL) in 1.5 mL of methanol pre-centrifugation (a), and post centrifugation for 10 minutes (b), 20 minutes (c), and 30 minutes (d) at 25000 g.

3.4.3. Evaluation of Extraction Time

During SPME, it takes time for equilibrium between the sample matrix and sorbent phase to be reached. The equilibrium time for each analyte is dependent on each individual partition coefficient, the diffusion properties of the analyte, sample temperature, the geometry of the sorbent which dictates the availability of sorption sites, the amount of agitation, and the influence of other analytes competing for sorption sites. The dispersive format can be advantageous over other SPME formats due to its shorter equilibrium time, thanks to increased contact between the sorbent and sample, and decreased diffusion distances. This is especially beneficial for more viscous samples such as plasma. Once equilibrium is reached, the extraction process is complete and increased extraction time will not increase the amount of analyte extracted.

3.4.3.1. Extraction Time for Standards in PBS

To evaluate the nature of the extraction using CNPs, multiple extraction times (2 min, 1 hour, and 17 hours) were initially tested using standards in PBS. The results, shown in Figure 3.6, cover a range of 0.01 to 5.55% recovery over all time points which is consistent with microextraction techniques. Several trends could be observed in the data including standards whose extraction had yet to reach equilibrium/reached equilibrium in 17 hours, reached equilibrium within 2 minutes, or possibly experienced displacement by other analytes with larger distribution coefficient decreasing the mass of analyte extracted with increasing extraction times. The occurrence of displacement could be indicative of CNPs being an adsorptive sorbent rather than an absorptive one. Alternatively, the layers of graphitic flakes that make up the particles could be allowing analyte molecules to intercalate between the layers when very long extraction times are employed (such as the 17-hr extraction). The large error bars for all time points made it difficult to conclusively evaluate whether equilibrium had been reached and warranted further investigation with an increased number of extraction time points. Additionally, these results were obtained prior to determining that CNPs needed to be washed to remove contaminants prior to use.

Standards in buffer were extracted with six different extraction times ranging from 2 minutes to 2 hours. The results of the analyses are shown in Figure 3.7. From this experiment it appears that, within experimental error, the amount of analyte extracted was not altered over time. This was confirmed for each standard by ANOVA. This indicates that equilibrium was reached within the first 2 minutes. This is consistent with extraction times used for D-SPME protocols with other carbon nanoparticles. For example, oxidized single walled carbon nanohorns have been used to extract triazines[143] and polyaromatic hydrocarbons[117] from water with a 2-minute extraction time. Magnetic MWCNTs have been used to extract the anticancer drug sunitinib from biological samples, including plasma, with a 5 minute extraction time.[116]

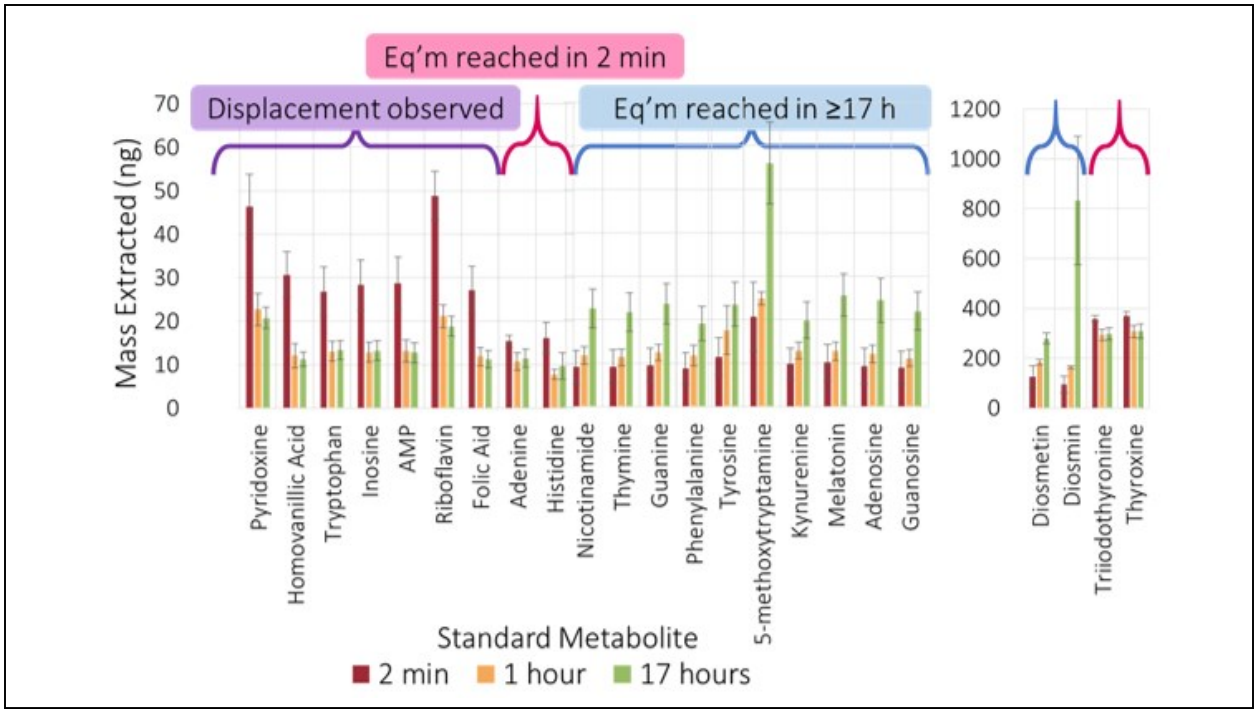

Figure 3.6 Effect of extraction time on the amount of standard metabolite extracted using D-SPME from metabolite standards (10 µg/mL) in PBS. The extraction of 1.5 mL samples was completed using 30 µL of CNP suspension and desorption with 200 µL of methanol. The metabolite standard thiamine is not shown since none was extracted. (n=6)

Taking into account the results of both experiments, it is possible that with extended extraction times, such as 17 hours, there may be some slow movement of the analytes between the graphitic flakes of the CNPs, however the evidence is not definitive. A second possibility for the discrepancy between Figure 3.6 and Figure 3.7 is suppression by contaminants, as the washing of CNPs prior to use was not incorporated for the experiment in Figure 3.6 but was incorporated for the experiment in Figure 3.7.

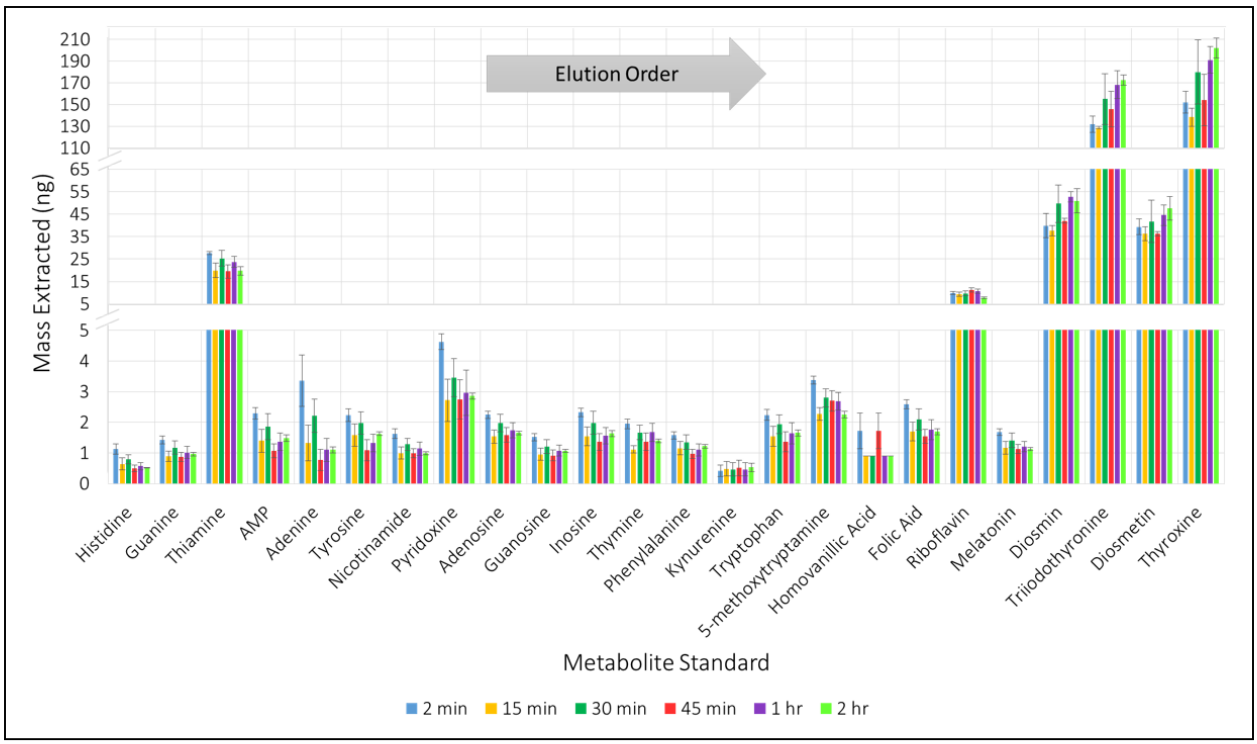

Figure 3.7 Effect of extraction time on the amount of standard metabolite extracted using D-SPME from metabolite standards (10 µg/mL) in PBS. The extraction of 1.5 mL samples was completed using 60 µL of CNP suspension and desorption with 25 µL of ACN. (n=3)

3.4.3.2. Extraction Time for Plasma

Sample matrix can affect the extraction process, influencing the equilibrium time for analytes. To evaluate the effect of extraction time on the amount of analyte extracted from plasma samples spiked with 10 µg/mL of each standard, a comparison of 2- and 30-minute extraction times was completed. The results of this experiment, shown in Figure 3.8, show that unlike in buffer, equilibrium is not reached within 2 minutes. An increase in the mass extracted was observed for multiple compounds (e.g. phenylalanine, adenosine, and 5-methoxytryptamine) while others may have experienced displacement (e.g. diosmetin and triiodothyronine).

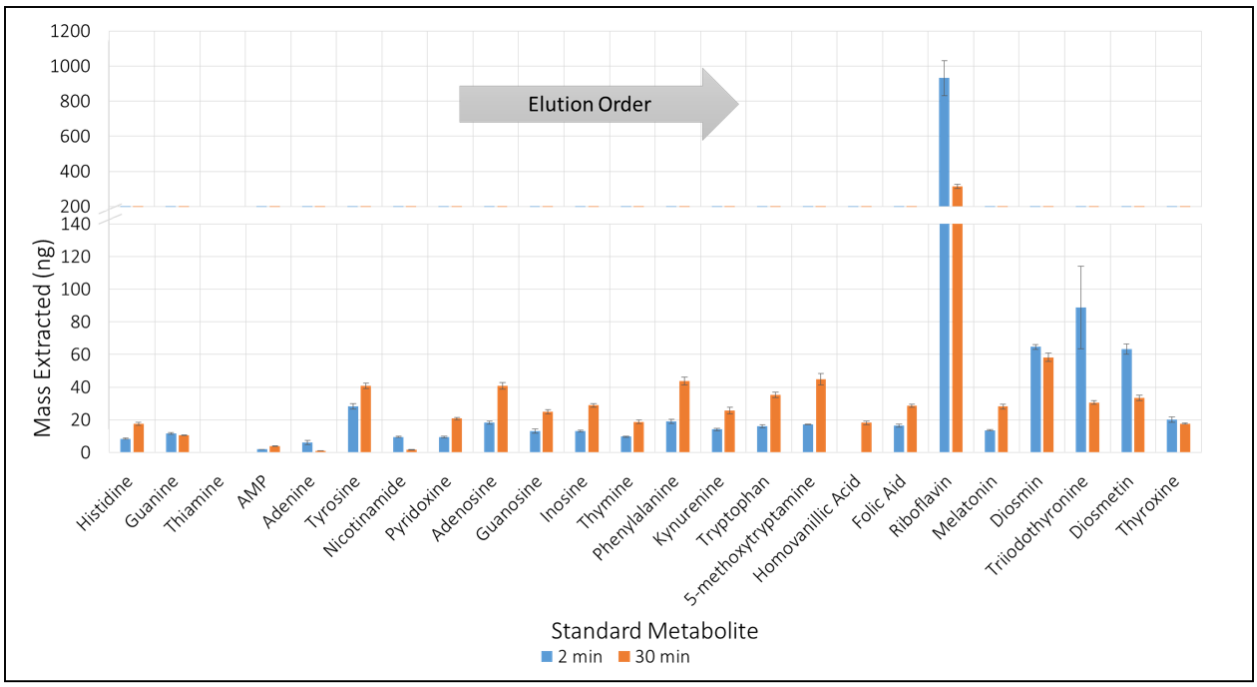

Figure 3.8 Effect of extraction time on the amount of standard metabolite extracted using D-SPME from metabolite standards (10 µg/mL) in plasma. The extraction of 1.5 mL samples was completed using 60 µL of CNP suspension and desorption with 25 µL of methanol. (n=3)

Global data processing to compare 2-minute and 30-minute extraction times showed that the 30 minute extraction time was more repeatable, with a lower average and median relative standard deviation (RSD) in both positive and negative mode ESI. This was consistent with the targeted results seen for the spiked standards. The distributions of RSD for each condition are shown in Figure 3.9. A comparison of peak areas for compounds observed with both conditions shows that the majority of compounds with greatly different peak areas are late eluting. Given the large number of compounds eluting in this chromatographic space, it is possible that the difference is due to a difference in the ionization suppression/enhancement that is occurring between sample groups. An extraction time of 30 minutes was chosen for all further experiments for the improvement in repeatability between replicates.

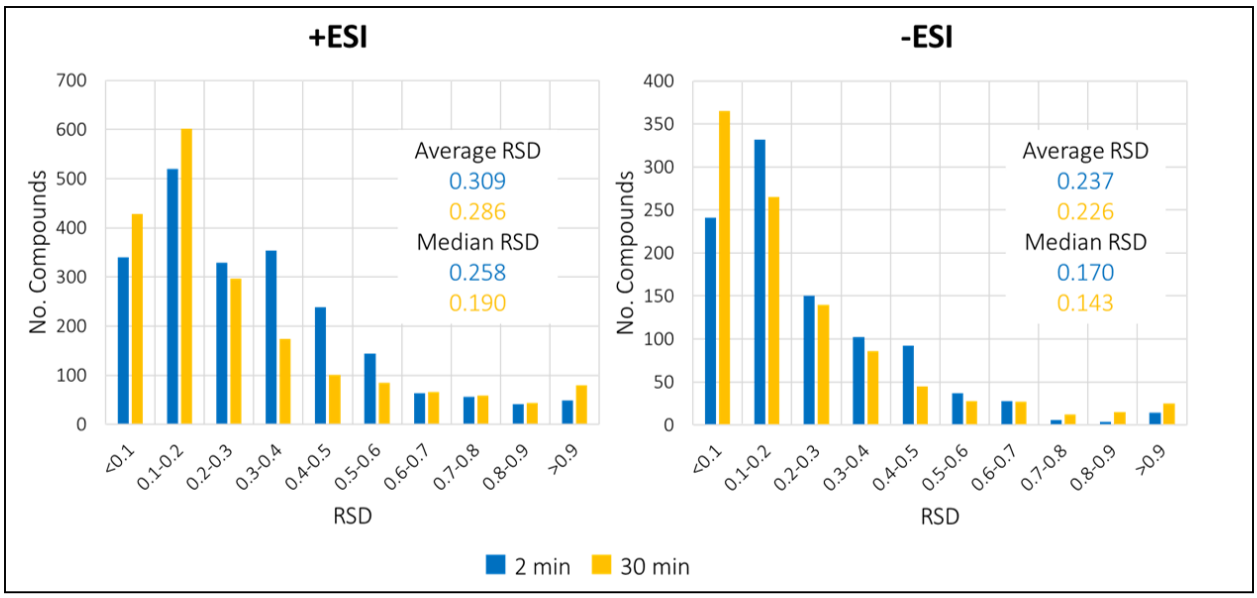

Figure 3.9 A comparison of the distribution of RSD for each compound detected in D-SPME extracted plasma samples with 2-minute and 30-minute extraction times. The extraction of 1.5 mL samples was completed using 60 µL of CNP suspension and desorption with 25 µL of methanol. RSD was calculated as standard deviation divided by the mean. (n=3) A total of 2135 and 1006 metabolites were observes in positive and negative ESI respectively with the 2-minute extraction time. A total of 1931 and 1008 metabolites were observes in positive and negative ESI respectively with the 30 minute extraction time.

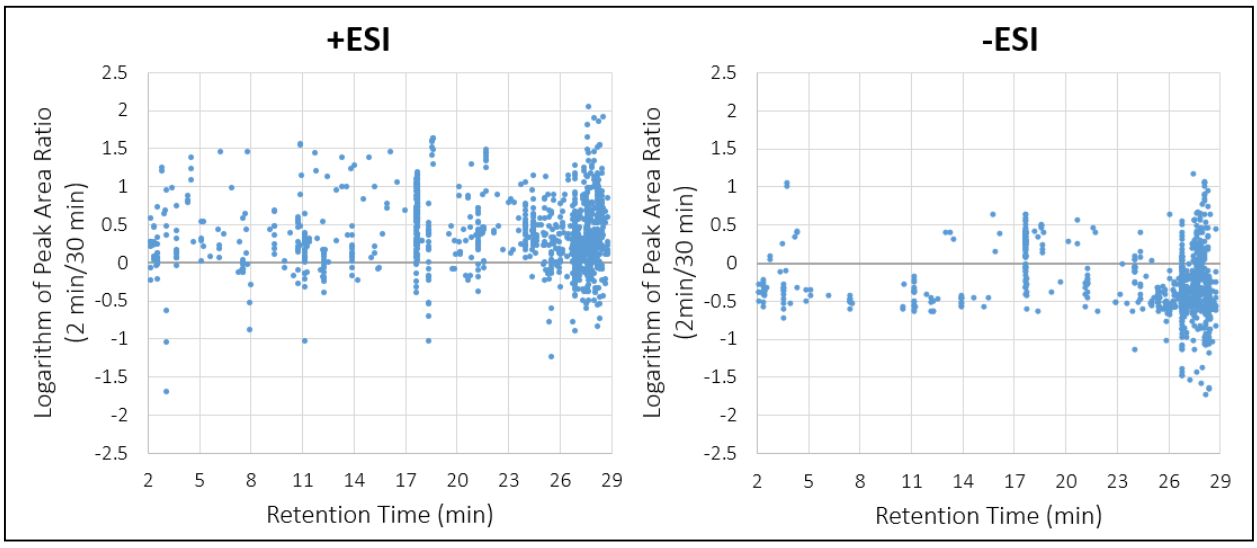

Figure 3.10 A comparison of peak area with respect to time for compounds detected in D-SPME extracted plasma samples with 2-minute and 30-minute extraction times. The extraction of 1.5 mL samples was completed using 60 µL of CNP suspension and desorption with 25 µL of methanol. (n=3)

3.4.4. Evaluation of Sample-to-Sorbent Ratio and Desorption Solvent Volume

The sensitivity of a SPME method, all other factors being held equal, is proportional to the number of moles of the analyte extracted.[25] From Equation 1.3, it follows that, in an ideal case, the number of moles extracted, and therefore the mass of analyte extracted, is dependent on the sample volume and the sorbent volume. An increase in either of these parameters will increase the sensitivity of the method. The sample-to-sorbent ratio was investigated by comparing the use of 30 µL or 60 µL of CNP suspension to extract 1.5 mL sample with a 10 µg/mL concentration of each standard metabolite. This represents a 6:5 and 3:5 total analyte mass to sorbent mass ratio respectively, and is not representative of typical microextraction conditions where sample should be in excess versus sorbent. With a specific surface area of 15 m^2/g, these ratios represent a total CNP surface area of 45 cm^2 and 90 cm^2 respectively. At the same time, the desorption volume was decreased from 200 µL to 25 µL. First, standards in PBS were extracted with both 30 µL of CNP suspension & 200 µL of methanol for desorption and with 60 µL of CNP suspension & 25 µL of methanol for desorption. The mass extracted for each standard with each condition are reported in Figure 3.11(a). Mass extracted was determined by calculating the concentration of the analyzed sample using a calibration curve, dividing by the dilution factor (1/10) and multiplying by the desorption volume. With mass extracted being reported, it was expected that the change in desorption solvent volume would increase the concentration of the extract, but not the total mass extracted. The doubling of the sorbent volume was expected to double the mass of analyte extracted. This was not observed, with the exception of riboflavin. A smaller increase in the mass extracted was seen for the late eluting compounds: diosmin, diosmetin, thyroxine, and triiodothyronine. Results obtained in buffer suggest that diosmin, diosmetin, triiodothyronine, and thyroxine have the highest distribution coefficients. This suggests that the selectivity of the CNPs as a sorbent is biased towards more hydrophobic compounds. These four compounds also contain multiple aromatic rings indicating aromaticity may be an important factor in extraction. Both thyroxine and triiodothyronine contain multiple iodine atoms which are capable of interacting with π electron systems, possibly contributing to their high distribution coefficients. Five standards not seen with the lower sorbent volume and higher desorption solvent were observed with the greater sorbent volume and lower desorption solvent. One or both of the changes to the extraction parameters could be responsible.

The experiment was repeated with standards spiked into human plasma samples. The quantitative results for the spiked standards, shown in Figure 3.11(b), show the same lack of the expected doubling of the mass of analyte extracted. There are several possible sources of error or uncertainty that could be impacting these results including the low number of replicates, irreproducibility in dispensing the CNPs

into each sample, and the 1/10 dilution before LC-MS analysis that diluted the sample concentrations to levels close to the lower limit of quantification for many of the standards The use of a greater number of replicates would increase confidence in the results. Any difference in the selectivity of the CNPs in buffer versus plasma remain unknown and should be investigate using unspiked plasma samples. The more complex matrix, plasma, contains many more metabolites as well as other matrix components such as proteins that may be responsible for the altered selectivity. It could also be that the available surface area of the particles is near saturation, such that large increases in the amount of analyte extracted are not possible. Unfortunately, endogenous levels were not measured independently during this experiment. Global processing results, shown in Figure 3.12 and Figure 3.13, show that the increased sorbent volume and decreased desorption solvent volume increased the number of compounds detected, as expected theoretically. The majority of the newly detected compounds were late eluting, indicating that they are hydrophobic in nature; however, an increase in the number of more hydrophilic compounds was also observed. The hydrophobic nature of the majority of the compounds extracted is consistent with the hydrophobic nature of the carbon nanopearls themselves, which allows for extraction by hydrophobic interactions.

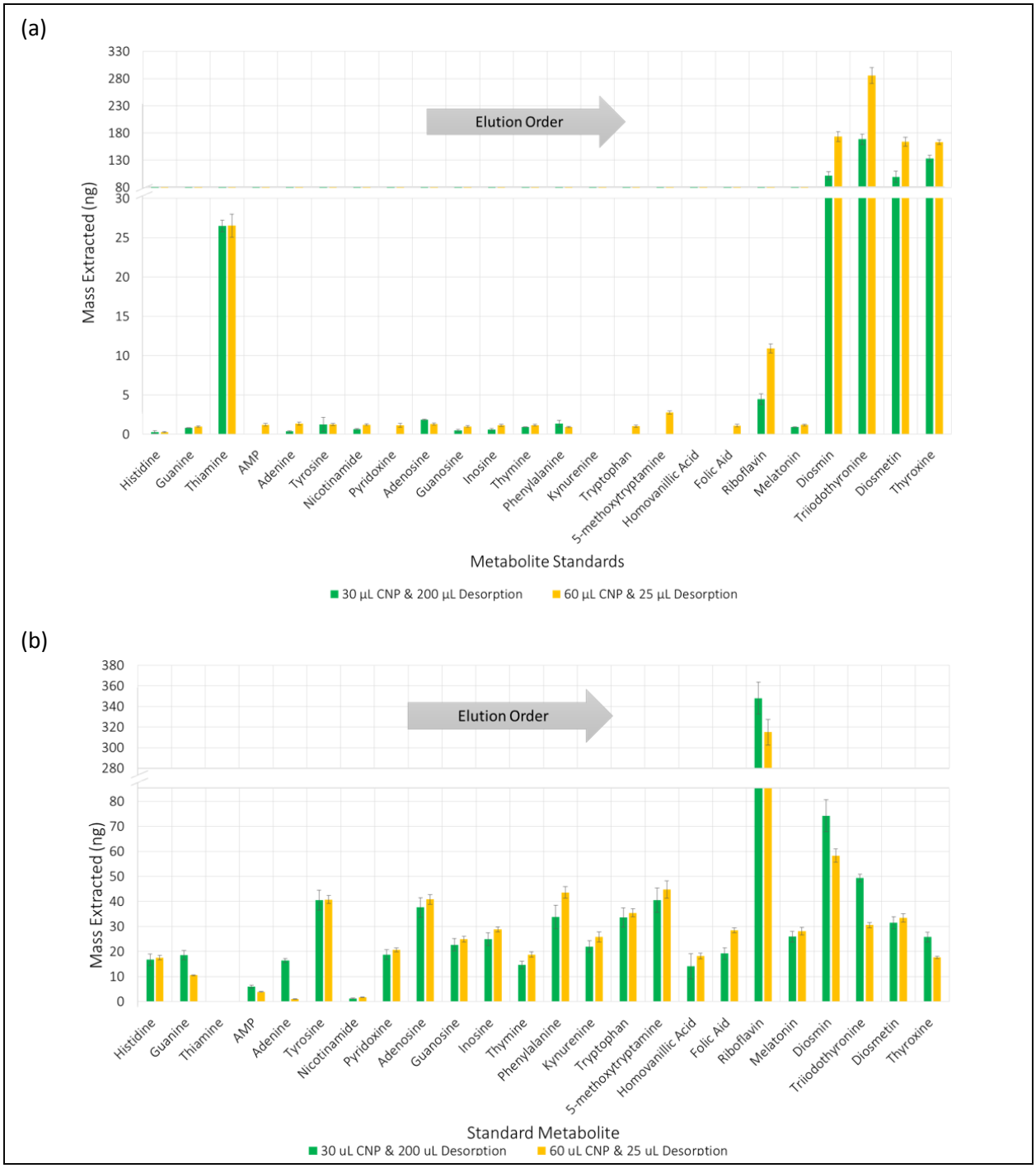

Figure 3.11 Effect of sorbent-to-sample ratio and desorption solvent volume on the amount of standard metabolite extracted using D-SPME from metabolite standards at 10 µg/mL in (a) PBS, and (b) plasma. The 30-minute extraction of 1.5 mL samples was completed using 30 µL of CNP (6:5 total standard analyte-to-CNP mass ratio) with 200 µL desorption volume or 60 µL of CNP (3:5 mass ratio) with 25 µL desorption volume. The 30-minute desorption was completed using methanol and the extracted samples were diluted 1/10 with water before LC-MS analysis. (n=3)

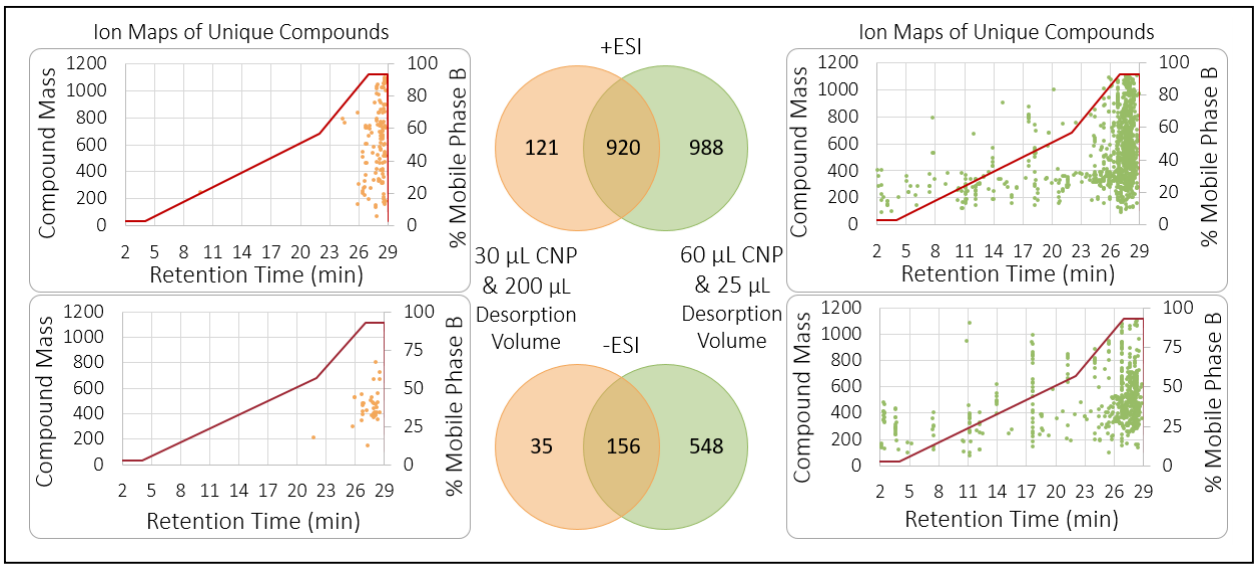

Figure 3.12 Effect of sorbent-to-sample ratio and desorption solvent volume on metabolite coverage for D-SPME of plasma samples. Metabolite maps show the unique compounds detected by each method in each ESI mode. Venn diagrams show the number of compounds unique to and shared by both methods. The 30-minute extraction of 1.5 mL samples was completed using 30 µL of CNP with 200 µL desorption volume or 60 µL of CNP with 25 µL desorption volume. The 30-minute desorption was completed using methanol and the extracted samples were diluted 1/10 with water before LC-MS analysis. (n=3)

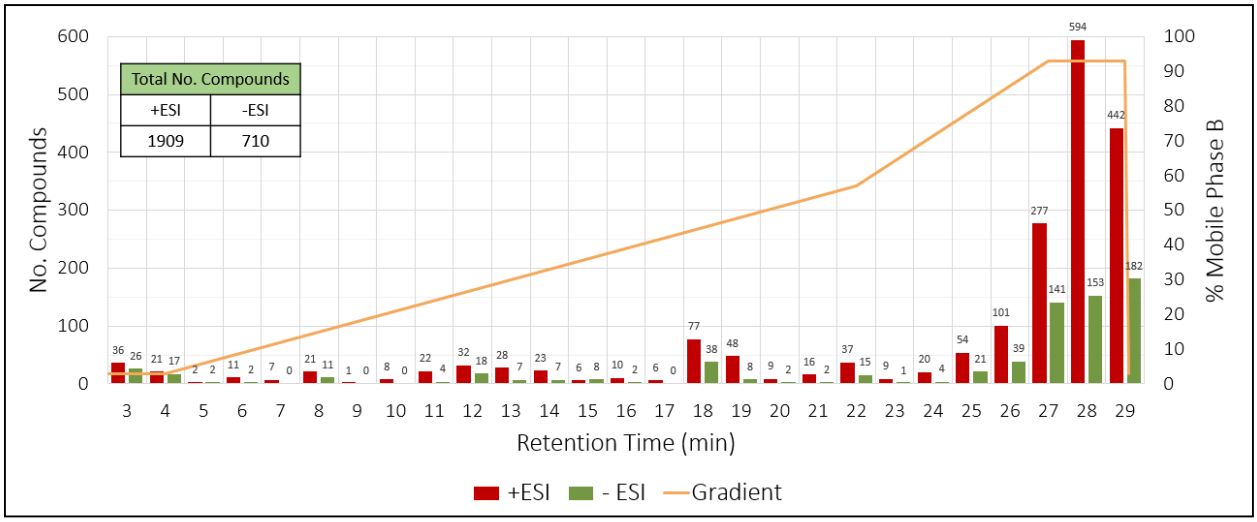

Figure 3.13 The distribution of compounds detected in D-SPME plasma extracts. The 30-minute extraction of 1.5 mL samples was completed using 60 µL of CNP with 25 µL desorption volume. The 30-minute desorption was completed using methanol and the extracted samples were diluted 1/10 with water before LC-MS analysis. (n=3)

3.4.5. Evaluation of the Choice of Desorption Solvent

The desorption of analytes off of the sorbent phase requires the use of a solvent with sufficient eluotropic strength to disrupt any interactions between the analyte and the sorbent site. If the solvent used does not sufficiently desorb the analytes, the recovery will be reduced. The choice of desorption solvent was evaluated by testing MeOH, ACN, and IPA. It was hypothesized that if aromatic compounds were preferentially extracted by the CNPs, the use of ACN, which disrupts pi-pi interactions[162] may provide improved desorption. The results (Figure 3.14a) seen for the aromatic standard metabolites spiked into plasma support this hypothesis. The global results (Figure 3.14b), especially in +ESI, show that IPA may provide improved desorption. This is consistent with previous results which showed that the majority of the compounds being extracted are highly non-polar. The aromatic nature of these compounds is currently unknown. Of the detected compounds unique to each desorption solvent, over 90% had retention times greater than 25 minutes when ACN or IPA was used. When methanol was used, approximately twenty more hydrophilic compounds, with retention times less than 10 minutes, were detected.

While using IPA resulted in the greatest number of compounds with positive ESI and ACN resulted in the most number of compounds detected with negative ESI, the use of methanol resulted in the detection of an increased number of earlier eluting compounds. It is possible that this is due to poor solubility of these more polar compounds in the stronger organic solvents.

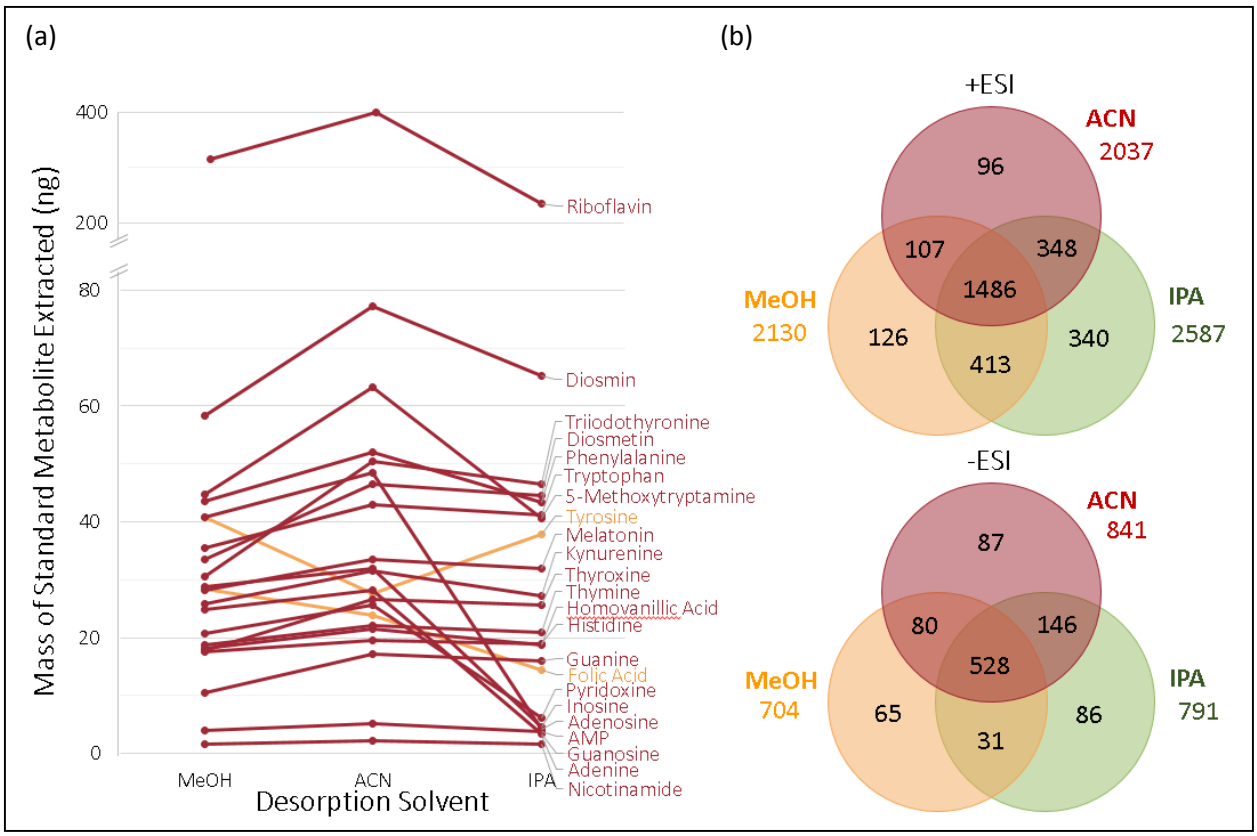

Figure 3.14 Effect of desorption solvent on the recovery of (a) standards (10 µg/mL) in plasma and (b) global results for plasma. Results for standards (a) indicate the solvent that provided the greatest mass of desorbed where red indicates ACN, yellow indicates MeOH, and green indicates IPA. RSD was less than 20% for all standards in all groups except for pyridoxine (22.4% with ACN desorption) so error bars were omitted for clarity. Global results (b) indicate the number of compounds detected with each desorption solvent and the overlap between sample groups. Extraction of 1.5 mL samples was completed using 60 µL of CNP suspension, 30-minute extraction time, and 30-minute desorption with 25 µL of solvent. Extracted samples were diluted 1/10 before LC-MS analysis. (n=3)

3.4.6. Evaluation of Temperature During Extraction and Desorption

The simplest description of the theory of SPME dictates that the distribution of each analyte between the two phases, sample and sorbent, is governed by the distribution constant for each analyte. Conditions used during extraction can influence the K_{fs} value.[25] In the case of temperature, an increase in sample temperature would theoretically decrease the K_{fs}, increasing the extraction rate, and therefore decreasing the time required to reach equilibrium.[164,165] Secondly, increasing the sample temperature decreases the viscosity of the sample, increasing the rate of diffusion and therefore, also decreasing the time required for analytes to migrate from the sample to the sorbent.[165] Increasing the extraction temperature can

however cause a loss of sensitivity due to decomposition of temperature sensitive analytes[165] as well as accelerating chemical reactions, such as oxidation.

To evaluate the effect of temperature during extraction, a 30-minute extraction of standards in buffer was performed at both room temperature (26°C) and 40°C. The results, shown in Figure 3.15, indicate that increasing the temperature during extraction did not significantly increase or decrease the mass of standard extracted. This conclusion was verified for each standard using a t-test.

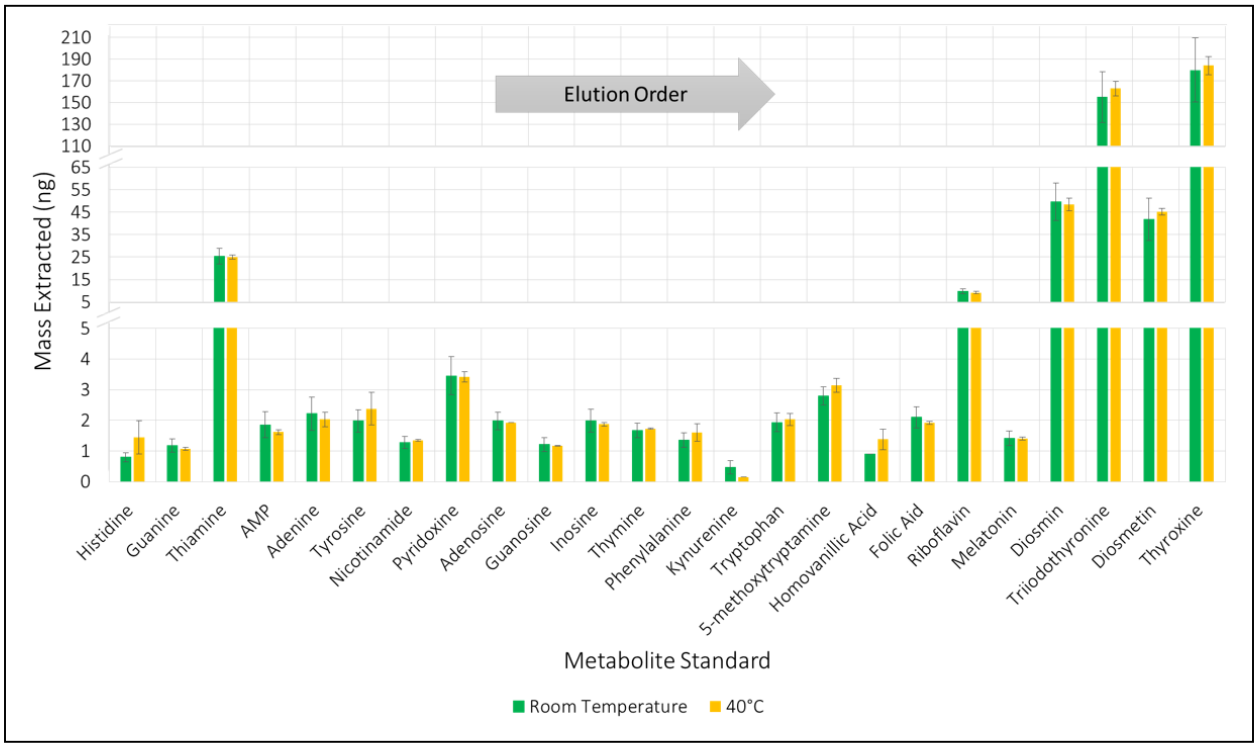

Figure 3.15 Effect of sample temperature on the efficiency of D-SPME extraction of standards (10 µg/mL) in PBS. The 30-minute extraction of 1.5 mL samples was completed using 60 µL of CNP with 25 µL desorption volume. The 30-minute desorption was completed using methanol and the extracted samples were diluted 1/10 with water before LC-MS analysis. (n=3)

Sample temperature can also affect the desorption of analytes from the sorbent into the desorption solvent. To evaluate the effect of temperature during desorption, a 30-minute extraction of standards in buffer was performed at both room temperature and 40°C. The results, shown in Figure 3.16, indicated that increasing the desorption temperature had no significant effect on desorption efficiency. This conclusion was verified for each standard using a t-test. Increased temperature during desorption provided no benefit to the desorption efficiency.

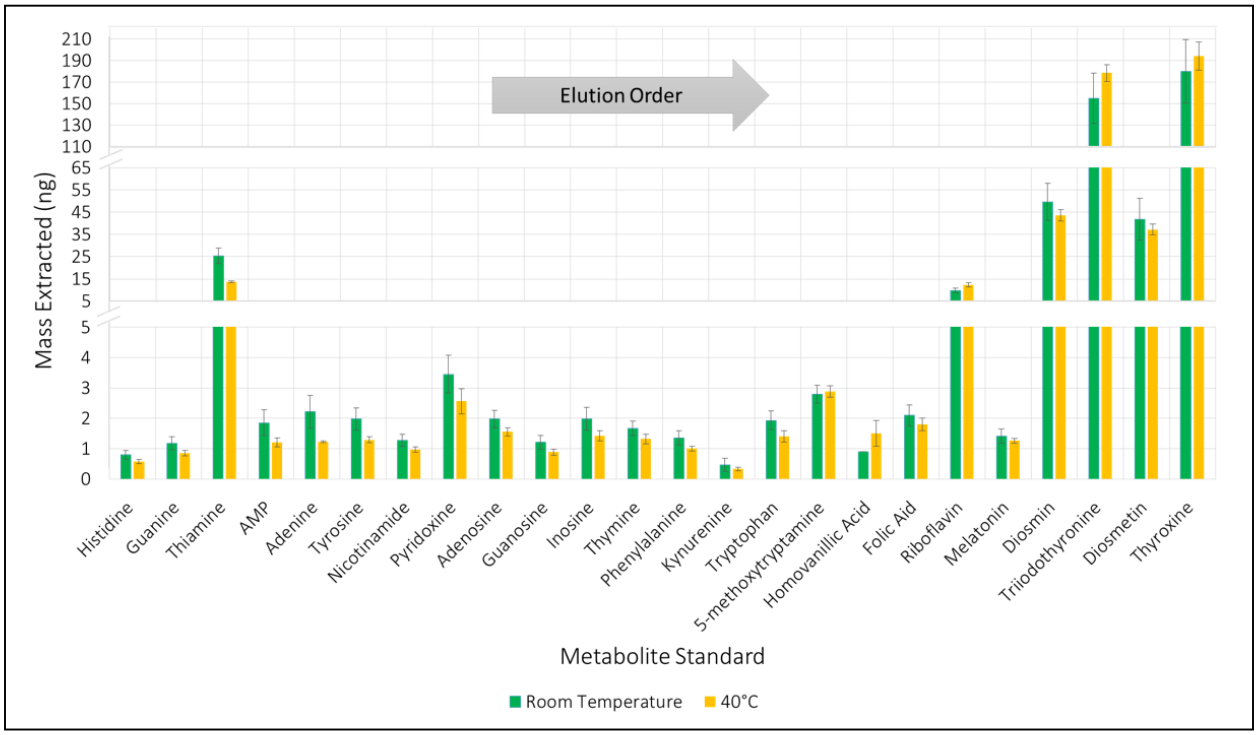

Figure 3.16 Effect of sample temperature on the efficiency of D-SPME desorption of standards (10 µg/mL) in PBS. The 30-minute extraction of 1.5 mL samples was completed using 60 µL of CNP at room temperature with 25 µL desorption volume. The 30-minute desorption was completed using methanol and the extracted samples were diluted 1/10 with water before LC-MS analysis. (n=3)

3.4.7. Testing the Addition of an Evaporation/Reconstitution Step

The one in ten dilution of extracts before LC-MS analysis decreased the concentration of the extracted sample, possibly decreasing the number of compounds detected, particularly for low abundance metabolites. To investigate the elimination of this step, it was replaced by an evaporation/reconstitution step using 10% MeOH/90% water as the reconstitution solvent. In addition, the addition of 6 µL of a 30% glycerol in methanol solution to the samples pre-evaporation was tested. The addition of small volumes of high boiling point solvents, like glycerol, before evaporation has been used to reduce the non-specific

adsorption of analytes onto the surface of the tube.[166] The number of compounds detected by each method (Figure 3.17) was within 2% for results obtained using both positive and negative ESI and the distribution of compounds was comparable between the two methods. The RSD of the peak areas for each compound detected for each method was calculated and the distribution for each method was plotted (Figure 3.18). Evaporation/reconstitution without the addition of glycerol presented lower average and median RSD for both positive and negative ESI, indicative of improved consistency between technical replicates. The addition of an evaporation/reconstitution step increased the number of detected compounds by 204% with positive ESI and 182% with negative ESI indicating that evaporation/reconstitution is advantageous over dilution.

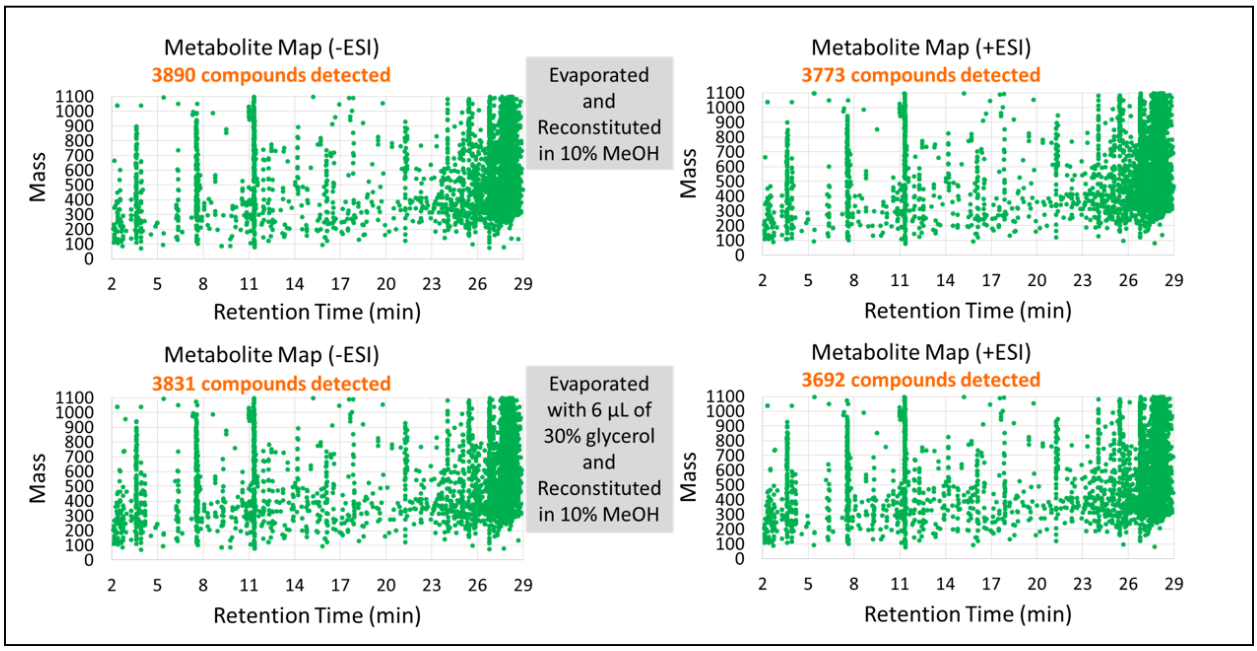

Figure 3.17 Metabolite maps showing compounds detected in extracted plasma samples with the addition of an evaporation/reconstitution step with and without the addition of 6 µL of 30% glycerol in methanol solution in place of the 1/10 dilution with water pre-LC-MS analysis. The 30-minute extraction of 1.5 mL samples was completed using 60 µL of CNP with 25 µL desorption volume. The 30-minute desorption was completed using methanol. (n=3)

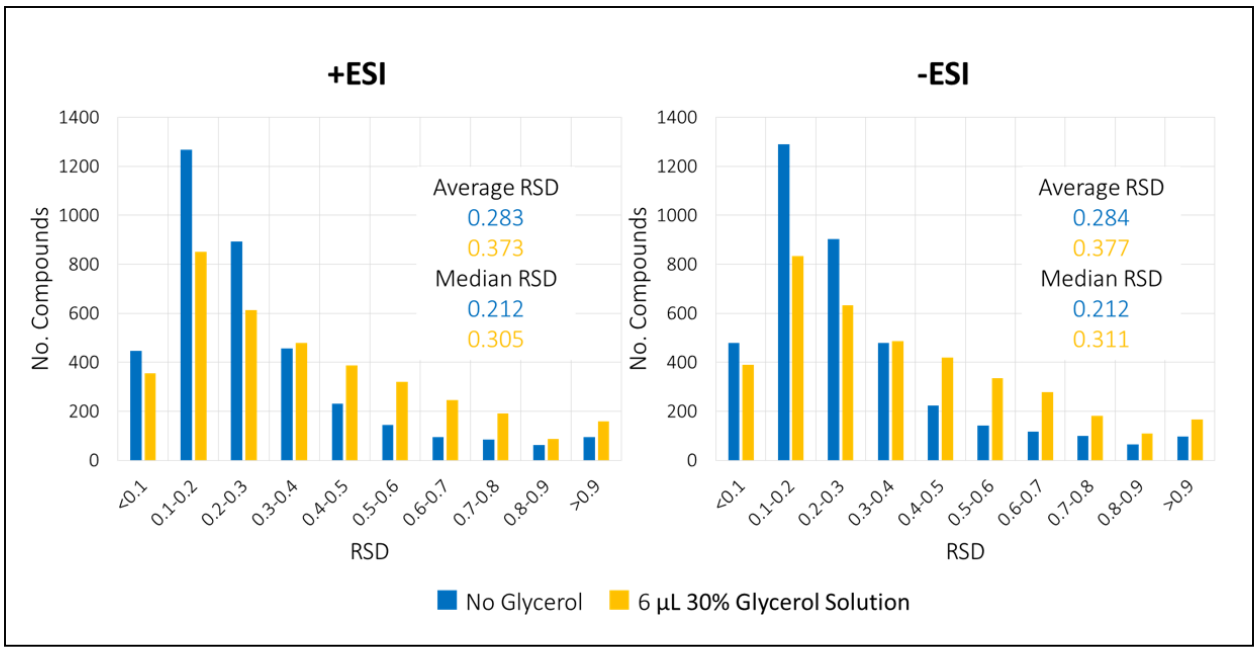

Figure 3.18 A comparison of the distribution of RSD for each compound detected in extracted plasma samples with the additon of an evaporation/reconstitution step with and without the addition of 6 µL of 30% glycerol in methanol solution in place of the 1/10 dilution with water pre-LC-MS analysis. The 30-minute extraction of 1.5 mL samples was completed using 60 µL of CNP with 25 µL desorption volume. The 30-minute desorption was completed using methanol. RSD was calculated as standard deviation divided by the mean. (n=3)

3.4.8. Evaluation of LC Injection volume

The solvent composition of a sample injected into an LC system can affect the chromatographic resolution achieved.[167] If the sample composition matches the mobile phase composition, then the analytes can interact with the stationary phase unhindered. If the sample composition contains a larger percentage of the stronger mobile phase solvent, the analytes in the middle of the sample "plug" travel faster than those on the perimeter, broadening peaks, decreasing resolution. Decreasing the injection volume can decrease this effect however, but decreasing the injection volume also decreases the moles of analyte injected. For low concentration analytes this can result in a loss of detection. Given that the addition of a step to the sample preparation process can result in losses and increased error, an evaluation of whether the 100% organic extracted sample can be analyzed directly and at what injection volume was done using standards spiked in plasma. Global analysis (Figure 3.19) shows that the number of compounds detected decreases with the decrease in injection volume from 10 µL to 5 µL to 2 µL. Peak shapes for spiked standards, examples of which are shown in Figure 3.20, and unknown compounds detected in plasma, examples of

which are shown in Figure 3.21, show that peak shape quality was maintained with decreasing injection volume. The number of compounds detected and peak shapes indicate that an injection volume of 5 µL may be acceptable. A comparison of peak shapes obtained after evaporation and reconstitution (with 90% water/10% MeOH) of samples showed peak shape quality equivalent, to or better than, those of direct injection of 5 µL especially for earlier eluting standards. Improved peak shape with increased aqueous content in the analyzed sample for earlier eluting analytes suggests that solvent content is more crucial for early eluting compounds.

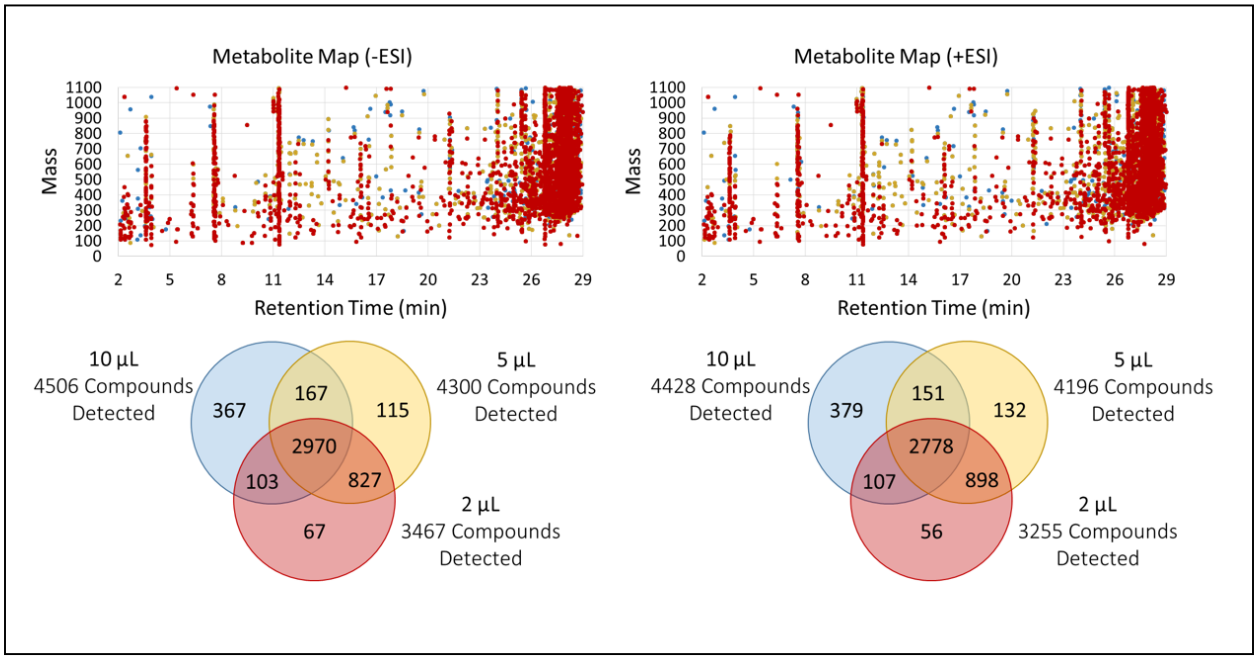

Figure 3.19 Metabolite maps and number of compounds detected demonstrating the effect of LC injection volume. The 30-minute extraction of 1.5 mL samples was completed using 60 µL of CNP.The 30-minute desorption was completed using 25 µL of methanol. Sample extract was injected directly after desorption without silution or evaporation/reconstitution step. (n=1)

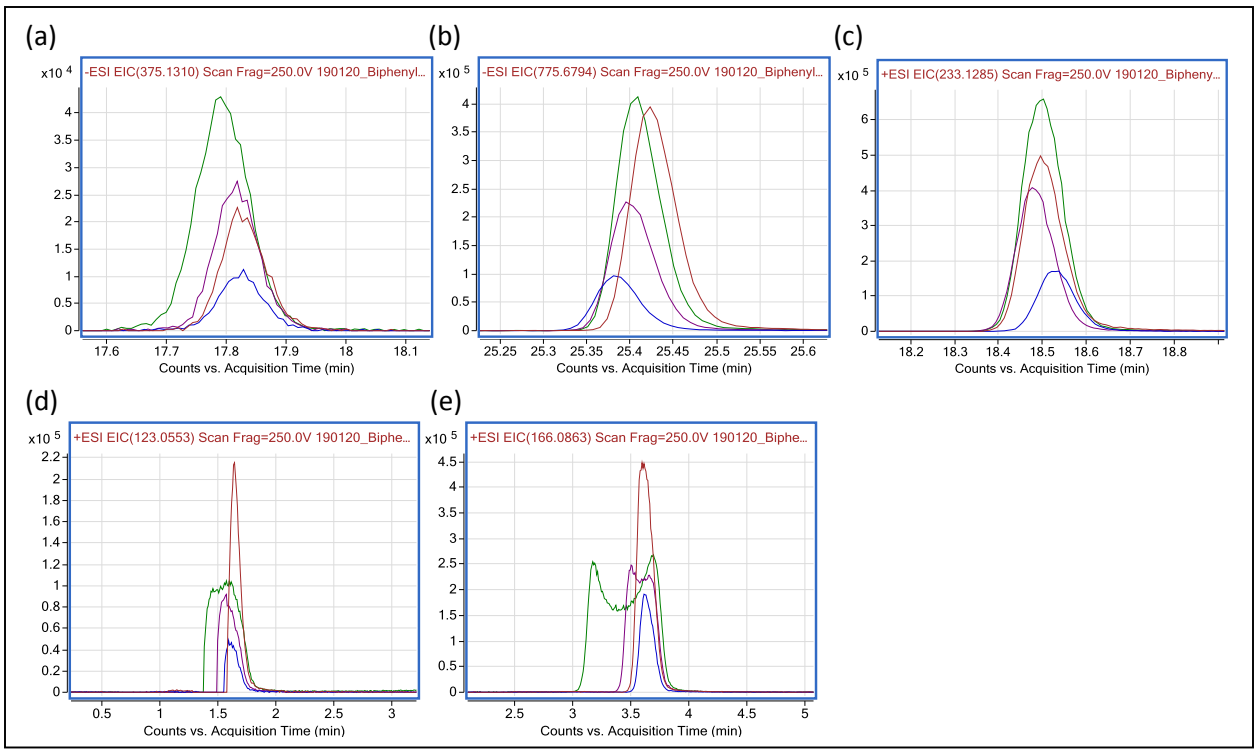

Figure 3.20 EIC for (a) riboflavin, (b) thyroxine, (c) melatonin, (d) nicotinamide, and (e) L-phenylalanine with injection volumes of 10 µL (green), 5 µL (purple), 2 µL (blue), and 10 µL after evaporation and reconstitution (red). The 30-minute extraction of 1.5 mL samples was completed using 60 µL of CNP with 25 µL desorption volume. The 30-minute desorption was completed using methanol. (n=1)

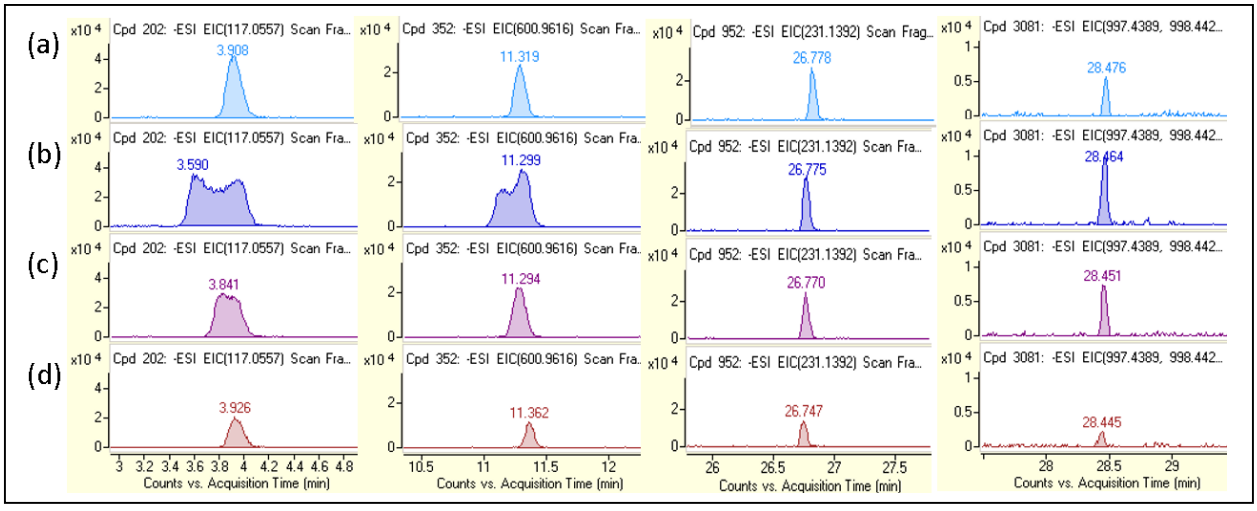

Figure 3.21 EICs of example compounds, shown in order of increasing retention time, from global results for (a) 10 µL injection after evaporation and reconstitution, (b) 10 µL injection, (c) 5 µL injection, and (d) 2 µL injection. The 30-minute extraction of 1.5 mL samples was completed using 60 µL of CNP with 25 µL desorption volume. The 30-minute desorption was completed using methanol. (n=1)

3.4.9 Detection of Endogenous Metabolites in Plasma Samples

To evaluate the ability of the optimized CNP D-SPME protocol to extract endogenous levels of the metabolite standards, extraction of unspiked plasma samples was performed. The EICs of the standards that were detected are shown in Figure 3.22.

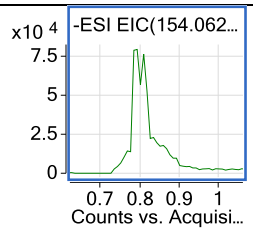	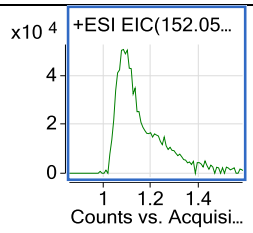	Not Detected	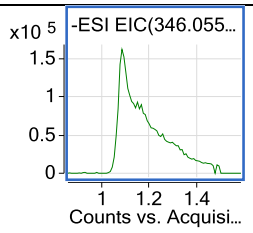
L-Histidine $[M-H]^-$	Guanine $[M+H]^+$	Thiamine $[M+H]^+$	AMP $[M-H]^-$
Not Detected	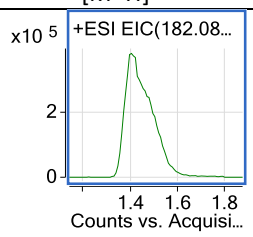	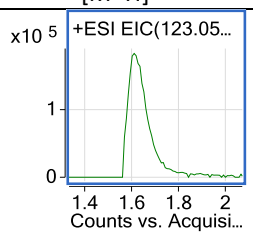	Not Detected
Adenine $[M-H]^-$	L-Tyrosine $[M+H]^+$	Nicotinamide $[M+H]^+$	Pyridoxine $[M-H]^-$
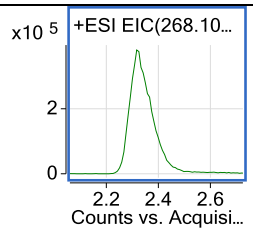	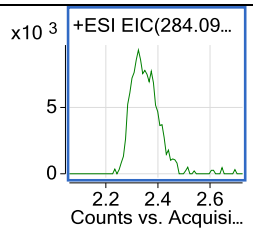	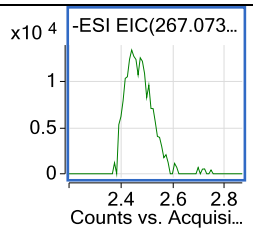	Not Detected
Adenosine $[M+H]^+$	Guanosine $[M+H]^+$	Inosine $[M-H]^-$	Thymine $[M+H]^+$
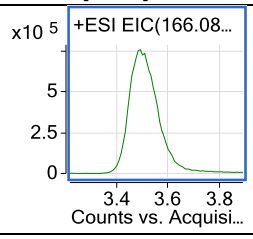	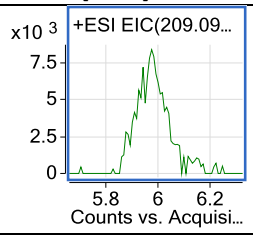	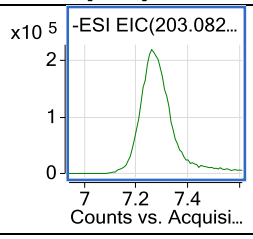	Not Detected
L-Phenylalanine $[M+H]^+$	Kynurenine $[M+H]^+$	L-Tryptophan $[M-H]^-$	5-methoxytryptamine $[M+H]^+$
Not Detected	Not Detected	Not Detected	Not Detected
Homovanillic Acid $[M-H]^-$	Folic Acid $[M-H]^-$	Riboflavin $[M-H]^-$	Melatonin $[M+H]^+$
Not Detected	Not Detected	Not Detected	Not Detected
Diosmin $[M+H]^+$	Triiodothyronine $[M-H]^-$	Diosmetin $[M+H]^+$	Thyroxine $[M-H]^-$

Figure 3.22 EICs of endogenous metabolite standards extracted using the final CNP D-SPME protocol shown in order by retention time.

3.4.10. Separation of Lipid Standards

To aid in the interpretation of the large number of late-eluting compounds extracted, lipid standards were analyzed to determine their retention times. The EICs for these lipids are shown in Figure 3.23 with their respective retention times. All of the lipid standards eluted after 27 minutes indicating that lipid species could be responsible for a large number of the late-eluting extracted compounds seen with all of the tested extraction conditions.

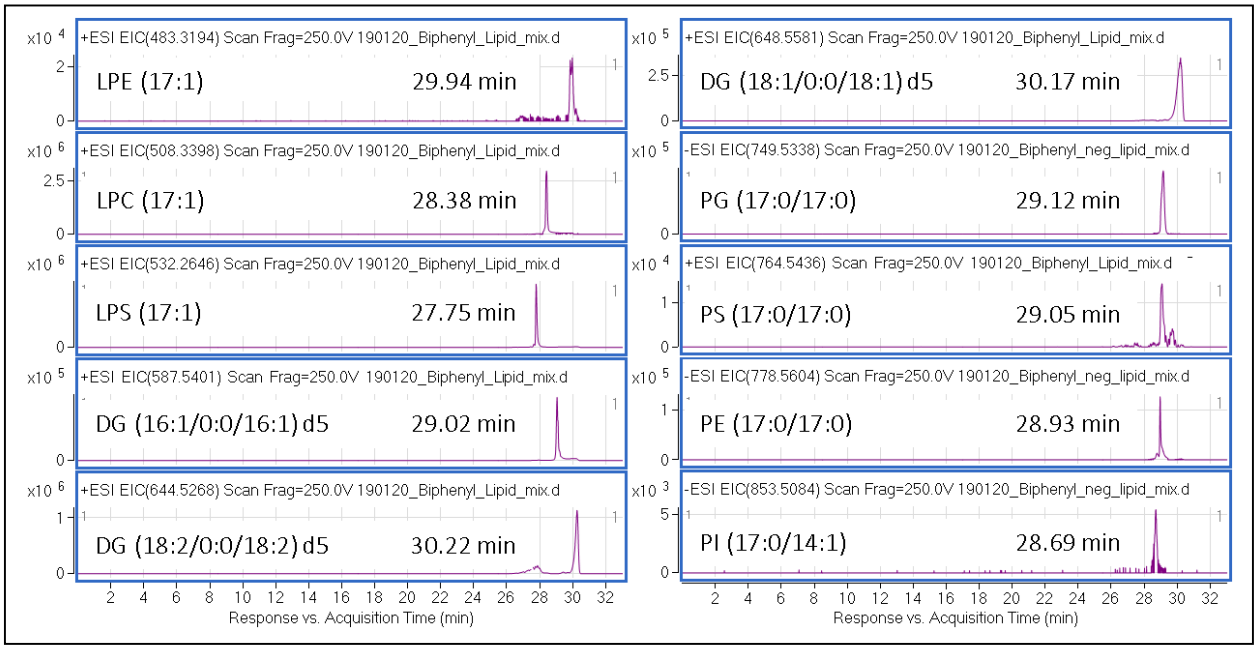

Figure 3.23 EICs of lipid standards (100 ng/mL) analyzed using the developed method for biphenyl column.

3.5. Conclusions

It has been demonstrated that CNPs can be used to extract metabolites from human plasma samples and that a variety of parameters from the extraction procedure can be altered to affect the results. It was determined that CNPs could be successfully separated from samples through centrifugation at 25000 g for 30-minutes. Centrifugation times below this were insufficient to pellet all of the CNPs in a sample. Extraction time was studied for both standards in PBS, and standards in plasma. In buffer, results obtained for 6 time points spanning 2 hours revealed that equilibrium was established within the first two minutes, however an earlier experiment suggested that displacement may occur when extended extraction times are used. The evidence for this phenomenon is not conclusive and will require further investigation. Another possible explanation for the increase in mass of analyte extracted for some standards with extended extraction times may be that the analyte molecules are slowly penetrating the CNPs between the graphitic flakes however, this also requires further investigation. When studied for standards in

plasma, a comparison of 2-minute and 30-minute extraction times showed that equilibrium was not reached within 2 minutes but additional time points would have been useful to further confirm this finding. A comparison of the mean and median RSD between replicates for compounds detected with each extraction time indicated that a 30-minute extraction time allowed for better control of the extraction procedure, as is required with an extraction time less than the equilibration time, and was used for all following experiments.

An evaluation of the sample-to-sorbent ratio, comparing a 6:5 and 3:5 mass ratio for total standard metabolite mass and CNP mass, did not result in the expected two fold increase in mass of analyte extracted. It did however, in combination with decreased desorption volume, allow for the detection of five standards not seen with the lower sorbent mass.

Extractions performed using standard metabolites in PBS suggested that the selectivity of the CNPs as a sorbent is biased toward more hydrophobic analytes. This is not unexpected given the hydrophobic nature of the particles themselves. Additionally, four standards, diosmin, diosmetin, triiodothyronine, and thyroxine, demonstrated greater extraction efficiency, possibly due to their multiple aromatic rings increasing the π-π interactions between analyte and sorbent. The latter two may also be interacting with the π electron systems of the sorbent through the iodine atoms in their structures.

Desorption with three different organic solvents showed that ACN improved the desorption of aromatic metabolite standards. Given that desorption efficiency is governed by the ability of the sorbent to disrupt interactions it is likely this is due to ACNs ability to disrupt π-π interactions between the aromatic metabolite standards and the sorbent. Both ACN and IPA desorbed an increased number of compounds for extracted plasma samples. This is consistent with their stronger eluotropic strength for reversed phase systems compared to MeOH and the observation that a large portion of the extracted compounds are relatively hydrophobic. MeOH, consistent with its more polar character, increased the number of more hydrophilic compounds detected. It is possible that these compounds had poor solubility in the stronger solvents, inhibiting their detection. Acetonitrile was chosen as the desorption solvent for the greater number of compounds detected and the improved desorption of aromatic analytes.

The temperature of samples, both during extraction and desorption, was evaluated comparing room temperature and 40°C. The increase in temperature showed no significant effect on the extraction or desorption efficiency for metabolite standards in buffer, indicating that extraction and desorption at room temperature was sufficient.

Replacing the dilution of samples prior to LC-MS analysis was shown to drastically increase the number of compounds detected in extracted plasma samples. This was achieved by either the addition of an evaporation to dryness and reconstitution in 10% MeOH/90% water step, or direct injection of the 100% organic sample. Direct injection was evaluated for three injection volumes and it was determined that a 5 µL injection volume allowed for the detection an adequate number of compounds. Ultimately the use of an evaporation/reconstitution step proved preferable for the improvement in peak shape for early eluting compounds. The addition of 6 µL of 30% glycerol solution to the desorbed sample pre-evaporation was evaluated to determine whether its ability to decrease non-specific adsorption of analytes onto the walls of the sample tube was required. Global results indicated that the addition of glycerol had no significant effect on the number of compounds detected. Given the small sample volume (25 µL) and 100% organic nature of the sample, which resulted in a drying time less than ten minutes, it is likely that the occurrence of non-specific adsorption, if any, is minimal.

Ultimately, CNPs can be used as a D-SPME sorbent for metabolomics analyses of human plasma, however further investigation of their selectivity is required as well as further development of the extraction protocol.

Chapter 4: Conclusions and Future Work

4.1 Conclusions

The body of this work aimed to achieve two objectives within the larger scope of global metabolomics: (i) to compare two HILIC stationary phases for the separation of methanol-precipitated plasma samples, and (ii) to evaluate the use of CNPs as a sorbent for D-SPME of plasma.

HILIC is used to separate the polar and charged portions of the metabolome. Although HILIC is routinely used in combination with RPLC to improve the metabolite coverage, there is currently no consensus in the literature regarding which HILIC stationary phase to use for this application. In this work, the choice of HILIC stationary phase was investigated, comparing the performance of an underivatized silica to a zwitterionic sulfobetaine using metabolite standards and methanol-precipitated plasma samples. During method development, the effect of mobile phase salt concentration was evaluated on the retention time of 37 metabolite standards consisting of 15 anions, 11 cations, and 11 uncharged. The results support previous literature which states that the effect of increasing salt concentration are twofold. First, increased salt concentration increases the retention time of analytes by increasing the thickness of the adsorbed water layer. This effect was most noticeable for the neutral standards which do not participate in electrostatic interactions with the stationary phase. Second, increased salt concentration decreases the effect of electrostatic interactions which in the case of the ZIC-HILIC column, with its dominant distal negative charge, resulted in decreased retention of most cation standards and increased retention of most anion standards. Overall, 5 mM ammonium acetate was chosen over 2 and 10 mM for allowing the detection of the highest number of standards, and for providing the best separation. This concentration of salt is lower than that used in previous comparisons of HILIC columns[103,168], indicating that the mobile phase salt concentration should be evaluated before comparing the performance of stationary phases.

Next, it was found that the ZIC-HILIC column was capable of successfully separating more standards than the silica column and produced higher quality peak shapes. Specifically the ZIC-HILIC column was able to separate 35 of the 37 tested standards, 14 with good quality peaks as determined by the developed scoring system, while the silica column was only able to separate 23 of the standards, among which only 7 were deemed good quality peaks. No trend was observed to explain why these twelve standards (tryptamine, 5-methoxytryptamine, 3-hydroxybutyric acid, epinephrine, histamine, L-tryptophan, L-lysine, L-histidine, ornithine, glutathione, ADP, and ATP) were observed with the ZIC-HILIC but not the silica column. A comparison of the retention times for standards observed with both columns showed that in general retention times for neutral compounds were within less than a minute of each other while cation

and anion standards showed increased retention times on the silica and ZIC-HILIC columns respectively. The improved peak quality on the ZIC-HILIC column was also observed during the analysis of plasma samples. However, a greater number of compounds, specifically 118% and 66% in positive and negative ESI respectively, were detected in 12 of 12 replicates using the silica column. These 12 replicates consisted of 6 replicated with no added ammonium phosphate, and 6 replicates with 10 mM ammonium phosphate added to the reconstitution solvent. The addition of trace amounts of ammonium phosphate to samples was evaluated for both standards and plasma. Improved peak shape quality was observed with the addition of ammonium phosphate on both columns when evaluating standards in solvent. However no significant change in peak shape, for example tryptophan, phenylalanine, and creatinine, or the number of compounds detected was seen for plasma samples. It is possible that ions already present in plasma, including phosphate, may already modulate electrostatic interactions making the addition of phosphate ions redundant. The discrepancy in these results compared to those obtained by Spalding *et al*.[149] may be caused by the difference in column support material which provided different electrostatic interaction sites, room for improvement due to higher water content in samples, or the difference in matrix components between the plasma used in this study and the E. coli samples used by Spalding *et al*.[149] Overall, the addition of ammonium phosphate to plasma samples before analysis on either the silica or ZIC-HILIC columns is unnecessary and further evaluation is required to make a definitive choice between the silica and ZIC-HILIC columns.

A dispersive solid-phase microextraction method was developed using the novel sorbent, carbon nanopearls, for the first time. In proof-of-concept studies, the effect of critical extraction parameters such as extraction time, sample-to-sorbent ratio, desorption solvent volume, extraction and desorption temperature, and desorption solvent was examined.

An evaluation of extraction time between 2 minutes and 2 hours for aromatic metabolite standards in buffer revealed that equilibrium was achieved within 2 minutes. An evaluation of an extended extraction time (17 hours) suggested that increased extraction may be possible, possibly due to the analyte molecules entering the space between the graphitic flakes that make up the CNPs. An evaluation of extraction time for metabolite standards in plasma indicated the equilibrium was not reached within 2 minutes and a longer extraction time (30 minutes) improved the repeatability of results between replicates.

Evaluation of the sample-to-sorbent ratio (6:5 and 3:5 mass ratio for total standard metabolite mass and CNP mass) did not produce the expected two-fold increase in mass of analyte extracted. However,

combined with decreased desorption volume, it did allow the detection of five more metabolite standards. The same experiment, completed using standard metabolites in plasma instead of buffer, showed the effects of the sample matrix on extraction, showing different extraction efficiencies than those seen for standards in buffer. For example, the recovery for diosmin was 1.15% in buffer but was only 0.39% in plasma. The recovery for unspiked plasma samples remains to be determined. It is possible that recoveries may be decreased by the need for a 30-minute centrifugation step to separate the CNPs from the wash solution. Extraction of metabolite standards in buffer shed some light on the selectivity of the CNPs, indicating that extraction efficiency is greater for more hydrophobic analytes, and that greater ability to interact with the π electron systems of the CNPs through aromatic rings, or iodine atoms, may play a role in determining extraction efficiency.

Desorption using three different organic solvents, ACN, IPA, and MeOH, showed increased desorption of aromatic standards when ACN was used. Desorption efficiency is governed by the sorbent's ability to disrupt interactions between the analyte and sorbent. ACN can disrupt π-π interactions between molecules, which may explain this increase in desorption efficiency. An increased number of compounds were detected in plasma extracts when ACN or IPA were used rather than MeOH, consistent with their stronger eluotropic strength. The more polar solvent, MeOH, increased the number of more hydrophilic compounds detected, possibly due to improved solubility in MeOH compared to IPA or ACN. Ultimately, ACN was chosen as desorption solvent.

The dilution of extracted sample prior to LC-MS analyses resulted in samples that were too dilute. To remedy this, both the direct injection of extracted samples and the addition of an evaporation/reconstitution step prior to LC-MS analysis were investigated. Both greatly increased the number of compounds detected in plasma extracts. The evaporation and reconstitution of samples in LC-MS compatible solvent (90% water/10 % MeOH) was chosen over direct injection of 5 µL of desorbed sample because of the better peak shape quality obtained for early eluting compounds. Overall, CNPs are capable of extracting metabolites from plasma in the context of D-SPME however, the benefit of CNPs over other sorbents as well as a more defined picture of their selectivity remains to be determined.

4.2 Future Work

Looking towards the future, evaluation of the robustness of the HILIC columns is required to determine stability over time and analysis of a large number of plasma samples. This is crucial prior to the use of these columns for long term studies involving hundreds to thousands of samples to ensure that trends observed in the data are not the result of changes in chromatographic performance. To determine the

column robustness, identical samples should be analyzed intermittently throughout a lengthy LC-MS run. Additionally, further investigation of the results seen with ammonium phosphate addition are required to determine why improved peak quality was observed for standards in solvent but not for compounds detected in plasma. We hypothesize that the complex matrix of plasma samples already contains ions which serve the same function as the added ammonium phosphate. Testing the addition of other ammonium salts to metabolite standard samples will hopefully help to identify which of the added ions, ammonium or phosphate, are responsible for the improved peak quality.

The increase in mobile phase salt concentration on the ZIC-HILIC revealed that several compounds, such as L-phenylalanine, did not follow the expected trends in terms of retention time. While we can hypothesize on the reason for these results, such as zwitterionic character, compound structure, or the presence of hydrophobic aromatic groups, a deeper understanding may be garnished through computer modeling of the interactions between these analytes and the stationary phase. It is surprising that more data is not available on the effect of mobile phase salt concentration of the retention of commonly studied metabolites such as amino acids.

Overall, HILIC remains a promising tool for studying the polar metabolome and further development of this technique should be completed. A deeper understanding of the retention mechanisms involved is required, either through experimental analysis or computer modeling. Additionally, although phospholipids were briefly evaluated on both HILIC columns, the evaluation of matrix effects was not performed. Phospholipids elute throughout the run time and likely cause matrix effects. Determining whether phospholipids should be removed from samples prior to HILIC separation to improve data quality needs to be determined.

On the sample preparation side, further investigation of the interday and intraday repeatability of the CNP D-SPME method should be completed, using isotopically labelled internal standards to evaluate where in the procedure issues may be occurring. The discrepancy between results for standards in buffer and in plasma should be further investigated to determine the effect of increased total analyte mass and to determine whether saturation of the CNP binding sites is occurring. This could be done using sorption isotherm experiments, and standard addition experiments in plasma by checking whether displacement occurs after long extraction times. The solid structure of the CNPs presents a lower surface are by mass compared to other carbon nanoparticles which may contribute to the possible saturation of binding sites. Also, results to date indicated that CNP selectivity is biased towards more hydrophobic analytes, especially those with multiple aromatic rings. Further investigation of the properties/classes of metabolites being

extracted should be determined to help evaluate the selectivity of the CNPs as an extraction sorbent. This could be done by determining the retention time of a large variety of metabolite standards on the biphenyl column using the developed method. If retention times of certain classes of metabolites align with the retention time of extracted compounds it could shed light on the physico-chemical properties of the extracted compounds. Alternatively, MS/MS could be used to fragment the extracted compounds and the spectra compared to a library to potentially identify parts of the extracted compounds structure. Additionally, the trend discrepancy between results for positive and negative ESI when comparing amounts extracted with 2 min and 30 min extraction times (Figure 3.10) bears further investigation to determine its cause. Although the CNPs carry no formal charge, it may be possible that they carry a surface charge that may influence the sorption process. It suggests possible preferential selectivity towards compounds that ionize preferentially in negative ESI, possible flavonoids and polyphenols as indicated by selectivity for standard for diosmin and diosmetin.

Biphenyl chromatography does not appear to be the optimal choice for separation of CNP D-SPME extracts. Either the gradient should be altered to better facilitate the separation of late eluting compounds or an alternative stationary phase should be implemented.

Once fully optimized, the method should be compared to the gold standard of sample preparation in global metabolomics, methanol precipitation. Matrix effects are one of the largest concerns when evaluating sample preparation methods and microextraction methods, including SPME, represent a possible way to address this concern. A comparison of the two techniques could shed light on whether D-SPME with CNPs can help to reduce matrix effects. Should the method prove valuable, ways of increasing sample throughput could be developed. For example, the elimination of the need to centrifuge samples to separate the CNPs by immobilization on a support or functionalization with magnetic nanoparticles could be explored. Additionally, it could be evaluated whether the addition of functional groups to the surface of the CNPs could alter the selectivity of the particles, possibly improving metabolome coverage.

The large discrepancy between number of expected metabolites and number of metabolites that have been detected indicates the need for further refinement of the global metabolomics workflow.[3] The application of CNPs as a D-SPME sorbent may improve the detection of some metabolites, possibly low abundance aromatic or halogen containing metabolites, however further investigation is required.

References

(1) Alonso, A.; Marsal, S.; Julia, A. Analytical Methods in Untargeted Metabolomics: State of the Art in 2015. *Front. Bioeng. Biotechnol.* **2015**, *3*, 1–20.

(2) Schrimpe-Rutledge, A. C.; Codreanu, S. G.; Sherrod, S. D.; McLean, J. A. Untargeted Metabolomics Strategies-Challenges and Emerging Directions. *J. Am. Soc. Mass Spectrom.* **2016**, *27* (12), 1897–1905.

(3) Wishart, D. S.; Feunang, Y. D.; Marcu, A.; Guo, A. C.; Liang, K.; Vázquez-Fresno, R.; Sajed, T.; Johnson, D.; Li, C.; Karu, N.; et al. HMDB 4.0: The Human Metabolome Database for 2018. *Nucleic Acids Res.* **2018**, *46*, D608–D617.

(4) Gertsman, I.; Barshop, B. A. Promises and Pitfalls of Untargeted Metabolomics. *J. Inherit. Metab. Dis.* **2018**, *41* (3), 355–366.

(5) Zhou, B.; Xiao, J. F.; Tuli, L.; Ressom, H. W. LC-MS-Based Metabolomics. *Mol. BioSyst.* **2012**, *8* (2), 470–481.

(6) Alvarez-Sanchez, B.; Priego-Capote, F.; Luque de Castro, M. D. Metabolomics Analysis I. Selection of Biological Samples and Practical Aspects Preceding Sample Preparation. *Trends Anal. Chem.* **2010**, *29* (2), 111–119.

(7) Fang, Z. Z.; Gonzalez, F. J. LC-MS-Based Metabolomics: An Update. *Arch. Toxicol.* **2014**, *88*, 1491–1502.

(8) Vuckovic, D. Improving Metabolome Coverage and Data Quality: Advancing Metabolomics and Lipidomics for Biomarker Discovery. *ChemComm* **2018**, *54*, 6728–6749.

(9) Paglia, G.; Del Greco, F. M.; Sigurdsson, B. B.; Rainer, J.; Volani, C.; Hicks, A. A.; Pramstaller, P. P.; Smarason, S. V. Influence of Collection Tubes during Quantitative Targeted Metabolomics Studies in Human Blood Samples. *Clin. Chim. Acta* **2018**, *486* (August), 320–328.

(10) Townsend, M. K.; Bao, Y.; Poole, E. M.; Bertrand, K. A.; Kraft, P.; Wolpin, B. M.; Clish, C. B.; Tworoger, S. S. Impact of Pre-Analytic Blood Sample Collection Factors on Metabolomics. *Cancer Epidemiol. Biomarkers Prev.* **2016**, *25* (5), 823–829.

(11) Gika, H.; Theodoridis, G. Sample Preparation Prior to the LC-MS-Based Metabolomics/Metabonomics of Blood-Derived Samples. *Bioanalysis* **2011**, *3* (14), 1647–1661.

(12) Liu, X.; Hoene, M.; Wang, X.; Yin, P.; Haring, H.-U.; Xu, G.; Lehmann, R. Serum or Plasma, What Is the Difference? Investigations to Facilitate the Sample Material Selection Decision Making Process for Metabolomics Studies and Beyond. *Anal. Chim. Acta* **2018**, *1037*, 293–300.

(13) Prehn, C.; He, Y.; Belcredi, P.; Mo, G.; Yu, Z.; Kastenmu, G. Differences between Human Plasma and Serum Metabolite Profiles. *PLoS One* **2011**, *6* (7), e21230.

(14) Vuckovic, D. Current Trends and Challenges in Sample Preparation for Global Metabolomics Using Liquid Chromatography-Mass Spectrometry. *Anal. Bioanal. Chem.* **2012**, *403* (6), 1523–1548.

(15) Want, E. J.; O'Maille, G.; Smith, C. A.; Brandon, T. R.; Uritboonthai, W.; Qin, C.; Trauger, S. A.; Siuzdak, G. Solvent-Dependent Metabolite Distribution, Clustering, and Protein Extraction for

Serum Profiling with Mass Spectrometry. *Anal. Chem.* **2006**, *78* (3), 743–752.

(16) Michopoulos, F.; Lai, L.; Gika, H.; Theodoridis, G.; Wilson, I. UPLC-MS-Based Analysis of Human Plasma for Metabonomics Using Solvent Precipitation or Solid Phase Extraction. *J. Proteome Res.* **2009**, *8*, 2114–2121.

(17) Polson, C.; Sarkar, P.; Incledon, B.; Raguvaran, V.; Grant, R. Optimization of Protein Precipitation Based upon Effectiveness of Protein Removal and Ionization Effect in Liquid Chromatography – Tandem Mass Spectrometry. *J. Chromatogr. B* **2003**, *785*, 263–275.

(18) Bruce, S. J.; Antti, H.; Cloarec, O.; Trygg, J.; Marklund, S. L.; Moritz, T. Evaluation of a Protocol for Metabolic Profiling Studies on Human Blood Plasma by Combined Ultra-Performance Liquid Chromatography/Mass Spectrometry: From Extraction to Data Analysis. *Anal. Chem.* **2008**, *372*, 237–249.

(19) Bruce, S. J.; Tavazzi, I.; Parisod, V.; Rezzi, S.; Kochhar, S.; Guy, P. A. Investigation of Human Blood Plasma Sample Preparation for Performing Metabolomics Using Ultrahigh Performance Liquid Chromatography/Mass Spectrometry. *Anal. Chem.* **2009**, *81* (9), 3285–3296.

(20) Pereira, H.; Martin, J.-F.; Joly, C.; Sebedio, J.-L.; Pujos-Guillot, E. Development and Validation of a UPLC/MS Method for a Nutritional Metabolomic Study of Human Plasma. *Metabolomics* **2010**, *6*, 207–218.

(21) Gika, H. G.; Macpherson, E.; Theodoridis, G. A.; Wilson, I. D. Evaluation of the Repeatability of Ultra-Performance Liquid Chromatography – TOF-MS for Global Metabolic Profiling of Human Urine Samples. *J. Chromaography B* **2008**, *871*, 299–305.

(22) Chang, M. S.; Ji, Q.; Zhang, J.; El-Shourbagy, T. A. Historical Review of Sample Preparation for Chromatographic Bioanalysis: Pros and Cons. *Drug Dev. Res.* **2007**, *68*, 107–133.

(23) Tiziani, S.; Emwas, A.; Lodi, A.; Ludwig, C.; Bunce, C. M.; Viant, M. R.; Gu, U. L. Optimized Metabolite Extraction from Blood Serum for 1H Nuclear Magnetic Resonance Spectroscopy. *Anal. Biochem.* **2008**, *377*, 16–23.

(24) Pawliszyn, J. Sample Preparation: Quo Vadis? *Anal Chem.* **2003**, *75* (11), 2543–2558.

(25) Pawliszyn, J. Theory of Solid-Phase Microextraction. *J. Chromatogr. Sci.* **2000**, *38*, 270–278.

(26) Ramautar, R.; Berger, R.; van der Greef, J.; Hankemeier, T. Human Metabolomics: Strategies to Understand Biology. *Curr. Opin. Chem. Biol.* **2013**, *17* (5), 841–846.

(27) Zelena, E.; Dunn, W. B.; Broadhurst, D. I.; Francis-McIntyre, S.; Carroll, K. M.; Begley, P.; O'Hagan, S.; Knowles, J. D.; Halsall, A.; Wilson, I. D.; et al. Development of a Robust and Repeatable UPLC−MS Method for the Long-Term Metabolomic Study of Human Serum. *Anal. Chem.* **2009**, *81* (4), 1357–1364.

(28) Want, E. J.; Wilson, I. D.; Gika, H.; Theodoridis, G.; Plumb, R. S.; Shockcor, J.; Holmes, E.; Nicholson, J. K. Global Metabolic Profiling Procedures for Urine Using UPLC – MS. *Nat. Protoc.* **2010**, *5* (6), 1005–1018.

(29) Martínez-Lozanoa, P.; Rusb, J. Separation of Isomers L-Alanine and Sarcosine in Urine by Electrospray Ionization and Tandem Differential Mobility Analysis-Mass Spectrometry. *J. Am. Soc. Mass Spectrom.* **2010**, *21*, 1129–1132.

(30) Yin, P.; Zhao, X.; Li, Q.; Wang, J.; Li, J.; Xu, G. Metabonomics Study of Intestinal Fistulas Based on Ultraperformance Liquid Chromatography Coupled with Q-TOF Mass Spectrometry (UPLC/Q-TOF MS). *J. Proteome Res.* **2006**, *5*, 2135–2143.

(31) Gowda, G. A. N.; Raftery, D. Quantitating Metabolites in Protein Precipitated Serum Using NMR Spectroscopy. *Anal. Chem.* **2014**, *86*, 5433–5440.

(32) Sitnikov, D. G.; Monnin, C. S.; Vuckovic, D. Systematic Assessment of Seven Solvent and Solid-Phase Extraction Methods for Metabolomics Analysis of Human Plasma by LC-MS. *Sci. Rep.* **2016**, *6* (November), 38885.

(33) Vuckovic, D.; Pawliszyn, J. Systematic Evaluation of Solid- Phase Microextraction Coatings for Untargeted Metabolomic Profiling of Biological Fluids By Liquid Chromatography-Mass Spectrometry. *Anal. Chem.* **2011**, *83*, 1944–1954.

(34) Wawrzyniak, R.; Kosnowska, A.; Macioszek, S.; Bartoszewski, R.; Markuszewski, M. J. New Plasma Preparation Approach to Enrich Metabolome Coverage in Untargeted Metabolomics: Plasma Protein Bound Hydrophobic Metabolite Release with Proteinase K. *Sci. Rep.* **2018**, *8* (9541), 1–10.

(35) Pesek, J. J.; Matyska, M. T.; Loo, J. A.; Fischer, S. M.; Sana, T. R. Analysis of Hydrophilic Metabolites in Physiological Fluids by HPLC-MS Using a Silica Hydride-Based Stationary Phase. *J. Sep. Sci.* **2009**, *32*, 2200–2208.

(36) Liu, C.; Sheng, X.; Wang, Y.; Yin, J.; Huang, W.; Fan, Y.; Li, Y.; Zhang, Y. A Sensitive Approach for Simultaneous Quantification of Carbonyl and Hydroxyl Steroids Using 96-Well SPE Plates Based on Stable Isotope Coded-Derivatization-UPLC-MRM: Method Development and Application. *RCS Adv.* **2018**, *8*, 19713–19723.

(37) Poschner, S.; Zehl, M.; Maier-salamon, A.; Jäger, W. Simultaneous Quantification of Estrogens, Their Precursors and Conjugated Metabolites in Human Breast Cancer Cells by LC – HRMS without Derivatization. *J. Pharm. Biomed. Anal.* **2017**, *138*, 344–350.

(38) Skov, K.; Hadrup, N.; Smedsgaard, J.; Frandsen, H. LC – MS Analysis of the Plasma Metabolome — A Novel Sample Preparation Strategy. *J. Chromatogr. B* **2015**, *978–979*, 83–88.

(39) Bojko, B.; Reyes-Garce´s, N.; Bessonneau, V.; Goryn´ski, K.; Mousavi, F.; Souza Silva, E. A.; Pawliszyn, J. Solid-Phase Microextraction in Metabolomics. *Trends Anal. Chem.* **2014**, *61*, 168–180.

(40) Zhang, Q. H.; Zhou, L. Di; Chen, H.; Wang, C. Z.; Xia, Z. N.; Yuan, C. S. Solid-Phase Microextraction Technology for in Vitro and in Vivo Metabolite Analysis. *TrAC - Trends Anal. Chem.* **2016**, *80*, 57–65.

(41) Silva, C. L.; Perestrelo, R.; Silva, P.; Tomás, H.; Câmara, J. S. Volatile Metabolomic Signature of Human Breast Cancer Cell Lines. *Sci. Rep.* **2017**, *7* (January), 1–9.

(42) Rodrigues, D.; Pinto, J.; Margarida, A.; Sara, A.; Reis, M.; Jerónimo, C. Volatile Metabolomic Signature of Bladder Cancer Cell Lines Based on Gas Chromatography – Mass Spectrometry. *Metabolomics* **2018**, *14* (62), 1–15.

(43) Vuckovic, D.; Lannoy, I. De; Gien, B.; Shirey, R. E.; Sidisky, L. M.; Dutta, S.; Pawliszyn, J. In Vivo Solid-Phase Microextraction: Capturing the Elusive Portion of Metabolome. *Angew. Chemie - Int. Ed.* **2011**, *50*, 5344–5348.

(44) Peng, J.; Li, L. Liquid – Liquid Extraction Combined with Differential Isotope Dimethylaminophenacyl Labeling for Improved Metabolomic Profiling of Organic Acids. *Anal. Chim. Acta* **2013**, *803*, 97–105.

(45) Delgado-Povedanoa, M. M.; Calderón-Santiagoa, M.; Castroa, M. D. L. de; Priego-Capotea, F. Metabolomics Analysis of Human Sweat Collected after Moderate Exercise. *Talanta* **2018**, *177* (July 2017), 47–65.

(46) Whiley, L.; Godzien, J.; Ruperez, F. J.; Legido-quigley, C.; Barbas, C. In-Vial Dual Extraction for Direct LC-MS Analysis of Plasma for Comprehensive and Highly Reproducible Metabolic Fingerprinting. *Anal. Chem.* **2012**, *84*, 5992–5999.

(47) Smith, C. A.; O'Maille, G.; Want, E. J.; Qin, C.; Trauger, S. A.; Brandon, T. R.; Custodio, D. E.; Abagyan, R.; Siuzdak, G. METLIN: A Metabolite Mass Spectral Database. *Ther. Drug Monit.* **2005**, *27* (6), 747–751.

(48) Gamagedara, S.; Kaczmarek, A. T.; Jiang, Y.; Cheng, X.; Rupasinghe, M.; Ma, Y. Validation Study of Urinary Metabolites as Potential Biomarkers for Prostate Cancer Detection. *Bioanalysis* **2012**, *4* (10), 1175–1183.

(49) Want, E. J.; Masson, P.; Michopoulos, F.; Wilson, I. D.; Theodoridis, G.; Plumb, R. S.; Shockcor, J.; Loftus, N.; Holmes, E.; Nicholson, J. K. Global Metabolic Profiling of Animal and Human Tissues via UPLC-MS. *Nat. Protoc.* **2013**, *8* (1), 17–32.

(50) Du, T.; Lin, Z.; Xie, Y.; Ye, X.; Tu, C.; Jin, K.; Xie, J. Metabolic Profiling of Femoral Muscle from Rats at Different Periods of Time after Death. *PLoS One* **2018**, *13* (9), 1–15.

(51) Wilson, I. D.; Plumb, R.; Granger, J.; Major, H.; Williams, R.; Lenz, E. M. HPLC-MS-Based Methods for the Study of Metabonomics. *J. Chromatogr. B* **2005**, *817*, 67–76.

(52) Guillarme, D.; Schappler, J.; Rudaz, S.; Veuthey, J. Coupling Ultra-High-Pressure Liquid Chromatography with Mass Spectrometry. *Trends Anal. Chem.* **2010**, *29* (1), 15–27.

(53) Nguyen, D. T.-T.; Guillarme, D.; Rudaz, S.; Veuthey, J.-L. Fast Analysis in Liquid Chromatography Using Small Particle Size and High Pressure. *J. Sep. Sci.* **2006**, *29*, 1836–1848.

(54) Berkecz, R.; Tömösi, F.; Körmöczi, T.; Szegedi, V.; Horváth, J.; Janáky, T. Comprehensive Phospholipid and Sphingomyelin Profiling of Different Brain Regions in Mouse Model of Anxiety Disorder Using Online Two-Dimensional (HILIC/RP)-LC/MS Method. *J. Pharm. Biomed. Anal.* **2018**, *149*, 308–317.

(55) Ivanisevic, J.; Zhu, Z.; Plate, L.; Tautenhahn, R.; Chen, S.; Johnson, C. H.; Marletta, M. A.; Patti, G. J.; Siuzdak, G. Toward Omic Scale Metabolite Profiling: A Dual Separation Mass Spectrometry Approach for Coverage of Lipids and Central Carbon Metabolism. *Anal. Chem.* **2013**, *10* (314), 1–11.

(56) Chalcraft, K. R.; McCarry, B. E. Tandem LC Columns for the Simultaneous Retention of Polar and Nonpolar Molecules in Comprehensive Metabolomics Analysis. *J. Sep. Sci.* **2013**, *36*, 3478–3485.

(57) Wang, D.; Stapleton, H. M. Analysis of Thyroid Hormones in Serum by Liquid Chromatography-Tandem Mass Spectrometry. *Anal. Bioanal. Chem.* **2010**, *397*, 1831–1839.

(58) Jiang, Y.; Cheng, X.; Wang, C.; Ma, Y. Quantitative Determination of Sarcosine and Related

Compounds in Urinary Samples by Liquid Chromatography with Tandem Mass Spectrometry. *Anal. Chem.* **2010**, *82* (21), 9022–9027.

(59) Townsend, M. K.; Clish, C. B.; Kraft, P.; Wu, C.; Souza, A. L.; Deik, A. A.; Tworoger, S. S.; Wolpin, B. M. Reproducibility of Metabolomic Profiles among Men and Women in 2 Large Cohort Studies. *Clin. Chem.* **2013**, *59* (11), 1–11.

(60) Chen, S.; Hoene, M.; Li, J.; Li, Y.; Zhao, X.; Häring, H.; Schleicher, E. D.; Weigert, C.; Xu, G.; Lehmann, R. Simultaneous Extraction of Metabolome and Lipidome with Methyl Tert-Butyl Ether from a Single Small Tissue Sample for Ultra-High Performance Liquid Chromatography/Mass Spectrometry. *J. Chromatogr. A* **2013**, *1298*, 9–16.

(61) Lindner, J. M.; Vogeser, M.; Grimm, S. H. Biphenyl Based Stationary Phases for Improved Selectivity in Complex Steroid Assays. *J. Pharm. Biomed. Anal.* **2017**, *142*, 66–73.

(62) Boggs, A. S. P.; Schock, T. B.; Schwacke, L. H.; Galligan, T. M.; Morey, J. S.; Mcfee, W. E.; Kucklick, J. R. Rapid and Reliable Steroid Hormone Profiling in Tursiops Truncatus Blubber Using Liquid Chromatography Tandem Mass Spectrometry (LC-MS/MS). *Anal. Bioanal. Chem.* **2017**, *409*, 5019–5029.

(63) Donnell, J. N. O.; Venkatesan, N.; Chang, J.; Nguyen, H.; Rhodes, N. J.; Pais, G.; Chapman, R. L.; Griffin, B.; Scheetz, M. H. High-Performance Liquid Chromatography Method for Rich Pharmacokinetic Sampling Schemes in Translational Rat Toxicity Models With Vancomycin. *Clin. Transl. Sci.* **2017**, *10*, 496–502.

(64) Wang, J.; Yang, Z.; Lechago, J. Rapid and Simultaneous Determination of Multiple Classes of Abused Drugs and Metabolites in Human Urine by a Robust LC-MS/MS Method – Application to Urine Drug Testing in Pain Clinics. *Biomed. Chromatogr.* **2013**, *27*, 1463–1480.

(65) Carlier, J.; Diao, X.; Wohlfarth, A.; Scheidweiler, K.; Huestis, M. A. In Vitro Metabolite Profiling of ADB-FUBINACA, A New Synthetic Cannabinoid. *Curr. Neuropharmacol.* **2017**, *15*, 682–691.

(66) Häkkinen, M. R.; Heinosalo, T.; Saarinen, N.; Linnanen, T. Analysis by LC–MS/MS of Endogenous Steroids from Human Serum, Plasma, Endometrium and Endometriotic Tissue. *J. Pharm. Biomed. Anal.* **2018**, *152*, 165–172.

(67) Lindahl, A.; Sääf, S.; Lehtiö, J.; Nordström, A. Tuning Metabolome Coverage in Reversed Phase LC-MS Metabolomics of MeOH Extracted Samples Using the Reconstitution Solvent Composition. *Anal. Chem.* **2017**, *89* (14), 7356–7364.

(68) Greco, G.; Letzel, T. Main Interactions and Influences of the Chromatographic Parameters in HILIC Separations. *J. Chromatogr. Sci.* **2013**, *51* (7), 684–693.

(69) Buszewski, B.; Noga, S. Hydrophilic Interaction Liquid Chromatography (HILIC)-a Powerful Separation Technique. *Anal. Bioanal. Chem.* **2012**, *402* (1), 231–247.

(70) Dole, M.; Hines, R. L.; Mack, L. L.; Mobley, R. C.; Ferguson, L. D.; Alice, M. B. Gas Phase Macroions. *Macromolecules* **1968**, *1* (1), 96–97.

(71) Yamashita, M.; Fenn, J. B. Electrospray Ion Source. Another Variation on the Free-Jet Theme. *J. Phys. Chem.* **1984**, *88* (20), 4451–4459.

(72) Yamashita, M.; Fenn, J. B. Negative Ion Production with the Electrospray Ion Source. *J. Phys.*

Chem. **1984**, *88* (20), 4671–4675.

(73) Ekman, R.; Silberring, J.; Westman-Brinkmalm, A.; Kraj, A. *Mass Spectrometry: Instrumentation, Interpretation, and Applications*; Ekman, R., Silberring, J., Westman-Brinkmalm, A. M., Kraj, A., Eds.; John Wiley & Sons, Inc.: New Jersey, 2008.

(74) Dass, C. *Fundamentals of Contemporary Mass Spectrometry*; John Wiley & Sons, Inc.: New Jersey, 2007.

(75) The Nobel Prize in Chemistry 2002 https://www.nobelprize.org/prizes/chemistry/2002/summary/ (accessed Sep 11, 2018).

(76) Konermann, L.; Ahadi, E.; Rodriguez, A. D.; Vahidi, S. Unraveling the Mechanism of Electrospray Ionization. *Anal. Chem.* **2013**, *85* (1), 2–9.

(77) Agilent. Agilent 6200 Series TOF and 6500 Series Q-TOF LC/MS System Concepts Guide. *Agilent Manual*. 2012, pp 17–43.

(78) Banerjee, S.; Mazumdar, S. Electrospray Ionization Mass Spectrometry: A Technique to Access the Information beyond the Molecular Weight of the Analyte. *Int. J. Anal. Chem.* **2012**, *2012*, 1–40.

(79) Mei, H. *Using Mass Spectrometry for Drug Metabolism Studies*, 2nd ed.; Korfmacher, W. A., Ed.; CRC Press: Boca Raton, 2010.

(80) Gosetti, F.; Mazzucco, E.; Zampieri, D.; Gennaro, M. C. Signal Suppression/Enhancement in High-Performance Liquid Chromatography Tandem Mass Spectrometry. *J. Chromatogr. A* **2010**, *1217* (25), 3929–3937.

(81) Matuszewski, B. K.; Constanzer, M. L.; Chavez-Eng, C. M. Strategies for the Assessment of Matrix Effect in Quantitative Bioanalytical Methods Based on HPLC-MS/MS. *Anal. Chem.* **2003**, *75* (13), 3019–3030.

(82) Volmer, B. D. A.; Jessome, L. L. Ion Suppression: A Major Concern in Mass Spectrometry. *LCGC North Am.* **2006**, *24* (5), 498–510.

(83) Lei, Z.; Huhman, D. V; Sumner, L. W. Mass Spectrometry Strategies in Metabolomics. *J. Biol. Chem.* **2011**, *286* (29), 25435–25442.

(84) Gowda, G. A. N.; Djukovic, D. Overview of Mass Spectrometry-Based Metabolomics: Opportunities and Challenges. *Methods Mol. Biol.* **2014**, *1198*, 3–12.

(85) Evans, A. M.; Bridgewater, B. R.; Liu, Q.; Mitchell, M. W.; Robinson, R. J.; Dai, H.; Stewart, S. J.; Dehaven, C. D.; Miller, L. A. D. High Resolution Mass Spectrometry Improves Data Quantity and Quality as Compared to Unit Mass Resolution Mass Spectrometry in High-Throughput Profiling Metabolomics Metabolomics: Open Access. *Metabolomics* **2014**, *4* (2), 1–7.

(86) Murray, K. K.; Boyd, R. K.; Eberlin, M. N.; Langley, G. J.; Li, L.; Naito, Y. Definitions of Terms Relating to Mass Spectrometry (IUPAC Recommendations 2013). *Pure Appl. Chem.* **2013**, *85* (7), 1515–1609.

(87) Chernushevich, I. V.; Loboda, A. V.; Thomson, B. A. An Introduction to Quadrupole-Time-of-Flight Mass Spectrometry. *J. Mass Spectrom.* **2001**, *36* (8), 849–865.

(88) Mamyrin, B. A.; Karataev, V. I.; Shmikk, D. V.; Zagulin, V. A. The Mass-Reflectron, a New Nonmagnetic Time-of-Flight Mass Spectrometer with High Resolution. *Sov. Physics, J. Exp. Theor. Phys.* **1973**, *37* (1), 45–48.

(89) Xian, F.; Hendrickson, C. L.; Marshall, A. G. High Resolution Mass Spectrometry. *Anal. Chem.* **2012**, *84*, 708–719.

(90) Lacorte, S.; Fernandez-Alba, A. R. Time of Flight Mass Spectrometry Applied to the Liquid Chromatographic Analysis of Pesticides in Water and Food. *Mass Spectrom. Rev.* **2006**, *25*, 866–880.

(91) Mamyrin, B. A. Time-of-Flight Mass Spectrometry (Concepts, Achievements, and Prospects). *Int. J. Mass Spectrom.* **2001**, *206* (3), 251–266.

(92) Berg, J. M.; Tymoczko, J. L.; Stryer, L. Section 30.1 Metabolism Consists of Highly Interconnected Pathways. In *Biochemistry*; W H Freeman: New York, 2002.

(93) Lindahl, A.; Forshed, J.; Nordstr, A. Overlap in Serum Metabolic Profiles between Non-Related Diseases: Implications for LC-MS Metabolomics Biomarker Discovery. *Biochem. Biophys. Res. Commun.* **2016**, *478*, 1472–1477.

(94) Yoric, G.; Julien, B.; Belén, P.; Serge, R. Metabolomics in Chronic Kidney Disease: Strategies for Extended Metabolome Coverage. *J. Pharm. Biomed. Anal.* **2018**, *161*, 313–325.

(95) Yang, Y.; Cruickshank, C.; Armstrong, M.; Mahaffey, S.; Reisdorph, R.; Reisdorph, N. New Sample Preparation Approach for Mass Spectrometry-Based Profiling of Plasma Results in Improved Coverage of Metabolome. *J. Chromatogr. A* **2013**, *1300*, 217–226.

(96) Chetwynd, A. J.; David, A. A Review of Nanoscale LC-ESI for Metabolomics and Its Potential to Enhance the Metabolome Coverage. *Talanta* **2018**, *182* (October 2017), 380–390.

(97) Tugizimana, F.; Steenkamp, P. A.; Piater, L. A.; Dubery, I. A. Mass Spectrometry in Untargeted Liquid Chromatography/Mass Spectrometry Metabolomics: Electrospray Ionisation Parameters and Global Coverage of the Metabolome. *Rapid Commun. Mass Spectrom.* **2018**, *32* (2), 121–132.

(98) Guo, K.; Li, L. Differential 12C-/13C-Isotope Dansylation Labeling and Fast Liquid Chromatography/Mass Spectrometry for Absolute and Relative Quantification of the Metabolome. *Anal. Chem.* **2009**, *81* (10), 3919–3932.

(99) Zhao, S.; Luo, X.; Li, L. Chemical Isotope Labeling LC-MS for High Coverage and Quantitative Profiling of the Hydroxyl Submetabolome in Metabolomics. *Anal. Chem.* **2016**, *88*, 10617–10623.

(100) Zhao, S.; Dawe, M.; Guo, K.; Li, L. Development of High-Performance Chemical Isotope Labeling LC − MS for Profiling the Carbonyl Submetabolome. *Anal. Chem.* **2017**, *89*, 6758–6765.

(101) Linden, J. C.; Lawhead, C. L. Liquid Chromatography of Saccharides. *J. Chromatogr. A* **1975**, *105* (1), 125–133.

(102) Alpert, A. J. Hydrophilic-Interaction Chromatography for the Separation of Peptides, Nucleic Acids and Other Polar Compounds. *J. Chromatogr. A* **1990**, *499* (C), 177–196.

(103) Wernisch, S.; Pennathur, S. Evaluation of Coverage, Retention Patterns, and Selectivity of Seven Liquid Chromatographic Methods for Metabolomics. *Anal. Bioanal. Chem.* **2016**, *408* (22), 6079–6091.

(104) Gallart-Ayala, H.; Konz, I.; Mehl, F.; Teav, T.; Oikonomidi, A.; Peyratout, G.; van der Velpen, V.; Popp, J.; Ivanisevic, J. A Global HILIC-MS Approach to Measure Polar Human Cerebrospinal Fluid Metabolome: Exploring Gender-Associated Variation in a Cohort of Elderly Cognitively Healthy Subjects. *Anal. Chim. Acta* **2018**, *1037*, 327–337.

(105) Ziarrusta, H.; Mijangos, L.; Picart-Armada, S.; Irazola, M.; Perera-Lluna, A.; Usobiaga, A.; Prieto, A.; Etxebarria, N.; Olivares, M.; Zuloaga, O. Non-Targeted Metabolomics Reveals Alterations in Liver and Plasma of Gilt-Head Bream Exposed to Oxybenzone. *Chemosphere* **2018**, *211*, 624–631.

(106) Huang, Y.; Li, W.; Minakova, A. S.; Anumol, T.; Keller, A. A. Quantitative Analysis of Changes in Amino Acids Levels for Cucumber (Cucumis Sativus) Exposed to Nano Copper. *NanoImpact* **2018**, *12*, 9–17.

(107) Yin, P.; Wan, D.; Zhao, C.; Chen, J.; Zhao, X. A Metabonomic Study of Hepatitis B-Induced Liver Cirrhosis and Hepatocellular Carcinoma by Using RP-LC and HILIC Coupled with Mass Spectrometry with Mass Spectrometry. *Mol. Biosyst.* **2009**, *5*, 868–876.

(108) Ortiz-Villanueva, E.; Navarro-Reig, M.; Jaumot, J.; Tauler, R. Chemometric Evaluation of Hydrophilic Interaction Liquid Chromatography Stationary Phases: Resolving Complex Mixtures of Metabolites. *Anal. Methods* **2017**, *9* (5), 774–785.

(109) Elmsjö, A.; Haglöf, J.; Engskog, M. K. R.; Erngren, I.; Nestor, M.; Arvidsson, T.; Pettersson, C. Method Selectivity Evaluation Using the Co-Feature Ratio in LC/MS Metabolomics: Comparison of HILIC Stationary Phase Performance for the Analysis of Plasma, Urine and Cell Extracts. *J. Chromatogr. A* **2018**, *1568*, 49–56.

(110) Contrepois, K.; Jiang, L.; Snyder, M. Optimized Analytical Procedures for the Untargeted Metabolomic Profiling of Human Urine and Plasma by Combining Hydrophilic Interaction (HILIC) and Reverse-Phase Liquid Chromatography (RPLC)–Mass Spectrometry. *Mol. Cell. Proteomics* **2015**, *14* (6), 1684–1695.

(111) Schwalbe-Herrmann, M.; Willmann, J.; Leibfritz, D. Separation of Phospholipid Classes by Hydrophilic Interaction Chromatography Detected by Electrospray Ionization Mass Spectrometry. *J. Chromatogr. A* **2010**, *1217* (32), 5179–5183.

(112) Vosse, C.; Wienken, C.; Cadenas, C.; Hayen, H. Separation and Identification of Phospholipids by Hydrophilic Interaction Liquid Chromatography Coupled to Tandem High Resolution Mass Spectrometry with Focus on Isomeric Phosphytidylglycerol and Bis(Monoacylglycero)Phosphate. *J. Chromatogr. A* **2018**, *1565*, 105–113.

(113) Arthur, C. L.; Pawliszyn, J. Solid Phase Microextraction with Thermal Desorption Using Fused Silica Optical Fibers. *Anal Chem* **1990**, *62*, 2145–2148.

(114) Kataoka, H.; Ishizaki, A.; Saito, K. Recent Progress in Solid-Phase Microextraction and Its Pharmaceutical and Biomedical Applications. *Anal. Methods* **2016**, *8* (29), 5773–5788.

(115) Vuckovic, D. Solid-Phase Microextraction as Sample Preparation Method for Metabolomics. **2010**, 337.

(116) Hooshmand, S.; Es'haghi, Z. Hydrophilic Modified Magnetic Multi-Walled Carbon Nanotube for Dispersive Solid/Liquid Phase Microextraction of Sunitinib in Human Samples. *Anal. Biochem.* **2018**, *542* (November 2017), 76–83.

(117) Jiménez-Soto, J. M.; Cárdenas, S.; Valcárcel, M. Evaluation of Single-Walled Carbon Nanohorns as Sorbent in Dispersive Micro Solid-Phase Extraction. *Anal. Chim. Acta* **2012**, *714*, 76–81.

(118) Hashemi, B.; Zohrabi, P.; Shamsipur, M. Recent Developments and Applications of Different Sorbents for SPE and SPME from Biological Samples. *Talanta* **2018**, *187*, 337–347.

(119) Lasarte-Aragonés, G.; Lucena, R.; Crdenas, S.; Valcrcel, M. Nanoparticle-Based Microextraction Techniques in Bioanalysis. *Bioanalysis* **2011**, *3* (22), 2533–2548.

(120) Herrero-Latorre, C.; Barciela-Garcia, J.; Garcia-Martin, S.; Pena-Crecente, R. M.; Otarola-Jimenez, J. Magnetic Solid-Phase Extraction Using Carbon Nanotubes as Sorbents: A Review. *Anal. Chim. Acta* **2015**, *892*, 10–26.

(121) Caris, J. A.; Silva, B. J. C.; Moises, E. C. D.; Lanchote, V. L.; Queiroz, M. E. C. Automated Analysis of Lidocaine and Its Metabolite in Plasma by In-Tube Solid-Phase Microextraction Coupled with LC-UV for Pharmacokinetic Study. *J. Sep. Sci.* **2012**, *35*, 734–741.

(122) Bojko, B.; Marcin, W.; Pawliszyn, J. Metabolic Profiling of Plasma from Cardiac Surgical Patients Concurrently Administered with Tranexamic Acid: DI-SPME–LC–MS Analysis. *J. Pharm. Anal.* **2014**, *4* (1), 6–13.

(123) Lee, J. H. J.; Jayaprakasha, G. K.; Avila, C. A.; Crosby, K. M.; Patil, B. S. Metabolomic Studies of Volatiles from Tomatoes Grown in Net-House and Open-Field Conditions. *Food Chem.* **2019**, *275*, 282–291.

(124) Li, M.; Liu, X.; Dong, F.; Xu, J.; Kong, Z.; Li, Y.; Zheng, Y. Simultaneous Determination of Cyflumetofen and Its Main Metabolite Residues in Samples of Plant and Animal Origin Using Multi-Walled Carbon Nanotubes in Dispersive Solid-Phase Extraction and Ultrahigh Performance Liquid Chromatography-Tandem Mass Spectrom. *Journal of Chromatography A*. 2013, pp 95–103.

(125) Lucena, R.; Simonet, B. M.; Cárdenas, S.; Valcárcel, M. Potential of Nanoparticles in Sample Preparation. *J. Chromatogr. A* **2011**, *1218* (4), 620–637.

(126) Lúcia de Toffoli, A.; Maciel, E. V. S.; Fumes, B. H.; Lanças, F. M. The Role of Graphene-Based Sorbents in Modern Sample Preparation Techniques. *J. Sep. Sci.* **2018**, *41*, 288–302.

(127) Bethune, D. S.; Kiang, C. H.; de Vries, M. S.; Gorman, G.; Savoy, R.; Vazquez, J.; Beyers, R. Cobalt-Catalysed Growth of Carbon Nanotubes with Single-Atomic-Layer Walls. *Nature* **1993**, *363*, 605–607.

(128) Files, B. S.; Mayeaux, B. M. CARBON NANOTUBES. *Adv. Mater. Process.* **1999**, *156* (4), 47.

(129) Kroto, H. W.; Heath, J. R.; O'Brien, S. C.; Curl, R. F.; Smalley, R. E. C60: Buckminsterfullerene. *Nature* **1985**, *318*, 162–163.

(130) Iijima, S. Helical Microtubules of Graphitic Carbon. *Nature* **1991**, *354*, 56–58.

(131) Iijima, S.; Ichihashi, T. Single-Shell Carbon Nanotubes of 1-Nm Diameter. *Nature* **1993**, *363*, 603–605.

(132) Levesque, A.; Binh, V. T.; Semet, V.; Guillot, D.; Fillit, R. Y.; Brookes, M. D.; Nguyen, T. P. Monodisperse Carbon Nanopearls in a Foam-like Arrangement: A New Carbon Nano-Compound for Cold Cathodes. *Thin Solid Films* **2004**, *464–465*, 308–314.

(133) Barnard, A. S.; Russo, S. P.; Snook, I. K. Structural Relaxation and Relative Stability of Nanodiamond Morphologies. *Diam. Relat. Mater.* **2003**, *12* (03), 1867–1872.

(134) The Nobel Prize in Chemistry 1996 http://www.nobelprize.org/nobel_prizes/chemistry/laureates/1996/ (accessed May 29, 2018).

(135) Liang, X.; Liu, S.; Wang, S.; Guo, Y.; Jiang, S. Carbon-Based Sorbents: Carbon Nanotubes. *J. Chromatogr. A* **2014**, *1357*, 53–67.

(136) Herascu, N.; Truong, V.-V. A Novel Carbon Nanopearls Based Electrode for Supercapacitor Applications.

(137) Mouton, R.; Semet, V.; Guillot, D.; Binh, V. T. Total Energy Distribution of Field Emission Electrons from a Film of Carbon Nanopearls. *J. Vac. Sci. Technol. B* **2006**, *24* (2), 993–996.

(138) Lasarte-Aragonés, G.; Lucena, R.; Cárdenas, S.; Valcárcel, M. Nanoparticle-Based Microextraction Techniques in Bioanalysis. *Bioanalysis* **2011**, *3* (22), 2533–2548.

(139) Rastkari, N.; Ahmadkhaniha, R.; Samadi, N.; Shafiee, A.; Yunesian, M. Single-Walled Carbon Nanotubes as Solid-Phase Microextraction Adsorbent for the Determination of Low-Level Concentrations of Butyltin Compounds in Seawater. *Anal. Chim. Acta* **2010**, *662* (1), 90–96.

(140) Rastkari, N.; Ahmadkhaniha, R.; Yunesian, M. Single-Walled Carbon Nanotubes as an Effective Adsorbent in Solid-Phase Microextraction of Low Level Methyl Tert-Butyl Ether, Ethyl Tert-Butyl Ether and Methyl Tert-Amyl Ether from Human Urine. *J. Chromaography B* **2009**, *877*, 1568–1574.

(141) Wu, F.; Lu, W.; Chen, J.; Liu, W.; Zhang, L. Single-Walled Carbon Nanotubes Coated Fibers for Solid-Phase Microextraction and Gas Chromatography-Mass Spectrometric Determination of Pesticides in Tea Samples. *Talanta* **2010**, *82* (3), 1038–1043.

(142) Jiménez-Soto, J. M.; Cárdenas, S.; Valcárcel, M. Evaluation of Single-Walled Carbon Nanohorns as Sorbent in Dispersive Micro Solid-Phase Extraction. *Anal. Chim. Acta* **2012**, *714*, 76–81.

(143) Jiménez-Soto, J. M.; Cárdenas, S.; Valcárcel, M. Dispersive Micro Solid-Phase Extraction of Triazines from Waters Using Oxidized Single-Walled Carbon Nanohorns as Sorbent. *J. Chromatogr. A* **2012**, *1245*, 17–23.

(144) Hooshmand, S.; Es'haghi, Z. Hydrophilic Modified Magnetic Multi-Walled Carbon Nanotube for Dispersive Solid/Liquid Phase Microextraction of Sunitinib in Human Samples. *Anal. Biochem.* **2018**, *542*, 76–83.

(145) Isabelle Kohler, Rico J.E. Derks, M. G. The Rise of Hydrophilic Interaction Chromatography in Untargeted Clinical Metabolomics. *LCGC Eur.* **2016**, *30* (1), 60–75.

(146) Tang, D.-Q.; Zou, L.; Yin, X.-X.; Ong, C. N. HILIC for Metabolomics: An Attractive and Complementary Approach to RPLC-MS. *Mass Spectrom. Rev.* **2016**, *35*, 574–600.

(147) Lu, W.; Bennett, B. D.; Rabinowitz, J. D. Analytical Strategies for LC-MS-Based Targeted Metabolomics. *J. Chromatogr. B Anal. Technol. Biomed. Life Sci.* **2008**, *871* (2), 236–242.

(148) Bajad, S. U.; Lu, W.; Kimball, E. H.; Yuan, J.; Peterson, C.; Rabinowitz, J. D. Separation and Quantitation of Water Soluble Cellular Metabolites by Hydrophilic Interaction Chromatography-Tandem Mass Spectrometry. **2006**, *1125*, 76–88.

(149) Spalding, J. L.; Naser, F. J.; Mahieu, N. G.; Johnson, S. L.; Patti, G. J. Trace Phosphate Improves ZIC-PHILIC Peak Shape, Sensitivity, and Coverage for Untargeted Metabolomics. *J. Proteome Res.* **2018**, *17*, 3537–3546.

(150) Millipore Sigma. SeQuant® ZIC®-pHILIC Polymeric http://www.emdmillipore.com/CA/en/products/analytics-sample-prep/chromatography-for-analysis/analytical-hplc/sequant-zic-hilic-hplc-columns/sequant-zic-philic-polymeric/aP6b.qB.Q4oAAAE_QfJ3.Lxi,nav (accessed Feb 22, 2019).

(151) Millipore Sigma. SeQuant® ZIC®-HILIC http://www.emdmillipore.com/CA/en/products/analytics-sample-prep/chromatography-for-analysis/analytical-hplc/sequant-zic-hilic-hplc-columns/sequant-zic-hilic/g0mb.qB.kYoAAAE_wOd3.Lxi,nav (accessed Feb 22, 2019).

(152) Sud, M.; Fahy, E.; Cotter, D.; Brown, A.; Dennis, E. A.; Glass, C. K.; Merrill, A. H.; Murphy, R. C.; Raetz, C. R. H.; Russell, D. W.; et al. LMSD: LIPID MAPS Structure Database. *Nucleic Acids Res.* **2007**, *35* (SUPPL. 1), 527–532.

(153) Alpert, A. J. Effect of Salts on Retention in Hydrophilic Interaction. *J. Chromatogr. A* **2018**, *1538*, 45–53.

(154) Agilent. Agilent ChemStation https://www.agilent.com/cs/library/usermanuals/public/G2070-91126_Understanding.pdf (accessed Jun 27, 2018).

(155) Mess, J. N.; Côôtéé, C.; Bergeron, A.; Furtado, M.; Garofolo, F. Selection of HILIC Columns to Handle Matrix Effect Due to Phospholipids. *Bioanalysis* **2009**, *1* (1), 57–62.

(156) Cífková, E.; Hájek, R.; Lísa, M.; Holcapek, M. Hydrophilic Interaction Liquid Chromatography–mass Spectrometry of (Lyso)Phosphatidic Acids, (Lyso)Phosphatidylserines and Other Lipid Classes. *J. Chromatogr. A* **2016**, *1439*, 65–73.

(157) Cífková, E.; Holčapek, M.; Lísa, M.; Ovčačíková, M.; Lyčka, A.; Lynen, F.; Sandra, P. Nontargeted Quantitation of Lipid Classes Using Hydrophilic Interaction Liquid Chromatography-Electrospray Ionization Mass Spectrometry with Single Internal Standard and Response Factor Approach. *Anal. Chem.* **2012**, *84* (22), 10064–10070.

(158) Xiao, C.; Han, S.; Wang, Z.; Xing, J.; Wu, C. Application of the Polysilicone Fullerene Coating for Solid-Phase Microextraction in the Determination of Semi-Volatile Compounds. **2001**, *927*, 121–130.

(159) Wang, J. X.; Jiang, D. Q.; Gu, Z. Y.; Yan, X. P. Multiwalled Carbon Nanotubes Coated Fibers for Solid-Phase Microextraction of Polybrominated Diphenyl Ethers in Water and Milk Samples before Gas Chromatography with Electron-Capture Detection. *Journal of Chromatography A*. 2006, pp 8–14.

(160) Liu, X.; Ji, Y.; Zhang, Y.; Zhang, H.; Liu, M. Oxidized Multiwalled Carbon Nanotubes as a Novel Solid-Phase Microextraction Fiber for Determination of Phenols in Aqueous Samples. **2007**, *1165*, 10–17.

(161) Gilar, M.; Jaworski, A.; McDonald, T. S. Solvent Selectivity and Strength in Reversed-Phase Liquid Chromatography Separation of Peptides. *J. Chromatogr. A* **2014**, *1337*, 140–146.

(162) Yang, M.; Fazio, S.; Munch, D.; Drumm, P. Impact of Methanol and Acetonitrile on Separations Based on π-π Interactions with a Reversed-Phase Phenyl Column. *J. Chromatogr. A* **2005**, *1097*,

124–129.

(163) Minder, E. I.; Schibli, A.; Mahrer, D.; Nesic, P.; Plüer, K. Effects of Different Centrifugation Conditions on Clinical Chemistry and Immunology Test Results. *BMC Clin. Pathol.* **2011**, *11* (6), 1–15.

(164) Li, J.; Wang, Y. Bin; Li, K. Y.; Cao, Y. Q.; Wu, S.; Wu, L. Advances in Different Configurations of Solid-Phase Microextraction and Their Applications in Food and Environmental Analysis. *TrAC - Trends Anal. Chem.* **2015**, *72*, 141–152.

(165) Ulrich, S. Solid-Phase Microextraction in Biomedical Analysis. *J. Chromatogr. A* **2000**, *902*, 167–194.

(166) Kortz, L.; Dorow, J.; Ceglarek, U. Liquid Chromatography-Tandem Mass Spectrometry for the Analysis of Eicosanoids and Related Lipids in Human Biological Matrices: A Review. *J. Chromatogr. B* **2014**, *964*, 1–11.

(167) Alsehli, B. B.; Dolan, J. W. The Role of the Injection Solvent. *LCGC Asia Pacific* **2012**, *15* (4), 19–21.

(168) Contrepois, K.; Jiang, L.; Snyder, M. Supplem Materials Optimized Analytical Procedures for the Untargeted Metabolomic Profiling of Human Urine and Plasma by Combining Hydrophilic Interaction and Reverse-Phase Liquid Chromatography - Mass Spectrometry. *Mol. Cell. Proteomics* **2015**, *14* (April), 1684–1695.